

Diffuse Scattering and Diffuse Optical Tomography on Graphs

by

Jeremy Hoskins

A dissertation submitted in partial fulfillment
of the requirements for the degree of
Doctor of Philosophy
(Applied and Interdisciplinary Mathematics)
in The University of Michigan
2017

Doctoral Committee:

Professor Anna C. Gilbert, Co-Chair
Professor John C. Schotland, Co-Chair
Professor Liliana Borcea
Professor Sergey Fomin
Professor Eric Michielssen

Jeremy G. Hoskins

jhoskin@umich.edu

ORCID iD: [0000-0001-5307-2452](https://orcid.org/0000-0001-5307-2452)

© Jeremy G. Hoskins 2017

To my parents, to Vivienne, and to Henri.

ACKNOWLEDGEMENTS

I owe many people many thanks. First and foremost I would like to thank my advisors, Anna Gilbert and John Schotland, for their guidance, their patience, their wisdom, and their humor. It was truly an honor to work with you. Over the last five years I have laughed much and learned more. I would also like to thank the members of my committee: Liliana Borcea, Eric Michielssen, and Sergey Fomin. Without their advice and teaching I would not be what and where I am today. Finally, I would like to thank Francis Chung for many valuable discussions.

While at the University of Michigan I was fortunate to have many amazing teachers. I learned much from the faculty in courses, seminars, and the occasional impromptu lecture at tea. I also owe much to my fellow graduate students, and my friends, and those who are both. They helped make the last five years pass as if it were no time at all. I would be remiss in my acknowledgements if I did not also thank the staff in the graduate student office. They treated my fiftieth question of the day like it was the first, and always greeted me with a smile. I would also like to thank the Mathematics department for giving me the opportunity to teach, and all of my former students for making it so easy. Additionally, I would like to thank

NSERC for funding my research.

Finally, I would like to thank my family. I would like to thank my mother and father for their constant support, for picking up the phone late at night to give advice on the day-to-day troubles which seemed so important at the time. I would like to thank them for their unwavering belief that this thesis would one day be written, and for all their help along the way. I would also like to thank the cat, Henri. What she lacks in understanding of mathematics and physics she makes up for in companionship. I hope she was able to learn something from the many versions of my talks she heard. Lastly, I would like to thank Vivienne: my best friend; my fiancée; and my partner in crime.

TABLE OF CONTENTS

DEDICATION	ii
ACKNOWLEDGEMENTS	iii
LIST OF FIGURES	vii
ABSTRACT	ix
CHAPTER	
I. Introduction	1
1.1 Introduction	1
1.2 The forward problem	3
1.3 The inverse problem	5
II. Preliminaries	8
2.1 Time-independent diffusion equations on graphs	8
2.2 Linear systems for finite boundary value problems	10
2.3 Spatially varying absorption	14
2.4 Green's functions for graphs	15
III. Diffuse Scattering on Graphs	17
3.1 Introduction	17
3.2 Born series	19
3.2.1 Construction	19
3.2.2 Convergence	20
3.3 Examples	22
3.4 Representation theory and the background Green's function	25
3.4.1 Cayley graphs of finite abelian groups	25
3.4.2 Cayley graphs of finite groups	28
3.5 Numerical experiments	36
3.5.1 Inhomogeneous absorption on a path	36
3.5.2 Inhomogeneous absorption on a complete graph with boundary	37

3.6	Point Absorbers	41
3.6.1	A single point absorber	41
3.6.2	Multiple point absorbers	43
3.7	Computation of background Green's functions	49
3.7.1	Analysis of a Möbius ladder	49
3.7.2	Analysis of the complete graph on d vertices	55
3.7.3	Analysis of a two-dimensional lattice	58
IV. Optical Tomography on Graphs		62
4.1	Introduction	62
4.2	Non-uniqueness of absorption recovery	65
4.3	Inverse Born series	72
4.3.1	Forward Born series	72
4.3.2	Inverse Born series	76
4.4	Implementation	90
4.4.1	Regularizing \mathcal{K}_1	90
4.4.2	Numerical examples	90
4.5	Incorporating potential structure	95
4.6	Inversion through Internal Polling	101
4.6.1	Internal Polling	101
V. Conclusion and Further Work		107
5.1	Conclusion	107
5.2	Future work	108
5.2.1	The inverse Born series in infinite dimensions	108
5.3	Operator bounds and the Inverse Born series	110
5.4	Sparsity and internal polling	111
5.5	Fast summation of the inverse Born series	116
BIBLIOGRAPHY		119

LIST OF FIGURES

Figure		
1.1	Experimental setup for optical tomography in diffuse media	2
2.2	The minimum eigenvalue of the operator H_0 as a function of the absorption α_0 for: a) a path of length 64 with Neumann boundary conditions, and b) a complete graph on 64 vertices and Neumann boundary conditions. For both plots the line corresponds to the bound in equation (2.18).	14
3.1	The permutahedron of order 4.	34
3.2	The background Green's function for the permutohedron of order 4, with $\alpha_0 = 0.1$	35
3.3	The absorption vector η used for the example of constructing a Green's function for the heterogeneous diffusion equation (2.6) via Born series. The support of η is chosen to be a random subset of the interior vertices of size $(2n + 2)/4$	37
3.4	Plots of the ℓ_∞ error of the truncated solution u_N . The green and red curves correspond to the bound on η_{\max} from Theorem III.1 and Proposition III.2, respectively. The other blue lines correspond to η_{\max} spaced 0.026 apart.	38
3.5	A typical absorption vector η used for the example of constructing a Green's function for the spatially-varying time-independent diffusion equation (2.6) via Born series. The support of η is once again chosen to be a random sample of the interior vertices of size $d/4$	39
3.6	Plots of the ℓ_∞ error of the truncated solution u_N . The green and red curves correspond to the bound on η_{\max} from Theorem III.1 and Proposition III.2, respectively.	40
3.7	Plots of $u_0 - u$ for the infinite path with two identical point scatterers equidistant from a point source located at the origin with $\alpha_0 = 0.001$ and $\kappa = 100$	47
3.8	A diagrammatic representation of the geometry of the point absorbers (blue circles), source (green diamond) and detector (red square) used to study the scattering properties of the two point absorber system on the infinite square lattice.	48

3.9	Plots of $u_0 - u$ for the infinite plane with two identical point scatterers equidistant from a point source located at $(-1, 0)$ and detector located at $(1, 0)$ with $\alpha_0 = 10^{-3}$ and $\kappa = 10^3$	50
3.10	The Möbius ladder with $2n + 2$ vertices.	51
3.11	The complete graph on 10 vertices with 10 boundary vertices.	56
4.1	A graph $G = (V, E)$ with a path subgraph (V', E') of length 4. The remainder of the vertices $V \setminus V'$ and edges $E \setminus E'$ are represented by the grey annulus.	66
4.2	A graph G with edges deleted to create an interior path of length four, as required by the conditions of Proposition IV.1. The blue circle, red square, green diamond, and orange star mark the vertices $x_1, x_2, x_3,$ and $x_4,$ respectively.	72
4.3	Left: Values of η restricted to an unconnected path subgraph of a lattice (see Figure 4.2), which are indistinguishable from $\eta \equiv 10$, for $\alpha = 0.2$. Right: ℓ^1 norm of the relative difference between the Robin to Dirichlet map of η and the Robin to Dirichlet map of $\tilde{\eta}_s$	73
4.4	The bound on the radius of convergence of the inverse Born series as a function of C_p/ν_p . The radius r_p (multiplied by μ_p/ν_p) is shown in blue. The red curve is the asymptotic estimate given in (4.52).	83
4.5	a) True potential b) first term of the inverse Born series, c) first two terms of the inverse Born series, d) first five terms of the inverse Born series. Here $\alpha_0 = 0.1,$ $t = 1,$ $\epsilon = 0,$ and every boundary vertex is both a source and a receiver. $\mu_2 = 0.0874,$ $\nu_2 = 0.4702,$ and $\tilde{r}_2 = 3.7 \times 10^{-7}$	92
4.6	a) True potential b) first term of the inverse Born series, c) first two terms of the inverse Born series, d) first five terms of the inverse Born series. Here $\alpha_0 = 0.1,$ $t = 1,$ $\epsilon = 10^{-7},$ and every boundary vertex is both a source and a receiver. $\mu_2 = 0.0874,$ $\nu_2 = 0.4702,$ and $\tilde{r}_2 = 1.215 \times 10^{-6}$. Note that without the regularization the inverse Born series diverges.	92
4.7	a) True potential b) first term of the inverse Born series, c) first two terms of the inverse Born series, d) first five terms of the inverse Born series. Here $\alpha_0 = 0.1,$ $t = 1,$ $\epsilon = 10^{-5},$ and every boundary vertex is both a source and a receiver. $\mu_2 = 0.0874,$ $\nu_2 = 0.4702,$ and $\tilde{r}_2 = 1.224 \times 10^{-4}$	93
4.8	a) True potential b) first term of the inverse Born series, c) first two terms of the inverse Born series, d) first five terms of the inverse Born series. Here $\alpha_0 = 0.1,$ $t = 0,$ $\epsilon = 10^{-5},$ and every boundary vertex is both a source and a receiver. $\mu_2 = 0.1738,$ $\nu_2 = 10.7463,$ and $\tilde{r}_2 = 2.677 \times 10^{-6}$	93

- 4.9 a) True potential b) first term of the inverse Born series, c) first two terms of the inverse Born series, d) first five terms of the inverse Born series. Here $\alpha_0 = 0.1$, $t = 1$, $\epsilon = 10^{-9}$, and every boundary vertex on the top and bottom edges of the lattice is both a source and a receiver. $\mu_2 = 0.0874$, $\nu_2 = 0.2351$, and $\tilde{r}_2 = 2.656 \times 10^{-7}$. . . 94
- 4.10 Reconstructions using the multi-frequency inverse Born series for $\alpha_i = 0.1 \left(1 + 4\frac{i}{N-1}\right)$, $i = 0, \dots, N - 1$, $t = 0.01$, and $\epsilon = 10^{-10}$ 102

ABSTRACT

We formulate and analyze difference equations on graphs analogous to time-independent diffusion equations arising in the study of diffuse scattering in continuous media and consider the associated inverse problem, which we call discrete diffuse optical tomography.

For the forward problem we show how to construct solutions in the presence of weak scatterers from the solution to the homogeneous (background problem) using Born series, providing necessary conditions for convergence and demonstrating the process through numerous examples. In addition, we outline a method for finding Green's functions for Cayley graphs for both abelian and non-abelian groups. Finally, we conclude our discussion of the forward problem by considering the effects of sparsity on our method and results, outlining the simplifications that can be made provided that the scatterers are weak and well-separated.

For the inverse problem, we present an algorithm for solving inverse problems on graphs analogous to those arising in diffuse optical tomography for continuous media. In particular, we formulate and analyze a discrete version of the inverse Born series, proving estimates characterizing the domain of convergence, approximation errors, and stability of our approach. We also present a modification which allows additional information on the structure of the potential to be incorporated, facilitating recovery

for a broader class of problems.

CHAPTER I

Introduction

1.1 Introduction

It is the nature of many systems, continuous or discrete, that given a quantity of interest, Q , and a region, R , it is infeasible to measure Q at every point in R . Instead, measurements are limited to the boundary of R , or a small subset of the vertices or edges of R . Often this limitation is imposed by cost, time, or the destructive nature of the measurement process. In medicine, for example, one wishes to ascertain the presence of a tumor without surgery. In material science, one might wish to find any cracks in an airplane wing without having to destroy it.

One possible way to circumvent this obstruction is to consider instead a related quantity Y , whose dependence on Q is non-local; changing Q on a subset, R_S , of R affects the value of Y at points far away from R_S . In this way, information about Q in the interior of R can propagate out to the boundary of R via Y . The goal of inverse problems is to understand to what extent knowledge of Q in R can be gained by measuring Y on the boundary of R . For example, in optical imaging light is sent into

biological tissue where it is scattered and absorbed. By measuring the light which comes out one wishes to deduce the internal structure of the tissue. In seismology, earthquakes propagate through the Earth's crust. The strength of the vibrations measured at the surface depends on the structure of the ground below. Using this information, one tries to infer the presence and location of oil or mineral deposits. In practice, Y is modelled by a differential, or difference, equation. The quantity, Q , arises in this model as either a coefficient in the differential equation or a source. The *forward problem* is to determine Y given knowledge of Q . The corresponding *inverse problem* is to find Q given Y at the boundary of the domain.

In this work we consider a discrete analog of diffuse scattering and its associated inverse problem: optical tomography. In continuous media, optical tomography is a biomedical imaging modality that uses scattered light as a probe of structural variations in the optical properties of tissue [6], see Figure 1.1. The inverse problem of optical tomography consists of recovering the absorption and diffusion coefficients from boundary measurements.

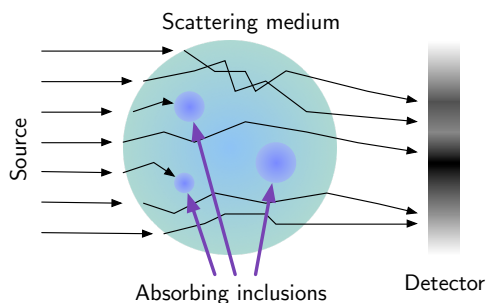


Figure 1.1: Experimental setup for optical tomography in diffuse media

1.2 The forward problem

Let $G = (V, E)$ be a graph with vertex set V and edge set E , and L be the combinatorial Laplacian L , or some suitably rescaled variant [28]. We can then formulate a graph analog of Poisson's equation

$$(1.1) \quad \begin{cases} (Lu)(x) = f(x), & x \in V \\ u(x) = g(x), & x \in \delta V \end{cases}$$

where δV is the set of boundary vertices, which will be discussed in more detail later, and the functions f and g represent internal and boundary sources, respectively. Equation (1.1) has been studied both when the edges are equally-weighted and when the edge weighting varies throughout the graph [13, 28, 29]. In this work, we consider the effect of introducing inhomogeneities on the vertices rather than on the edges, as represented by the addition of a (vertex) potential term to equation (1.1). We call this problem *diffuse scattering on graphs* because of its analogy to a related problem in the continuous setting, where the vertex potential is often called the *absorption*. A similar problem arises in the study of Schrödinger operators on graphs, see for example [12, 10, 19, 20, 21, 72]. In order to develop the necessary foundations to formulate corresponding inverse problems, which will be analyzed in subsequent works, we also study the role of boundary conditions on the solutions. In particular, we consider Dirichlet, Neumann and Robin, or mixed, boundary conditions, which are often employed in the continuous setting.

The graph analog of Poisson's equation is related to the classical problem of

resistor networks first studied by Kirchhoff in 1847 [55]. In that setting, one is given a collection of interconnected resistors to which a voltage source is attached at various points [35]. The resulting system can be thought of as a weighted graph, with each edge corresponding to a particular resistor and the vertices representing the connections between them [35]. In the event that all the resistors are identical, the voltage at each point satisfies Poisson's equation on the associated graph [31]. In this setting, one seeks either to map the network, finding its corresponding graph [35], solely by measuring the current or potential at various points in the network. This physical analogy is also employed for graph sparsification [73], as well as in near linear-time solvers for symmetric, diagonally dominant linear systems [36, 56, 80].

Discrete analogs of PDEs on graphs are not limited to Poisson-type problems and are used extensively in lattice dynamics where we consider the graph analog of the Helmholtz equation [61, 76], which arises when considering time-harmonic waves. In lattice theory, one problem of particular importance is to examine the propagation of phonons through a crystal in order to determine the size and location of imperfections [61, 76].

In Chapter III we consider the graph analog of a different PDE, which we call the problem of diffuse scattering on graphs, though the equation also arises in the study of discrete Schrödinger operators [19]. A key component of our analysis will be constructing methods for obtaining the appropriate Green's functions for the problems we wish to consider. The idea of discrete Green's functions has a long

history arising in many important problems and fields such as the study of inverses of tri-diagonal matrices [42], potential theory [15, 26, 37], the study of Schrödinger operators on graphs [5, 10, 19, 20, 21, 22, 72, 81], and the graph-theoretic analog of Poisson's equation [29, 52, 77, 78]. Additionally, Green's function methods have yielded interesting results in many areas including the properties of random walks [29, 53], chip-firing games [40], analysis of online communities [58], machine learning algorithms [68, 82] and load balancing in networks [24].

1.3 The inverse problem

Inverse problems arise in numerous settings within discrete mathematics, including graph tomography [79, 48, 49, 45, 27] and resistor networks [32, 33, 34, 35, 50, 17, 16]. In such problems, one is typically interested in reconstructing a function defined on edges of a fixed graph or, in some cases, the edges themselves. Here we focus on recovering vertex properties of a graph from boundary measurements. The problem we consider is the discrete analog of optical tomography, and the inverse problem associated with diffuse scattering on graphs.

The underlying model of discrete optical tomography also arises in the study of the Schrödinger equation on graphs and its related inverse problems [67, 51, 3, 17, 18]. For circular planar graphs, or lattice graphs in two or more dimensions, [67, 51, 3, 17] outline an algorithm that can be used to recover the vertex potential. In particular, the first three employ special combinations of boundary sources which force the solution in the interior to be zero except on a small, controllable set of vertices.

Using this approach, the potential at each vertex can be calculated. Then, starting at the boundary, the entire potential can be recovered. The resulting algorithm relies on the lattice structure of the graphs and is unstable for potentials with large support.

In Chapter IV we present a reconstruction method for graph optical tomography that is based on inversion of the Born series solution to the forward problem [64, 9, 59, 65, 60, 7, 54]. Using this approach, we show that it is possible to recover vertex potentials for a general class of graphs under certain smallness conditions on the boundary measurements. Our results are complementary to those in [18], where a discrete analog of complex geometrical optics solutions are used to show that if the linearized problem is solvable, then the Robin-to-Dirichlet map is invertible almost everywhere. We also note that our algorithm applies to complex η , a case that arises in optical tomography. In addition, we obtain sufficient conditions under which the inverse Born series converges to the vertex potential. We also obtain a corresponding stability estimate, which is independent of the support of the potential. In numerical studies of the inverse Born series for large potentials or large graphs, where exact recovery is not guaranteed, we nevertheless find that good qualitative recovery of large scale features of the potential is possible. Moreover, our approach can be easily modified to incorporate additional information on the structure of the potential, improving both the speed and accuracy of the algorithm. As an application of this idea, we show how to determine the potential η using data for multiple values of

α_0 , assuming η is independent of α_0 . This allows us to apply our method to graphs whose structure makes exact potential recovery otherwise impossible.

CHAPTER II

Preliminaries

2.1 Time-independent diffusion equations on graphs

Let $\Gamma = (V', E)$ be a connected locally finite loop-free graph with edge set E and vertex set V' . Given a subset, V , of the vertex set V' , we define the *vertex boundary* of V , δV , by [28]

$$(2.1) \quad \delta V = \{y \in V' \setminus V \mid \exists x \in V \text{ such that } x \sim y \in E\},$$

where $x \sim y$ if x is adjacent to the vertex y , i.e. there is an edge in E joining the vertex x to y . Here we assume that V is a proper subset of V' so that δV is not empty. As in [28], if d_x is the degree of the vertex x , we consider the (vertex) Laplacian $L : (V \cup \delta V) \times (V \cup \delta V) \rightarrow \mathbb{R}$ defined by

$$(2.2) \quad L(x, y) = \begin{cases} d_x & \text{if } y = x \\ -1 & \text{if } y \sim x \\ 0 & \text{otherwise.} \end{cases}$$

Note that in the following, by a slight abuse of notation, we will use the same symbol, L , to denote the Laplacian operator, its kernel, and the corresponding matrix. In

later sections we will employ a similar convention when discussing operators for the time-independent diffusion equation and their associated Green's functions.

To develop the time-independent diffusion equation on graphs we require suitable boundary conditions analogous to those arising in partial differential equations (PDEs). We say a function $u : V \rightarrow \mathbb{R}$ satisfies a homogeneous *Dirichlet* boundary condition if its restriction to δV is identically zero [28]. To obtain appropriate derivative-type boundary conditions we define the discrete analog of the normal derivative $\partial : \ell^2(V \cup \delta V) \rightarrow \ell^2(\delta V)$ by

$$(2.3) \quad \partial u(y) = \sum_{\substack{x \in V \\ x \sim y}} [u(y) - u(x)].$$

A function $u : (V \cup \delta V) \rightarrow \mathbb{R}$ satisfies a homogeneous *Neumann* boundary condition [28] if $\partial u(x) = 0$ for all $x \in \delta V$ and satisfies a *Robin* boundary condition [11] if there exists a constant $t \geq 0$ such that

$$(2.4) \quad t u(x) + \partial u(x) = 0$$

for all $x \in \delta V$. Note that choosing $t = 0$ yields Neumann boundary conditions while letting $t \rightarrow \infty$ produces Dirichlet boundary conditions. Given a function $g : \delta V \rightarrow \mathbb{R}$ we can also define corresponding inhomogeneous boundary conditions

$$(2.5) \quad t u(x) + \partial u(x) = g(x), \quad x \in \delta V$$

which arise when sources or sinks are located on the boundary. For a given interior

source f and boundary source g we define the constant absorption diffusion equation

$$(2.6) \quad \begin{cases} \sum_{y \in V'} L(x, y) u(y) + \alpha_0 u(x) = f(x), & x \in V \\ t u(x) + \partial u(x) = g(x), & x \in \delta V. \end{cases}$$

Here, in analogy with the physical problem of diffuse scattering, α_0 is a strictly positive constant which represents the absorption of the medium. Note that L is positive semidefinite [11, 28].

2.2 Linear systems for finite boundary value problems

In the case where $|V|$ and $|\delta V|$ are both finite the boundary value problem (2.6) can be written as a linear system of equations for u . We first index the vertices of V by $1, \dots, n = |V|$ and those of δV by $n + 1, \dots, n + k$ where $k = |\delta V|$. Next we construct the $(n + k) \times (n + k)$ matrix

$$(2.7) \quad H_0 = L + \begin{pmatrix} \alpha_0 I_{n \times n} & 0_{n \times k} \\ 0_{k \times n} & t I_{k \times k} \end{pmatrix}$$

where $I_{n \times n}$ and $I_{k \times k}$ are the $n \times n$ and $k \times k$ identity matrices, respectively, and $0_{n \times k}$ is the $n \times k$ zero matrix. If we let $u = (u(x_1), \dots, u(x_{n+k}))^*$ and

$$\tilde{f} = (f(x_1), \dots, f(x_n), g(x_{n+1}), \dots, g(x_{n+k}))^*,$$

where w^* denotes the conjugate transpose of w , then we can rewrite the diffusion equation (2.6) as

$$(2.8) \quad H_0 u = \tilde{f}.$$

Similarly, we obtain Dirichlet boundary conditions by replacing the matrix operator H_0 in (2.7) by the matrix

$$(2.9) \quad H_0^{\text{D}} = \begin{pmatrix} L(V; V) + \alpha_0 I_{n \times n} & L(V; \delta V) \\ 0_{k \times n} & I_{k \times k} \end{pmatrix}$$

Here we have used the convention that given any two sets $A, B \subset V \cup \delta V$, $L(A; B)$ is the submatrix of the Laplacian matrix, L , obtained by taking the rows corresponding to the elements in A and the columns corresponding to the elements in B . We say the vector u satisfies the diffusion equation with Dirichlet boundary conditions if

$$(2.10) \quad H_0^{\text{D}} u = \tilde{f}.$$

Alternatively, one can obtain u by noting that

$$(2.11) \quad u = \lim_{t \rightarrow \infty} u_t$$

where u_t satisfies the equation

$$(2.12) \quad H_0 u_t = \begin{pmatrix} f \\ t g \end{pmatrix}$$

and H_0 is the matrix operator corresponding to Robin boundary conditions depending on the parameter t as in (2.5).

It is clear by construction that H_0 is symmetric. As shown in the following proposition, under certain restrictions, the matrix H_0 is also positive definite and hence has a well-defined inverse. This is equivalent to the existence of a unique solution to the diffusion equation (2.6).

Proposition II.1. *For all t such that $0 \leq t < \infty$ the smallest eigenvalue λ_m of H_0 satisfies*

$$(2.13) \quad \lambda_m \geq \min\{t, \alpha_0\},$$

and hence the matrix H_0 is positive definite if $t > 0$ and H_0 is positive semidefinite if $t = 0$, though later, in Proposition II.2, we will show that in the latter case H_0 is also positive definite provided that $\alpha_0 > 0$, see also [12].

Proof. The desired inequality follows immediately from an analysis of the variational formulation of the problem, as in [11, 12]. Alternatively, the result can also be shown by applying the Gerschgorin circle theorem to the operator H_0 .

□

Proposition II.2. *Consider the diffusion equation (2.6) on a connected graph Σ with Neumann boundary conditions corresponding to $t = 0$. The associated matrix operator H_0 is positive definite for all $\alpha_0 > 0$ and moreover*

$$(2.14) \quad \lambda_m = \frac{|V|}{|V| + |\delta V|} \alpha_0 + O(\alpha_0^2)$$

as $\alpha_0 \rightarrow 0^+$.

Proof. The proof is by contradiction. Suppose v is an eigenvector of H_0 with eigenvalue 0. Let A be the matrix defined by

$$(2.15) \quad A_{i,j} = \begin{cases} 1, & i = j, 1 \leq i \leq n, \\ 0, & \text{otherwise,} \end{cases} .$$

By construction it is clear that

$$(2.16) \quad H_0 = L + \alpha_0 A$$

and, that both A is positive semidefinite. Note that

$$(2.17) \quad \begin{aligned} 0 &= v^* H_0 v \\ &= v^* L v + \alpha_0 v^* A v. \end{aligned}$$

Since L and A are positive semidefinite and A is diagonal it is clear that v is in the kernel of A and is an eigenvector of L with eigenvalue 0. Since $v \in \ker A$ it follows that its first n entries must be identically zero. From [28] we observe that since Γ is connected, the eigenvalue 0 of L has multiplicity one corresponding to the eigenvector $(1, \dots, 1)^*$. Thus, since v is a scalar multiple of the all ones vector and its first n entries are zero, it follows that v is the zero vector and hence cannot be an eigenvector of H_0 , completing the proof.

It follows immediately from the theory of asymptotic analysis of linear systems, see [63] for example, that the smallest eigenvalue of $L + \alpha_0 A$ is

$$(2.18) \quad \lambda_m = \alpha_0 \frac{v^* A v}{v^* v} + O(\alpha_0^2),$$

from which the required result follows immediately.

□

Plots of the minimum eigenvalue of H_0 as a function of α_0 are shown for a path in Figure 2.2a and for a complete graph in Figure 2.2b. As we can see, for small

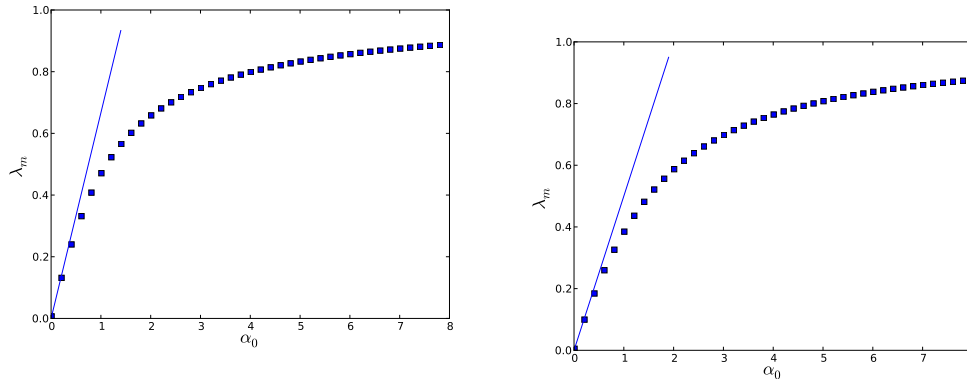


Figure 2.2: The minimum eigenvalue of the operator H_0 as a function of the absorption α_0 for: a) a path of length 64 with Neumann boundary conditions, and b) a complete graph on 64 vertices and Neumann boundary conditions. For both plots the line corresponds to the bound in equation (2.18).

α_0 the curve approaches the bound given in (2.18), which is shown in both plots for reference.

2.3 Spatially varying absorption

When discussing diffusion problems in the continuous setting we often wish to consider media with spatially varying properties. A similar idea can be applied to graphs through a suitable modification of the graph diffusion problem (2.6). Suppose the absorption at each vertex in V is given by a non-negative function $\eta : V \rightarrow \mathbb{R}_{\geq 0}$. The resulting perturbed diffusion equation is

$$(2.19) \quad \begin{cases} \sum_{y \in V'} L(x, y) u(y) + \alpha_0 [1 + \eta(x)] u(x) = f(x), & x \in V, \\ t u(x) + \partial u(x) = g(x), & x \in \delta V. \end{cases}$$

Note that equation (2.19) also arises in the study of Schrödinger equations on graphs where it can be interpreted as the Robin boundary value problem for the Schrödinger

operator with potential $q = \alpha_0(1 + \eta)$. To write this as a linear system we let D_η be the $(n + k) \times (n + k)$ matrix with entries

$$(2.20) \quad (D_\eta)_{ij} = \begin{cases} \eta(x_i), & i = j \leq n, \\ 0, & \text{otherwise.} \end{cases}$$

It follows that u solves the boundary value problem (2.19) if and only if it satisfies

$$(2.21) \quad [H_0 + \alpha_0 D_\eta]u = \tilde{f}.$$

For convenience we define $H = H_0 + \alpha_0 D_\eta$ to be the matrix operator corresponding to the more general diffusion equation.

In many physical applications we are often interested in inhomogeneities confined to a region whose volume is significantly smaller than that of the whole domain. An analogous idea for diffuse scattering on graphs is to consider absorption functions, $\alpha(x)$, with small *support*. Given a function $\alpha(x)$ defined on a graph with vertex set V , its *support* is the set of all vertices in V for which the function $\alpha(x)$ is non-zero.

We also note that in some cases it is useful to consider graphs with no boundary. In this case we take δV in (2.19) to be the empty set and consider the effects of sources placed in the interior, ie. the support of \tilde{f} in (2.21) is contained in V .

2.4 Green's functions for graphs

Green's functions are a useful tool for obtaining and analyzing solutions to PDEs. When discussing similar equations on graphs, the analogous operator $G(x, y)$ is the inverse of H [28]. Suppose the number of interior vertices of Σ and the number of

boundary vertices of Σ are both finite. If we define $G_y = (G(x_1, y), G(x_2, y), \dots, G(x_{n+k}, y))^*$ and let H^* denote the adjoint of the operator H , then G_y satisfies the linear system

$$(2.22) \quad H^*G_y = \delta_y$$

where δ_y is the vector whose components are all zero except for the one corresponding to y which is one. Observe that since $H = H_0 + \alpha_0 D_\eta$, where H_0 and α_0 are symmetric, it follows that H is also symmetric, and so is its inverse G . Using (2.22) we see that if u is a solution of (2.19) then

$$(2.23) \quad \begin{aligned} G_y^* \tilde{f} &= G_y^* H u \\ &= (H^* G_y)^* u \\ &= \delta_y^* u \\ &= u(y). \end{aligned}$$

In this work the examples in which we are primarily interested are those for which $|V|$ and $|\delta V|$ are both finite, though when $|V| + |\delta V|$ is infinite Green's functions can also be defined, see [11, 77] for example.

CHAPTER III

Diffuse Scattering on Graphs

3.1 Introduction

Here we consider a graph analog of the time-independent diffusion equation, which we call diffuse scattering on graphs. This model also arises in the study of discrete Schrödinger operators [19]. As in the continuous problem, we are particularly interested in systems with nearly uniform absorption. By this we mean that the variations in the absorption are small relative to the mean and are typically limited to a small subset of vertices. By defining and applying a discrete version of the Born series we obtain, under suitable conditions, a series solution to the forward problem for a heterogeneous medium, given in terms of the Green's function for the diffusion equation on the same graph but with uniform absorption, called the *background Green's function*. We then provide sufficient conditions on the inhomogeneities for the series solution to converge to the correct solution and provide estimates for the rate of convergence.

In Section 3.2 we develop the necessary tools to construct the Born series from

the background Green's function. In particular, we prove necessary conditions for the convergence of the series, and discuss the dependence of the rate of convergence on the structure of the graph.

Before applying the Born series to a specific graph, it is first necessary to obtain the background Green's function. In Section 3.3 we provide examples of various families of graphs for which the background Green's function is explicitly known and in Section 3.4 we discuss the connection between the symmetries of vertex-transitive graphs and group representation theory, showing how to use knowledge of the symmetry group of a graph to obtain an expression for the corresponding background Green's function.

In Section 3.5 we present a few representative numerical experiments demonstrating the convergence of the Born series for small perturbations to the absorption and compare the empirical convergence results to the bounds obtained in Section 3.2. Finally, in Section 3.6, we consider the discrete analogue of a classical problem in scattering theory; the scattering due to a small collection of point absorbers. In the case where there are only one or two point absorbers present, we explicitly sum the Born series and give exact formulae for the scattered fields provided the Green's function for the homogeneous medium is known. We conclude with a comparison of the scattering of light from point absorbers on infinite one-dimensional and two-dimensional lattice graphs to the well-known formulae for the continuous problem of the same dimensions.

3.2 Born series

We next discuss a useful perturbative method, called *Born series*, for constructing series solutions to (2.19) using the homogeneous Green's function.

3.2.1 Construction

Consider the matrix operator H_0 for the unperturbed diffusion equation (2.6) and let G_0 be the matrix such that $G_0 H_0 = I$. In particular we require the columns of H_0 to be linearly independent so that H_0 has a well-defined inverse. As in the previous section, we define the matrix operator H for the perturbed problem (2.19) by

$$(3.1) \quad H = H_0 + \alpha_0 D_\eta,$$

where D_η is once again the matrix defined in (2.20). Since $\eta \geq 0$, H^{-1} exists and satisfies

$$(3.2) \quad H^{-1} = (I + \alpha_0 G_0 D_\eta)^{-1} G_0$$

and we can write a corresponding Neumann series

$$(3.3) \quad B = \left[\sum_{n=0}^{\infty} (-1)^n \alpha_0^n (G_0 D_\eta)^n \right] G_0,$$

which, under suitable conditions on G_0 and D_η , is equal to the inverse of H . In the context of scattering theory such an expansion is often called a *Born series*. Assuming the series in (3.3) converges to H^{-1} it follows immediately that for any source vector \tilde{f} the corresponding solution u of the time-independent diffusion equation (2.19) is

given by

$$(3.4) \quad u = \left[\sum_{n=0}^{\infty} (-1)^n (\alpha_0)^n (G_0 D_\eta)^n \right] G_0 \tilde{f}.$$

3.2.2 Convergence

To show convergence of the Born series (3.3) with respect to a norm $\|\cdot\|$ it is sufficient to show that the induced operator norm of B , denoted by $\|B\|$, is bounded, as shown in the following theorem.

Theorem III.1. *The series*

$$(3.5) \quad B = \left[\sum_{n=0}^{\infty} (-1)^n \alpha_0^n (G_0 D_\eta)^n \right] G_0$$

converges to the Green's function of the perturbed problem (2.19) if $\alpha_0 \|G_0\| \cdot \|D_\eta\| < 1$. Moreover, if B_N , the truncated operator formed by taking the first $N + 1$ terms of the Born series, we have the following estimate of the error

$$(3.6) \quad \|B - B_N\| \leq \|G_0\|^2 \frac{\alpha_0^N \|G_0\|^N \|\eta\|_\infty}{1 - \alpha_0 \|G_0\| \|\eta\|_\infty}$$

Proof. The proof is an immediate consequence of the existing theory of *Neumann series*, see [30] for example. □

In particular we see from the previous theorem that approximating the Green's function by a truncated Born series is more accurate when $\|D_\eta\| \|G_0\|^{-1} \alpha_0^{-1}$ are small, sometimes called the *weak scattering limit* [8]. We can also obtain tighter bounds if additional information about the structure of the absorption matrix D_η

is used. In particular it is natural to assume that the matrix D_η has few non-zero diagonal entries. This is analogous to the physical situation where the spatial support of the scatterers is much smaller than the total volume.

Proposition III.2. *Suppose η has support $\Lambda \subseteq V$ and let I_Λ be the restriction of the identity matrix to the support of η . Further define $G_{0,\Lambda} = I_\Lambda G_0 I_\Lambda$ and let $\eta_{\max} = \sup_{x \in \Lambda} \eta(x)$. The series*

$$(3.7) \quad B = \left[\sum_{n=0}^{\infty} (-1)^n \alpha_0^n (G_0 D_\eta)^n \right] G_0$$

converges to the Green's function of the perturbed problem (2.19) if $\eta_{\max} \alpha_0 \|G_{0,\Lambda}\| < 1$. Moreover, the truncation error associated with taking the first $N + 1$ terms of the Born series,

$$(3.8) \quad B_N = \left[\sum_{n=0}^N (-1)^n \alpha_0^n (G_0 D_\eta)^n \right] G_0,$$

is $O(\alpha_0^N \|G_{0,\Lambda}\|^N \cdot \eta_{\max}^N)$ as $N \rightarrow \infty$.

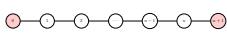
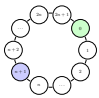
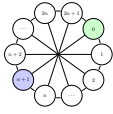
Proof. Since D_η is a diagonal matrix it follows that $\|D_\eta\| = \eta_{\max} = \sup_{x \in V} |\eta(x)|$. Let Λ be the support of η and let I_Λ be the restriction of the identity matrix to the support of η . In particular, I_Λ is the diagonal matrix $I_\Lambda(x, y) = \delta_{x,y} \chi_{\{x \in \Lambda\}}$, where χ_A denotes the characteristic function of the set A . Note that $D_\eta = I_\Lambda D_\eta = D_\eta I_\Lambda$ and thus if we define $G_{0,\Lambda} = I_\Lambda G_0 I_\Lambda$ and let $n > 1$, then $(G_0 D_\eta)^n = G_0 D_\eta (I_\Lambda G_0 I_\Lambda D_\eta)^{n-1} = G_0 D_\eta (G_{0,\Lambda} D_\eta)^{n-1}$. Defining the truncated operator $B_N = \sum_{n=0}^N (-1)^k \alpha_0 (G_0 D_\eta)^n G_0$, we note that

$$(3.9) \quad B_N = G_0 + G_0 D_\eta \sum_{n=1}^{N-1} (-1)^k \alpha_0^n (G_{0,\Lambda} D_\eta)^{n-1} G_0.$$

The result now follows immediately from the theory of Neumann series. \square

3.3 Examples

Having developed the theory of Born series in the previous section, provided the perturbations to the absorption are sufficiently small, we can now apply this method to approximate Green's functions for which the background Green's function is known. A non-exhaustive list of families graphs for which the background Green's function is known is given in Table 3.1.

Name	Figure	Background Green's function	Reference
Path		$G(i, j) = \frac{(ar^i - a^{-1}r^{-i})(ar^{n+1-j} - a^{-1}r^{-(n+1-j)})}{(r - \frac{1}{r})(a^2r^{n+1} - a^{-2}r^{-(n+1)})}, \quad 0 \leq i \leq j \leq n+1,$ $r + 1/r = 2 + \alpha_0, \text{ and } a = \left[1 + \frac{(r^2 - 1)}{r[1 + \alpha_0 - r]}\right]^{1/2}$	[10, 29]
Cycle		$G(i, j) = \frac{r^{n+1 - i-j _{\min}} + r^{-(n+1 - i-j _{\min})}}{(r - \frac{1}{r})(r^{n+1} - r^{-(n+1)})},$ <p>for all $0 \leq i, j \leq 2n+1$, where $i-j _{\min} = \min\{ i-j , 2n+2 - i-j \}$.</p>	[10, 39]
Möbius ladder		$G(i, j) = \begin{cases} g_1(i-j _{\min}) + g_2(i-j _{\min}), & i-j \leq \frac{n+1}{2} + 1 \\ g_1(i-j _{\min}) - g_2(i-j _{\min}), & i-j > \frac{n+1}{2} \end{cases}$ <p>for all $0 \leq i, j \leq 2n+1$, where $i-j _{\min} = \min\{ i-j , 2n+2 - i-j , i-j - (n+1) \}$,</p> $g_k(s) = \frac{\left(a_k r_k^{\frac{n+1}{2}} - \frac{r_k^{-\frac{n+1}{2}}}{a_k}\right) \left(a_k r_k^{\frac{n+1}{2} - s} - \frac{r_k^{-[\frac{n+1}{2} - s]}}{a_k}\right)}{(r_k - r_k^{-1})(a_k^2 r_k^{n+1} - a_k^{-2} r_k^{-(n+1)})},$ <p>$k \in \{1, 2\}$, r_k satisfies $r_k + 1/r_k = 2k + \alpha_0$, $a_1 = \left[1 + \frac{r_1^2 - 1}{r_1(1 + \frac{\alpha_0}{2} - r_1)}\right]^{\frac{1}{2}}$, $a_2 = 1$.</p>	Section 3.7

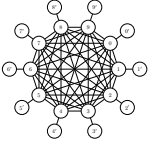
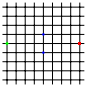
Complete graph		$G(x, y) = \begin{cases} \frac{\sigma}{(\sigma-1)(\sigma-1+d)} & \text{if } x = y \in V, \\ \frac{1}{(\sigma-1)(\sigma-1+d)} & \text{if } x \neq y, x, y \in V, \\ \frac{\gamma^2 \sigma}{(\sigma-1)(\sigma-1+d)} + \gamma & \text{if } x = y \in \delta V, \end{cases}$ <p>where $\gamma = 1/(1+t)$ and $\sigma = 2 + \alpha_0 - \gamma$.</p>	Section 3.7
Infinite plane		$G((m_1, n_1), (m_2, n_2)) = \frac{1}{2\pi} \int_0^\pi \frac{\cos(d_- v) (\cos(v))^{d_+}}{(a + \sqrt{a^2 - \cos(v)})^{d_+} \sqrt{a^2 - \cos(v)}} dv$ <p>where $a = 1 + \alpha_0/4$, and $d_\pm = m_2 - m_1 \pm n_2 - n_1$.</p>	Section 3.7

Table 3.1: Summary of Green's function results

3.4 Representation theory and the background Green's function

In the previous section we obtained the background Green's function for a variety of examples by solving corresponding recurrence relations. In every example, excluding the finite path, clearly-visible symmetries were employed in an intuitive way to reduce the problem to a more tractable set of equations. This connection between symmetry and PDE analogues on graphs can be formalized using the language of representation theory.

3.4.1 Cayley graphs of finite abelian groups

As a particularly important special case we first consider Cayley graphs of abelian groups. In particular, let G be a finite abelian group and S be a symmetric subset of the elements of G . Recall that S is a symmetric subset of a group G if $g \in S$ implies $g^{-1} \in S$. This condition is required to ensure that the resulting graph is undirected and the associated Laplacian operator is symmetric. We can then define the Cayley graph $X(G, S)$ to be the graph whose vertices are indexed by the elements of G with edge set [75]

$$(3.10) \quad E = \{(g, h) \in G \times G \mid gh^{-1} \in S\}.$$

Looking at the examples considered in the previous section we note that the loop, Möbius ladder, and complete graph are all Cayley graphs with group $G = \mathbb{Z}/n\mathbb{Z}$, for some n , and $S = \{-1, 1\}$, $\{-1, 1, -n/2, n/2\}$ and $\{-n+1, -n+2, \dots, -1, 1, \dots, n-2, n-1\}$, respectively. The infinite path is the Cayley graph of the free group on

2 generators and the Bethe lattice with coordination number k is the Cayley graph of the free group on k generators. Finally, the two-dimensional lattice is the Cayley graph with group $\mathbb{Z} \times \mathbb{Z}$ and generator set $S = \{(-1, 0), (0, -1), (1, 0), (0, 1)\}$.

For Cayley graphs the combinatorial Laplacian can be compactly expressed using the convolution operator $*$: $\ell^2(G) \times \ell^2(G) \rightarrow \ell^2(G)$ defined by

$$(3.11) \quad (f * g)(x) = \sum_{y \in G} f(y) g(y^{-1}x).$$

It is clear that the adjacency matrix A for $X(G, S)$ is given by [75]

$$(3.12) \quad A(f)(x) = (\delta_S * f)(x)$$

where δ_S is the characteristic function on the set S and hence if $k = |S|$ then

$$(3.13) \quad L(f)(x) = (kI - A)(f)(x) = kf(x) - (\delta_S * f)(x).$$

In order to diagonalize this operator using Fourier analysis, we next define the *dual group*

$$(3.14) \quad \hat{G} = \text{Hom}(G, \mathbb{T})$$

where \mathbb{T} is the multiplicative group of complex numbers with modulus one. If $\chi \in \hat{G}$ then we call χ a *character*. If G is a finite abelian group then it is self-dual [70], and hence G is isomorphic to \hat{G} . We then have the following proposition, proved in [75].

Proposition III.3. *If $h \in \ell^2(G)$ then the eigenvectors of the corresponding convolution operator are equal to the characters of G . In particular, if $\chi \in \hat{G}$ then*

$$(3.15) \quad (h * \chi)(x) = \hat{h}(\chi) \chi(x)$$

for all $x \in G$ and where $\hat{h}(\chi) = \sum_{x \in G} h(x) \overline{\chi(x)}$.

The following corollaries are immediate consequences of Proposition III.3.

Corollary III.4. *The characters of G are the eigenvectors of L with corresponding eigenvalues*

$$(3.16) \quad \lambda_\chi = k - \sum_{s \in S} \overline{\chi(s)}.$$

Corollary III.5. *The Green's function for the uniform diffusion equation is*

$$(3.17) \quad G(f)(x) = \sum_{\chi \in \hat{G}} \sum_{y \in G} \frac{1}{\lambda_\chi + \alpha_0} f(y) \overline{\chi(y)} \chi(x).$$

Proof. We begin by observing that since the eigenfunctions of L are the characters of G through an appropriate change of basis we may diagonalize L . If we denote the elements of G by x_1, \dots, x_k and the characters of G by χ_1, \dots, χ_k then we can form the corresponding $k \times k$ matrix defined by

$$(3.18) \quad X_{i,j} = \chi_j(x_i).$$

It follows from the above results that the matrix representation of L can be written as

$$(3.19) \quad L = X \begin{pmatrix} \lambda_{\chi_1} & & & & & \\ & \lambda_{\chi_2} & & & & \\ & & \ddots & & & \\ & & & \lambda_{\chi_{k-1}} & & \\ & & & & \lambda_{\chi_k} & \end{pmatrix} X^\dagger,$$

where X^\dagger denotes the conjugate transpose of the matrix X . Since $XX^\dagger = I$, the $k \times k$ identity matrix, it follows that

$$(3.20) \quad \begin{aligned} H_0 &= L + \alpha_0 I \\ &= X \begin{pmatrix} \lambda_{\chi_1} + \alpha_0 & & & & & \\ & \lambda_{\chi_2} + \alpha_0 & & & & \\ & & \ddots & & & \\ & & & \lambda_{\chi_{k-1}} + \alpha_0 & & \\ & & & & \lambda_{\chi_k} + \alpha_0 & \\ & & & & & \lambda_{\chi_k} + \alpha_0 \end{pmatrix} X^\dagger, \end{aligned}$$

from which the formula (3.17) follows immediately, using the fact that $G = H_0^{-1}$. \square

3.4.2 Cayley graphs of finite groups

The results of the previous section can be extended to non-abelian groups in a natural way. As before, we use the fact that the operator H_0 can be written as a convolution operator on $\ell^2(G)$ to find a spectral decomposition of its Fourier transform. Applying the inverse Fourier transform yields a complete set of eigenvectors and eigenvalues of H_0 from which it is straightforward to obtain an expression for the background Green's function G_0 of the corresponding Cayley graph.

Before presenting the main results we first introduce some basic definitions and results associated with Fourier analysis on finite non-abelian groups (for a more complete description see [75], for example). As in [70], let ρ be a homomorphism from the group G to the automorphism group of V , a k -dimensional vector space over \mathbb{C} . Such a map ρ is called a *k-dimensional representation* of G and is said to be *irreducible*

if the only subspaces of V which are invariant under $\rho(g)$ for all $g \in G$ are $\mathbf{0}$ and V . We say that two representations $\rho : G \rightarrow \text{GL}(V)$ and $\tau : G \rightarrow \text{GL}(W)$ are *equivalent* [70] if there exists an isomorphism $f : V \rightarrow W$ such that $\tau(g) = f \circ \rho(g) \circ f^{-1}$.

Given a representation $\rho : G \rightarrow \text{GL}(V)$ of G , let $d_\rho = \dim(V)$ denote its degree. If $f \in \ell^1(G)$ then its *Fourier transform* is the map $\mathcal{F}[f] : \rho \rightarrow \mathbb{C}^{d_\rho} \times \mathbb{C}^{d_\rho}$ defined by [75]

$$(3.21) \quad \mathcal{F}[f](\rho) = \sum_{g \in G} f(g)\rho(g).$$

Observe that the Fourier transform of a function f at a representation ρ will, in general, be matrix-valued and is called the *Fourier coefficient* matrix of f at ρ . If two representations ρ_1 and ρ_2 are equivalent then it is straightforward to show that the corresponding Fourier coefficient matrices are similar and hence the Fourier transform of f is completely determined by its value on a maximal set of inequivalent irreducible representations, called the *dual* and denoted by \hat{G} . Note that if G is abelian then its irreducible representations must be of degree one and this definition of \hat{G} is equivalent to the one given in (3.14).

Given a function $h : \rho \in \hat{G} \rightarrow \mathbb{C}^{d_\rho} \times \mathbb{C}^{d_\rho}$ we can define its inverse Fourier transform by the following expression [75]

$$(3.22) \quad \check{h} = \mathcal{F}^{-1}[h](g) = \frac{1}{|G|} \sum_{\rho \in \hat{G}} d_\rho \text{Tr}(\rho(g^{-1})h(\rho)).$$

The proof that $\mathcal{F}^{-1}\mathcal{F}$ is the identity operator on $\ell^2(G)$ and is independent of the choice of the elements in \hat{G} , provided they form a maximal set of irreducible inequivalent representations can be found in [75].

From the definitions given above it is straightforward to prove the following result [75] which will be useful in decomposing the operator H_0 .

Proposition III.6. *Consider the convolution operator $*$: $\ell^1(G) \times \ell^1(G) \rightarrow \ell^1(G)$ defined by*

$$(3.23) \quad f * h(g) = \sum_{r \in G} f(r^{-1})h(rg).$$

If $\hat{f} = \mathcal{F}[f]$ and $\hat{h} = \mathcal{F}[h]$ then

$$(3.24) \quad \mathcal{F}[f * h](\rho) = \hat{f}(\rho)\hat{h}(\rho).$$

We can now employ the theory developed above to analyze the spectrum of the Cayley graph $X(G, S)$ with vertices once again indexed by the elements of G and edge generating set S . We begin by observing that the adjacency operator A for $X(G, S)$ can be written as

$$(3.25) \quad A[f](g) = \chi_S * f(g), \quad \forall g \in G$$

where χ_S is the characteristic function of S . It follows immediately that if $e \in G$ is the identity element then

$$(3.26) \quad H_0[f](g) = ((|S| + \alpha_0)\chi_e - \chi_S) * f(g)$$

and thus from Proposition III.6 that

$$(3.27) \quad \hat{H}_0[\hat{f}](\rho) = (|S| + \alpha_0)\hat{f}(\rho) - \sum_{g \in S} \rho(g)\hat{f}(\rho).$$

The problem then becomes to diagonalize the operator \hat{H}_0 in Fourier space by finding suitable eigenfunctions of (3.27). Using the properties of the Fourier transform outlined above we can then find the corresponding eigenfunctions of H_0 in $\ell^2(G)$.

For ease of exposition, let $M(\rho) = \sum_{g \in S} \rho(g)$ in which case we have the following useful lemma.

Lemma III.7. *If $M(\rho) = \sum_{g \in S} \rho(g)$ where ρ is a representation of a finite group, G , then $M(\rho)$ is diagonalizable.*

Proof. We begin by noting that since G is finite, ρ is equivalent to a representation ρ' such that $\rho'(g)$ is unitary for all $g \in G$. In particular, there exists a $d_\rho \times d_\rho$ matrix B such that

$$(3.28) \quad M(\rho) = B M(\rho') B^{-1}.$$

Since $\rho'(g)$ is unitary observe that $\rho'(g^{-1}) = \rho'(g)^{-1} = \rho'(g)^*$, where $*$ once again denotes the adjoint of a matrix. Furthermore, we note that since S is symmetric, if $g \in S$ then $g^{-1} \in S$ so that

$$(3.29) \quad M(\rho') = \frac{1}{2} \sum_{g \in S} [\rho'(g) + \rho'(g^{-1})].$$

It follows immediately that

$$\begin{aligned}
(3.30) \quad M(\rho')^* &= \left[\sum_{g \in S} \rho'(g) \right]^* \\
&= \frac{1}{2} \sum_{g \in S} [\rho'(g) + \rho'(g^{-1})]^* \\
&= \frac{1}{2} \sum_{g \in S} [\rho'(g) + \rho'(g)^*]^* \\
&= M(\rho'),
\end{aligned}$$

and so $M(\rho')$ is Hermitian. Since $M(\rho)$ is similar to $M(\rho')$ it follows that it too is diagonalizable. \square

Fixing a maximal set of inequivalent irreducible representations $\hat{G} = \{\rho_1, \dots, \rho_L\}$, let v_j^i be the j th eigenvector of $M(\rho_i)$ with eigenvalue ν_j^i . Furthermore, let H_{jk}^i be the $d_{\rho_i} \times d_{\rho_i}$ zero matrix with the k th column replaced by v_j^i . We then define the function $f_{jk}^i : \rho \in \hat{G} \rightarrow \mathbb{C}^{d_\rho} \times \mathbb{C}^{d_\rho}$ by

$$(3.31) \quad f_{jk}^i(\rho) = \delta_{\rho_i}(\rho) H_{jk}^i$$

where $\delta_{\rho_i}(\rho)$ is 1 if $\rho = \rho_i$ and zero otherwise. We remark that the function f has only been defined on the set of representations \hat{G} though it has a natural, and unique, extension, \tilde{f} , to all representations of G by requiring the following two conditions hold:

- i) if ρ and ρ' are equivalent representations such that $\rho = B \rho'(g) B^{-1}$ for all $g \in G$ then $\tilde{f}_{jk}^i(\rho) = B^{-1} f_{jk}^i(\rho') B$, and
- ii) if $\rho = \rho_1 \oplus \rho_2$ then $\tilde{f}_{jk}^i(\rho) = f_{jk}^i(\rho_1) \oplus f_{jk}^i(\rho_2)$.

The following proposition is an immediate consequence of the previous definitions.

Proposition III.8. *The function $f_{jk}^i(\rho)$ defined in (3.31) is an eigenfunction of the operator \hat{H}_0 with corresponding eigenvalue*

$$(3.32) \quad \lambda_{jk}^i = |S| + \alpha_0 - \nu_j^i.$$

for all $i = 1, \dots, L$ and $1 \leq j, k \leq d_{\rho_i}$.

Notice that Proposition III.8 tells us that given the irreducible representations of G we can reduce the problem of finding the eigenfunctions and eigenvalues of the operator \hat{H}_0 to that of finding the eigenvectors and eigenvalues of the matrices $\{M(\rho_i)\}_{i=1}^L$. To find the corresponding eigenfunctions of the operator H_0 we observe that

$$(3.33) \quad H_0[f](g) = \mathcal{F}^{-1} [H_0 \mathcal{F}[f]](g)$$

from which it follows that H_0 has eigenfunctions $u_{jk}^i = \mathcal{F}^{-1} f_{jk}^i$ with eigenvalues λ_{jk}^i . Proceeding in this way will generate $\sum_{\rho \in \hat{G}} d_\rho^2$ distinct eigenfunctions of H_0 . However, we know that [70]

$$(3.34) \quad n = |G| = \sum_{\rho \in \hat{G}} d_\rho^2,$$

and so the above procedure will produce a complete set of eigenfunctions for the operator H_0 . Since H_0 is Hermitian we can use Gram-Schmidt orthogonalization to produce a complete orthonormal set of eigenvectors ϕ_{jk}^i , with eigenvalues once again

given by λ_{jk}^i , from which it follows that

$$(3.35) \quad G_0 = \sum_{i=1}^L \sum_{1 \leq j, k \leq d_{\rho_i}} \frac{1}{\lambda_{jk}^i} \phi_{jk}^i \phi_{jk}^{i*}.$$

As an illustration of this procedure we now consider the background Green's function for the permutohedron of order 4, shown in Figure 3.1, though the following analysis generalizes to permutohedra of arbitrary order.

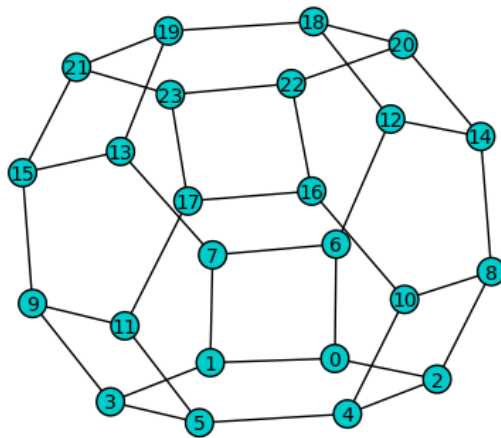


Figure 3.1: The permutahedron of order 4.

We begin by noting that the permutohedron of order n is isomorphic to the Cayley graph $X(S_n, S)$, where S_n is the symmetric group on n letters and S is the symmetric set of generators consisting of all transpositions which interchange neighbouring elements [4]. For each irreducible representation ρ of S_n we can construct the matrix $M(\rho)$, given by

$$(3.36) \quad M(\rho) = \sum_{g \in S} \rho(g).$$

Next, for each non-equivalent irreducible representation ρ , we diagonalize the matrix $M(\rho)$ and form the eigenvectors of \hat{H}_0 using (3.31). Taking the inverse Fourier transform of each of these eigenvectors yields eigenvectors of the original operator H_0 , with corresponding eigenvalues (3.32). After normalizing the eigenvectors we construct the background Green's function using (3.35). The matrix given by this procedure, plotted in Figure 3.2, agrees to within machine precision with the inverse of H_0 calculated numerically.

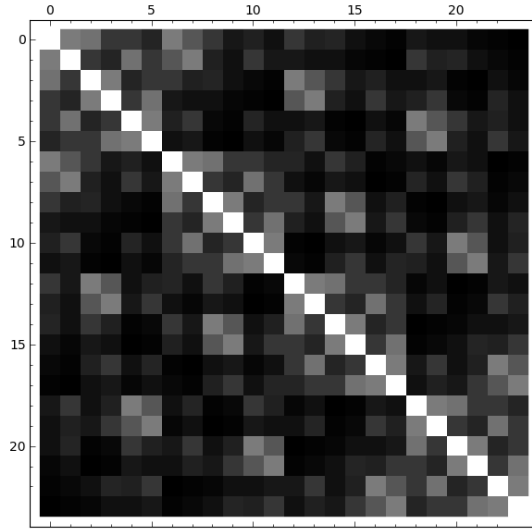


Figure 3.2: The background Green's function for the permutohedron of order 4, with $\alpha_0 = 0.1$.

3.5 Numerical experiments

In this section we demonstrate the use of the Born series for two illustrative examples to approximate Green's functions when the absorption is a small perturbation of a constant background value α_0 , comparing the convergence we observe with the bounds obtained in Section 3.2.

3.5.1 Inhomogeneous absorption on a path

Using the background Green's function for the path given in Table 3.1, we can solve the diffusion equation (2.19) on a path provided the absorption coefficients $\eta(x)$ are sufficiently small. Let $u_N = B_N \tilde{f}$ where \tilde{f} is the source vector and B_N is the truncated Born series matrix operator. Figure 3.4 gives the numerical results obtained when using the particular η given in Figure 3.3 with a unit source located at the left boundary vertex and $t = 1/2$. As predicted the error decays exponentially as $N \rightarrow \infty$ if η_{\max} is less than a cut-off value, which is approximately 1.15. The comparison between the empirically determined cut-off for η_{\max} and the upper bounds given by Section 3.2.2 is summarized in Table 3.2.

Bound	Cut-off η_{\max}
Numerical Experiment	1.15
Theorem III.1	0.8333
Proposition III.2	1.14655

Table 3.2: Comparison of theoretical bounds and experimental results for the maximum possible value of η_{\max} for which the Neumann series converges.

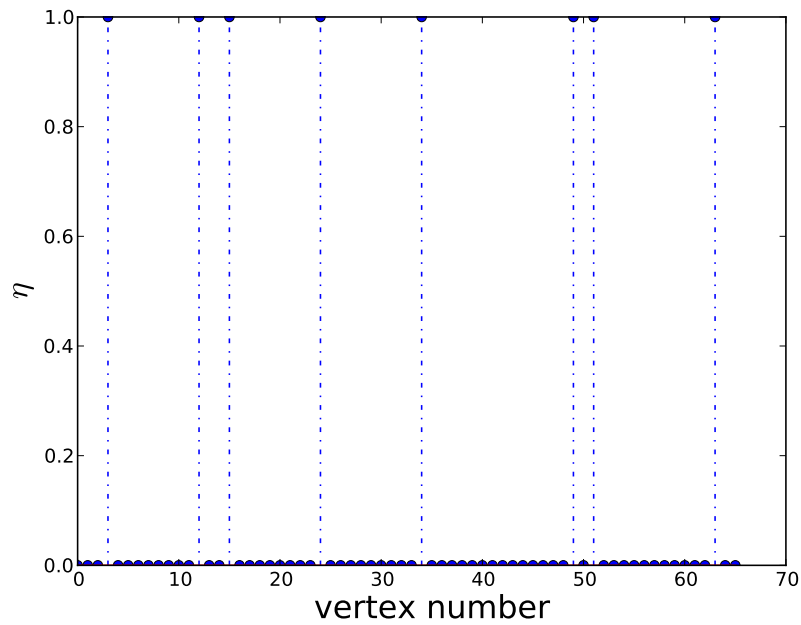


Figure 3.3: The absorption vector η used for the example of constructing a Green's function for the heterogeneous diffusion equation (2.6) via Born series. The support of η is chosen to be a random subset of the interior vertices of size $(2n + 2)/4$.

3.5.2 Inhomogeneous absorption on a complete graph with boundary

As a second example, using the background Green's function for the complete graph obtained in Appendix A, and listed in Table 3.1, we can once again solve the time-independent diffusion problem (2.19) for sufficiently small perturbations. In particular, choosing η to be that given in Figure 3.5, the associated errors for various values of η_{\max} are given in Figure 3.6.

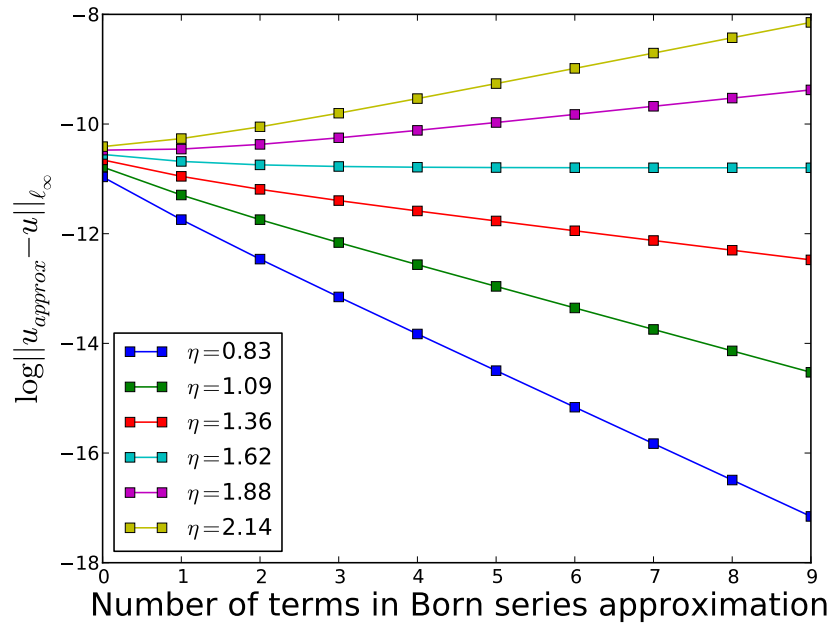


Figure 3.4: Plots of the ℓ_∞ error of the truncated solution u_N . The green and red curves correspond to the bound on η_{\max} from Theorem III.1 and Proposition III.2, respectively. The other blue lines correspond to η_{\max} spaced 0.026 apart.

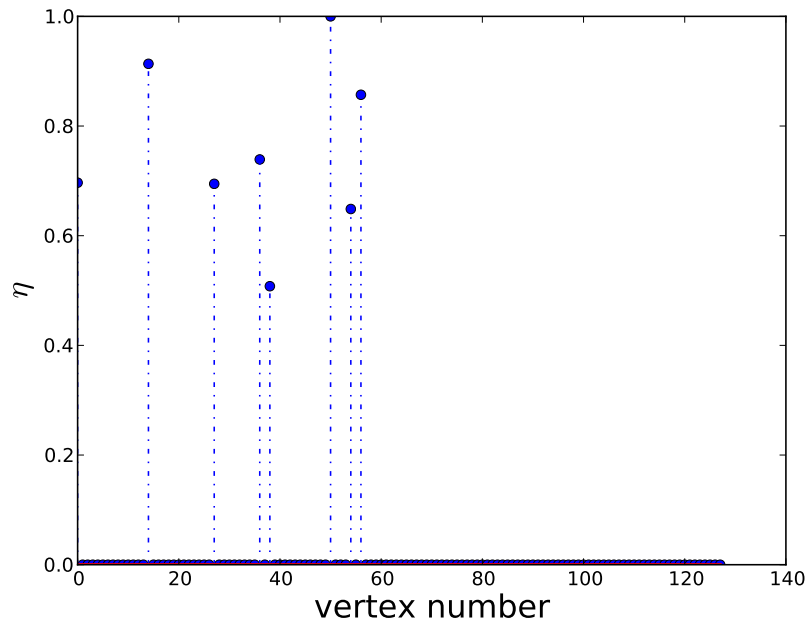


Figure 3.5: A typical absorption vector η used for the example of constructing a Green's function for the spatially-varying time-independent diffusion equation (2.6) via Born series. The support of η is once again chosen to be a random sample of the interior vertices of size $d/4$.

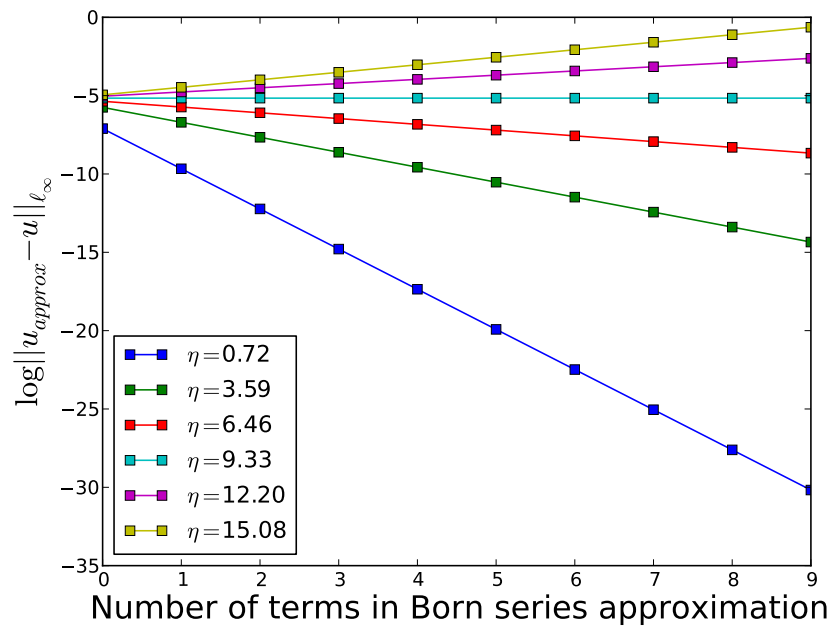


Figure 3.6: Plots of the ℓ_∞ error of the truncated solution u_N . The green and red curves correspond to the bound on η_{\max} from Theorem III.1 and Proposition III.2, respectively.

3.6 Point Absorbers

In scattering theory a classic problem is to consider a medium which is entirely homogeneous except for a few small inhomogeneities referred to as point absorbers [41]. For convenience we typically assume that the inhomogeneities are sufficiently far apart relative to their diameters, so that each can be thought of as being supported on a single point.

3.6.1 A single point absorber

As above let $\Gamma = (V', E)$ be a graph, let $V \subset V'$ and let δV be defined as in (2.1). If a single point absorber is present then $\eta : (V \cup \delta V) \rightarrow \mathbb{R}$ is of the form

$$(3.37) \quad \eta(x) = \kappa \delta_y,$$

where $y \in V$ is the location of the point absorber and κ is a positive constant. For potentials of this form, we have the following theorem.

Theorem III.9. *Let G_0 be the background Green's function for the diffusion equation (2.6). If the potential, η , is due to a single point absorber located at the vertex labelled by y , then the Green's function, G , for (2.19) satisfies*

$$(3.38) \quad G_0 - G = \frac{\alpha_0 \kappa}{1 + \alpha_0 \kappa G_0(y, y)} G_0(\cdot, y) G_0(\cdot, y)^*.$$

Proof. Let G denote the Green's function for the diffusion equation (2.19). By definition, we see that

$$(3.39) \quad G = H^{-1} = [H_0 + \alpha_0 \kappa e_y e_y^T]^{-1},$$

and hence that H is a rank one perturbation of the operator H_0 . The Sherman-Morrison formula, see [19] for example, then yields

$$(3.40) \quad (G_0 - G)(i, j) = \frac{\alpha_0 G_0^*(j, y) G_0(i, y)}{1 + \alpha_0 \kappa G_0(y, y)},$$

which completes the proof. \square

For example, consider the infinite path whose background Green's function can be obtained by taking the limit as n goes to infinity of the Green's function for the finite path given in Table 3.1. If the point absorber is located at the vertex k then equation (3.38) yields

$$(3.41) \quad (G_0 - G)(i, j) = \frac{\alpha_0 \kappa}{1 + \frac{\alpha_0 \kappa}{r-r^{-1}}} e^{-\log(r)(|i-k|+|j-k|)}.$$

Note that unlike the continuous case [41], no renormalization is required to obtain equation (3.41). This is an immediate consequence of the fact that in the discrete setting the operator G_0 is bounded for all i and j , whereas for the continuous problem G_0 is a singular integral operator. Physically, renormalization corresponds to giving each point absorber a non-zero size which we assume is small relative to the wavelength of the incident field. For the infinite path, since the system is discrete, the point absorbers automatically have a non-zero width and so no additional length scales need to be introduced.

As a second example, we consider the complete graph with boundary. For convenience we assume that the absorber is located in the interior of the graph and that the source and detector are located on the boundary of V . Using the Green's function

given in equation (3.72) with the formula (3.38) we obtain

$$(3.42) \quad (G_0 - G)(i, j) = \frac{\alpha_0 \kappa}{1 + \frac{\alpha_0 \kappa \sigma}{(\sigma-1)(\sigma-1+d)}} \frac{\gamma^2 \sigma^2}{(\sigma-1)^2 (\sigma-1+d)^2},$$

where $i, j \in \delta V$, $\gamma = 1/(1+t)$ and $\sigma = 2 + \alpha_0 - \gamma$.

3.6.2 Multiple point absorbers

We now consider the case where there are m identical point scatterers.

Theorem III.10. *Let G_0 be the background Green's function for the diffusion equation (2.6). Further suppose that the potential, η , consists of m identical point absorbers of strength κ , located at the vertices $\Lambda = \{x_{k_1}, \dots, x_{k_m}\} \subset V$. Let I_Λ be the $(|V| + |\delta V|) \times m$ submatrix of the identity obtained by taking the columns of I indexed by Λ . The Green's function, G , for (2.19) satisfies*

$$(3.43) \quad G_0 - G = \alpha_0 \kappa G_0 I_\Lambda [I + \alpha_0 \kappa I_\Lambda^T G_0 I_\Lambda]^{-1} I_\Lambda^T G_0.$$

Proof. We begin by observing that by definition, G satisfies

$$(3.44) \quad H_0 G = I - \alpha_0 D_\eta G.$$

Using our definition of I_Λ , we can rewrite this as

$$(3.45) \quad H_0 G = I - \alpha_0 \kappa I_\Lambda I_\Lambda^T G.$$

Similarly, we observe that

$$(3.46) \quad G = G_0 - \alpha_0 \kappa G I_\Lambda I_\Lambda^T G_0,$$

from which it follows that

$$(3.47) \quad H_0 G = I - \alpha_0 \kappa I_\Lambda I_\Lambda^T [G_0 - \alpha_0 \kappa G I_\Lambda I_\Lambda^T G_0],$$

where we have used the fact that

$$(3.48) \quad H_0 G_0 = I.$$

Thus

$$(3.49) \quad (G_0 - G) = \alpha_0 \kappa [G_0 (I_\Lambda I_\Lambda^T) G_0 - \alpha_0 \kappa G_0 I_\Lambda (I_\Lambda^T G I_\Lambda) I_\Lambda^T G_0],$$

and hence

$$(3.50) \quad G_0 - G = \alpha_0 \kappa (G_0 I_\Lambda) [I_\Lambda^T I_\Lambda - \alpha_0 \kappa (I_\Lambda^T G I_\Lambda)] (I_\Lambda^T G_0).$$

To find $I_\Lambda^T G I_\Lambda$ we left multiply (3.46) by I_Λ^T and right multiply by I_Λ to obtain

$$(3.51) \quad G' = G'_0 - \alpha_0 \kappa G' G'_0,$$

where $G'_0 = I_\Lambda^T G_0 I_\Lambda$ and $G' = I_\Lambda^T G I_\Lambda$. It follows that

$$(3.52) \quad G' = G'_0 [I_\Lambda^T I_\Lambda + \alpha_0 \kappa G'_0]^{-1}.$$

Note that the inverse of the matrix in (3.52) exists since the smallest eigenvalue of G'_0 must be greater than the smallest eigenvalue of G_0 , which is positive definite.

Since $I_\Lambda^T I_\Lambda$ is the $m \times m$ identity matrix it follows that $I_\Lambda^T I_\Lambda + \alpha_0 \kappa G'_0$ has positive eigenvalues and is therefore invertible.

Finally, observe that

$$(3.53) \quad I_\Lambda^T I_\Lambda - \alpha_0 \kappa G'_0 [I_\Lambda^T I_\Lambda + \alpha_0 \kappa G'_0]^{-1} = [I_\Lambda^T I_\Lambda + \alpha_0 \kappa G'_0]^{-1},$$

from which it follows that

$$(3.54) \quad G_0 - G = \alpha_0 \kappa (G_0 I_\Lambda) [I_\Lambda^T I_\Lambda + \alpha_0 \kappa I_\Lambda^T G_0 I_\Lambda]^{-1} (I_\Lambda^T G_0),$$

which completes the proof. Alternatively we could iterate the Sherman-Morrison formula, or follow the approach of [19]. \square

As an example, we once again consider the infinite path and suppose there are two point absorbers located at the vertices corresponding to k_1 and k_2 . Here

$$(3.55) \quad G'_0 = \frac{1}{2 \sinh \log r} \begin{pmatrix} 1 & e^{-\log(r)|k_2 - k_1|} \\ e^{-\log(r)|k_2 - k_1|} & 1 \end{pmatrix}.$$

If $f_{i,j} = e^{-\log(r)|i-j|}/2 \sinh \log r$ and $s = \sinh(\log(r))$ a straightforward calculation yields

$$(3.56) \quad e_j^* (G_0 - G) e_i = \frac{1}{2} \begin{pmatrix} f_{j,k_1} + f_{j,k_2} & f_{j,k_1} - f_{j,k_2} \end{pmatrix} \begin{pmatrix} \frac{\alpha_0 \kappa}{1 + \alpha_0 \kappa (s^{-1} + f_{k_1, k_2})} & 0 \\ 0 & \frac{\alpha_0 \kappa}{1 + \alpha_0 \kappa (s^{-1} - f_{k_1, k_2})} \end{pmatrix} \\ \times \begin{pmatrix} f_{i,k_1} + f_{i,k_2} \\ f_{i,k_1} - f_{i,k_2} \end{pmatrix}.$$

Observe that in the limit as $|k_1 - k_2| \rightarrow \infty$, $f_{k_1, k_2} = o(1)$ and hence equation (3.56)

becomes

(3.57)

$$\begin{aligned}
e_j^*(G_0 - G)e_i &\approx \frac{\alpha_0\kappa}{2(1 + \alpha_0\kappa s^{-1})} \begin{pmatrix} f_{j,k_1} + f_{j,k_2} & f_{j,k_1} - f_{j,k_2} \end{pmatrix} \begin{pmatrix} f_{i,k_1} + f_{i,k_2} \\ f_{i,k_1} - f_{i,k_2} \end{pmatrix} \\
&= \frac{\alpha_0\kappa}{2(1 + \alpha_0\kappa s^{-1})} [f_{i,k_1}f_{j,k_1} + f_{i,k_2}f_{j,k_2}] \\
&= G_1(i, j; k_1) + G_1(i, j; k_2)
\end{aligned}$$

where $G_1(i, j; k)$ is the Green's function for one point absorber located at the point k . Thus as the separation of the two point absorbers increases, the Green's function tends toward the sum of the Green's functions for two non-interacting point absorbers. Sample plots are shown in Figure 3.7 for the infinite path with two point absorbers equidistant from a point source located at the origin. Here u_0 represents the solution to the homogeneous problem and u denotes the solution to the full time-independent diffusion equation.

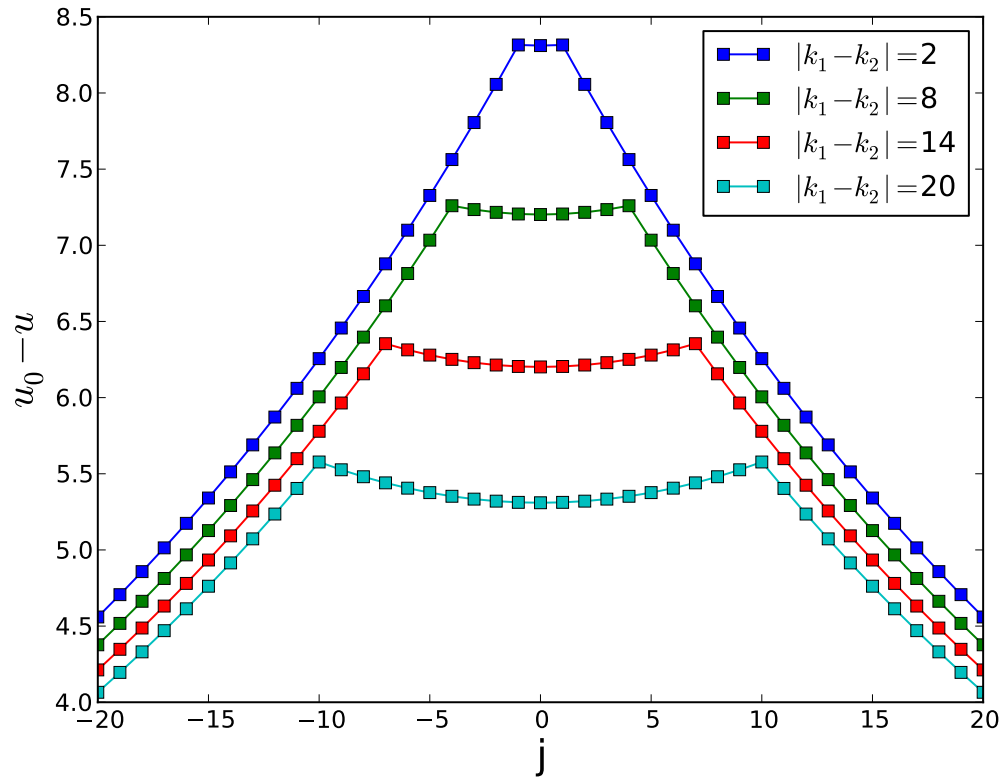


Figure 3.7: Plots of $u_0 - u$ for the infinite path with two identical point scatterers equidistant from a point source located at the origin with $\alpha_0 = 0.001$ and $\kappa = 100$.

As a second example we consider the scattering from two point absorbers on the infinite two-dimensional lattice. An analysis of the scattering properties of this system requires an expression for the Green's function of the diffusion equation (2.6) on $\mathbb{Z} \times \mathbb{Z}$, an integral formula for which was found in Proposition III.13 of Appendix A. For simplicity we specialize to the case in which the two point absorbers are positioned on the y-axis and the source and detector are located on the x-axis as in Figure 3.8.

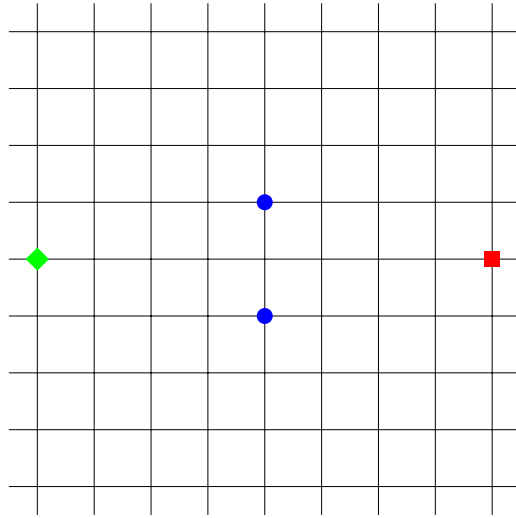


Figure 3.8: A diagrammatic representation of the geometry of the point absorbers (blue circles), source (green diamond) and detector (red square) used to study the scattering properties of the two point absorber system on the infinite square lattice.

If we assume the source is located at $(s, 0)$ the detector is at $(j, 0)$, and the point absorbers are located at $(0, k_1)$, and $(0, k_2)$, then an analogous calculation to the one

performed for the one-dimensional case yields

$$(3.58) \quad e_j^*(G_0 - G)e_s = \frac{1}{2} \begin{pmatrix} f_{j,k_1} + f_{j,k_2} & f_{j,k_1} - f_{j,k_2} \end{pmatrix} \begin{pmatrix} \frac{\alpha_0 \kappa}{1 + \alpha_0 \kappa \lambda_+} & 0 \\ 0 & \frac{\alpha_0 \kappa}{1 + \alpha_0 \kappa \lambda_-} \end{pmatrix} \\ \times \begin{pmatrix} f_{s,k_1} + f_{s,k_2} \\ f_{s,k_1} - f_{s,k_2} \end{pmatrix}.$$

where

$$(3.59) \quad \lambda_{\pm} = g(0, 0) \pm g(0, k_2 - k_1) \\ = \frac{1}{\pi a} K \left(\frac{1}{a^2} \right) \pm \frac{1}{2\pi} \int_0^{\pi} \frac{\cos[(k_2 - k_1)v] (\cos v)^{|k_2 - k_1|}}{(a + \sqrt{a^2 - \cos^2 v})^{|k_2 - k_1|} \sqrt{a^2 - \cos^2 v}} dv$$

and $f_{s,k} = g(|s|, |k|)$. Results for $-s = j = 1$ and $k_1 = -k_2$ are shown in Figure 3.9 for various values of the point absorber separation $|k_2 - k_1|$ with $\alpha_0 = 10^{-3}$ and $\kappa = 10^3$. Note that due to the nature of our expression for the isotropic Green's function we cannot evaluate equation (3.58) exactly and must make use of numerical integration both to evaluate $g(|s|, |k|)$ and to find values for the integrals in (3.59).

3.7 Computation of background Green's functions

3.7.1 Analysis of a Möbius ladder

Another family of vertex-transitive graphs of particular interest in material science [71, 62, 74] and computer science [44] are the Möbius ladders on $2n+2$ vertices. Using a similar approach as above we can compute the background Green's function for the diffusion equation on this family of graphs. For convenience we assume n is odd

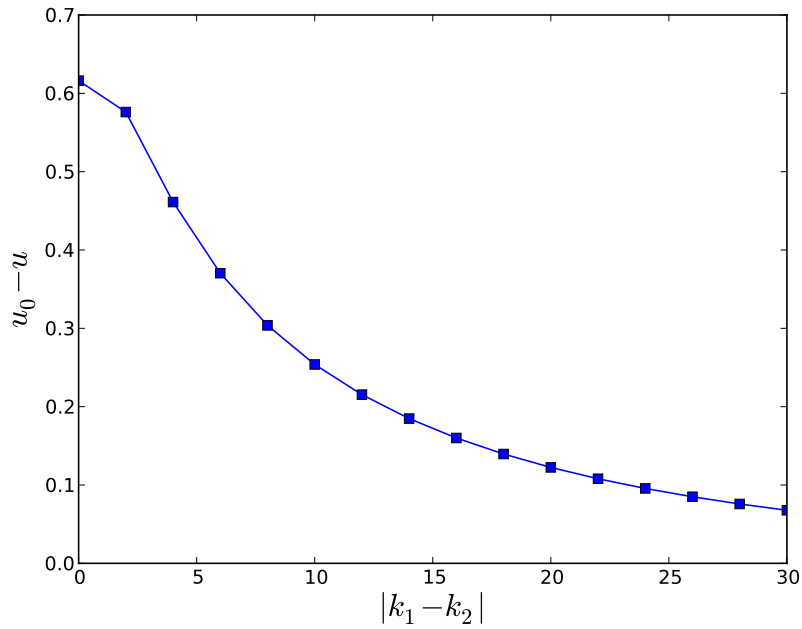


Figure 3.9: Plots of $u_0 - u$ for the infinite plane with two identical point scatterers equidistant from a point source located at $(-1, 0)$ and detector located at $(1, 0)$ with $\alpha_0 = 10^{-3}$ and $\kappa = 10^3$.

though a similar result can be obtained in the even case by a slight modification to the proof of the following theorem.

Theorem III.11. *Consider the Möbius ladder with $2n+2$ vertices $\{0, 1, \dots, 2n+1\}$, n odd, as shown in Figure 3.10. The associated Green's function for the diffusion equation with uniform absorption (2.6) is*

$$(3.60) \quad G(i, j) = \begin{cases} g_1(|i - j|_{\min}) + g_2(|i - j|_{\min}), & |i - j| \leq \frac{n+1}{2} + 1 \\ g_1(|i - j|_{\min}) - g_2(|i - j|_{\min}), & |i - j| > \frac{n+1}{2} \end{cases}$$

for all $0 \leq i, j \leq 2n+1$, where $|i-j|_{\min} = \min\{|i-j|, 2n+2-|i-j|, ||i-j| - (n+1)|\}$,

(3.61)

$$g_k(s) = \frac{(a_k r_k^{(n+1)/2} - a_k^{-1} r_k^{-(n+1)/2})(a_k r_k^{(n+1)/2-s} - a_k^{-1} r_k^{-[(n+1)/2-s]})}{(r_k - r_k^{-1})(a_k^2 r_k^{n+1} - a_k^{-2} r_k^{-(n+1)})}, \quad k = 1, 2,$$

r_k satisfies $r_k + 1/r_k = 2k + \alpha_0$,

$$(3.62) \quad a_1 = \left[1 + \frac{r_1^2 - 1}{r_1(1 + \frac{\alpha_0}{2} - r_1)} \right]^{\frac{1}{2}},$$

and $a_2 = 1$.

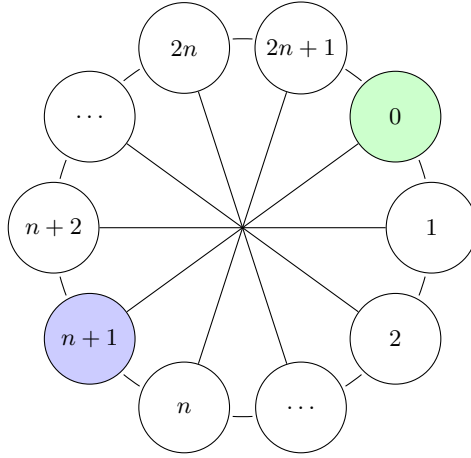


Figure 3.10: The Möbius ladder with $2n + 2$ vertices.

Proof. The result is proved in a manner similar to the method of images used in PDEs. We decompose the Green's function into two functions one of which is symmetric and the other antisymmetric with respect to reflection through the origin. Unlike in the case of method of images, however, the 'mirror charges' are located within the domain of interest and we rely on cancellations to recover the desired

solution. In considering the symmetries of the problem, it is clear that $G(i, j)$ must depend only on the number of vertices of the loop lying between the two vertices x_i and x_j , since the graph Σ is invariant under cyclic permutations of its vertices. Thus, without loss of generality, we can fix $j = 0$. Letting H_0 be the operator associated with the homogeneous time-independent diffusion equation (2.6) we now consider two related problems:

(A) find the vector $g_2 \in \mathbb{R}^{2n+2}$ such that $H_0 g_2 = \frac{1}{2}(e_0 - e_{n+1})$, where e_k is the k th canonical basis vector

(B) find the vector $g_1 \in \mathbb{R}^{2n+2}$ such that $H_0 g_1 = \frac{1}{2}(e_0 + e_{n+1})$.

In considering subproblem (A), we see by inspection that if g_2 is a solution then it must satisfy

$$(3.63) \quad g_2(i) = g_2(2n+2-i) = -g_2(n+1-i) = -g_2(n+1+i),$$

where once again for ease of notation we take all indices modulo $2n+2$. It follows immediately that

$$(3.64) \quad g_2((n+1)/2) = g_2(-(n+1)/2) = 0.$$

Moreover, applying H_0 we see that

$$(3.65) \quad \begin{aligned} \frac{1}{2}\delta_{0,i} &= (3 + \alpha_0)g_2(i) - g_2(i+n+1) - g_2(i+1) - g_2(i-1), \\ &= (4 + \alpha_0)g_2(i) - g_2(i+1) - g_2(i-1), \end{aligned}$$

for $-(n+1)/2 < i < (n+1)/2$. Hence $2g_2(i)$, $-(n+1)/2 < i < (n+1)/2$ satisfies the same equation as the Green's function for the centered path with source at $j = 0$,

α_0 replaced by $2 + \alpha_0$ and with Dirichlet boundary conditions at $i = \pm(n+1)/2$. A slight modification to the first example of Table 3.1 then yields

$$(3.66) \quad g_2(i) = \frac{(r^{(n+1)/2} - r^{-(n+1)/2})(r^{(n+1)/2-i} - r^{-(n+1)/2+i})}{2(r - r^{-1})(r^{n+1} - r^{-(n+1)})}$$

where $r + r^{-1} = 4 + \alpha_0$.

To solve subproblem (B), we begin by noting that

$$(3.67) \quad g_1(i) = g_1(2n+2-i) = g_1(n+1-i) = g_1(n+1+i),$$

for all $i = 0, \dots, 2n+1$ and where all indices are taken modulo $2n+2$. It follows that it is sufficient to find $g_1(i)$ for $i = -(n+1)/2, \dots, -2, -1, 0, 1, 2, \dots, (n+1)/2$. By symmetry we know that $g_1((n+1)/2 - 1) = g_1((n+1)/2 + 1)$ and $g_1(-(n+1)/2) = g_1((n+1)/2)$ so that

$$(3.68) \quad \begin{aligned} 0 &= (3 + \alpha_0)g_1((n+1)/2) - g_1(-(n+1)/2) - g_1((n+1)/2 - 1) - g_1((n+1)/2 + 1) \\ &= (2 + \alpha_0)g_1((n+1)/2) - 2g_1((n+1)/2 - 1). \end{aligned}$$

Similar reasoning applies to $g_1(-(n+1)/2)$ and hence

$$(3.69) \quad \left(1 + \frac{\alpha_0}{2}\right)g_1\left(\frac{n+1}{2}\right) - g_1\left(\frac{n+1}{2} - 1\right) = 0, \text{ and } \left(1 + \frac{\alpha_0}{2}\right)g_1\left(-\frac{n+1}{2}\right) - g_1\left(-\frac{n+1}{2} + 1\right) = 0.$$

For all i , $-(n+1)/2 < i < (n+1)/2$ we find from the above symmetries that

$$(3.70) \quad (2 + \alpha_0)g_1(i) - g_1(i-1) - g_1(i+1) = \frac{1}{2}\delta_{i,0}.$$

It follows immediately that the equations satisfied by $2g_1(i)$, $i = -(n+1)/2, \dots, (n+1)/2$ are identical to those defining the Green's function for the centered path with source at $j = 0$ and with Robin boundary conditions $t = \alpha_0/2$. Once again using a slight modification of the first line of Table 3.1, we find that if $r + 1/r = 2 + \alpha_0$, $t = \alpha_0/2$ and $a = \left[1 + \frac{r^2-1}{r(1+t-r)}\right]^{\frac{1}{2}}$ then

$$(3.71) \quad g_1(i) = \frac{(ar^{(n+1)/2} - a^{-1}r^{-(n+1)/2})(ar^{(n+1)/2-i} - a^{-1}r^{-(n+1)/2+i})}{2(r - r^{-1})(a^2r^{n+1} - a^{-2}r^{-(n+1)})}.$$

The remaining entries can then be found immediately by reflection.

□

3.7.2 Analysis of the complete graph on d vertices

We can perform a similar computation for the complete graph on d vertices, an example of which is shown in Figure 3.11 for $d = 10$.

Proposition III.12. *Let R be the complete graph on d vertices $\{0, 1, \dots, d - 1\}$ with d boundary vertices $\{0', \dots, (d - 1)'\}$. The associated Green's function for the diffusion equation (2.6) with Robin boundary conditions is*

$$(3.72) \quad G(x, y) = \begin{cases} \frac{\sigma}{(\sigma-1)(\sigma-1+d)} & \text{if } x = y \in V, \\ \frac{1}{(\sigma-1)(\sigma-1+d)} & \text{if } x \neq y, x, y \in V, \\ \frac{\gamma^2 \sigma}{(\sigma-1)(\sigma-1+d)} + \gamma & \text{if } x = y \in \delta V, \end{cases}$$

where $\gamma = 1/(1 + t)$ and $\sigma = 2 + \alpha_0 - \gamma$. The remaining entries can be obtained via the Robin boundary conditions and the identity

$$(3.73) \quad G(x, y) = G(y, x)$$

which holds for all $x, y \in V \cup \delta V$.

Proof. We first consider the case where the source is located at an interior vertex. By symmetry we may assume without loss of generality that $y = 0$. Note that upon fixing $y = 0$ the graph is invariant under a permutation of all remaining vertices, provided it preserves the edge between the vertex in R and the corresponding boundary point.

If $x \neq 0$ we observe that

$$(3.74) \quad [(d + \alpha_0)G(x, 0) - (d - 2)G(x, 0) - G(0, 0) - G(x', 0)] = 0.$$

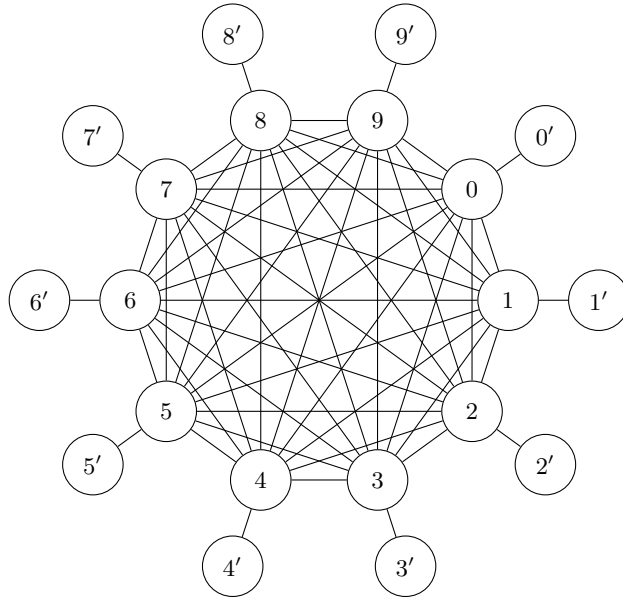


Figure 3.11: The complete graph on 10 vertices with 10 boundary vertices.

Using Robin boundary conditions we see that $G(x', 0) = G(x, 0)/(1 + t)$ and hence

$$(3.75) \quad G(0, 0) = [2 + \alpha_0 - \gamma] G(x, 0).$$

Let $g = G(x, 0)$ and $\sigma = [2 + \alpha_0 - \gamma]$ in which case we obtain

$$(3.76) \quad \begin{aligned} 1 &= [(d + \alpha_0)G(0, 0) - (d - 1)g - \gamma G(0, 0)] \\ &= [(d + \alpha_0)\sigma g - (d - 1)g - \gamma \sigma g] \\ &= g(\sigma - 1)(\sigma + d - 1) \end{aligned}$$

and thus

$$(3.77) \quad g = \frac{1}{(\sigma - 1)(\sigma + d - 1)}.$$

The remainder of the result follows immediately from noting that $G(0, 0) = \sigma g$ and by using the symmetries of the complete graph described above.

Now suppose the source is located on the boundary. Again, without loss of generality, we may assume that the source is located at the vertex $0'$. If $x \neq 0$ then

$$(3.78) \quad 0 = [(d + \alpha_0) G(x, 0') - (d - 2)G(x, 0') - G(0, 0') - G(x', 0)].$$

If $G(x, 0') = g$ then $G(0, 0') = (2 + \alpha_0 - \gamma)g = \sigma g$. If $x = 0$ then

$$(3.79) \quad 0 = [(d + \alpha_0)\sigma g - (d - 1)g - G(0', 0')].$$

The Robin boundary condition $tG(0', 0') + [G(0', 0') - G(0, 0')] = 1$ implies that

$$(3.80) \quad g = \gamma \frac{1}{(d + \alpha_0)\sigma - (d - 1) - \sigma\gamma} = \frac{\gamma}{(\sigma - 1)(\sigma + d - 1)}.$$

□

3.7.3 Analysis of a two-dimensional lattice

We conclude our catalogue of examples with a discussion of the Green's function for the two-dimensional lattice $\Sigma = \mathbb{Z} \times \mathbb{Z}$. For convenience, we index the vertices with ordered tuples $V = \{(m, n) \mid m, n \in \mathbb{Z}\}$ and hence if $x = (m_1, n_1)$ and $y = (m_2, n_2)$ are two vertices then $x \sim y$ if and only if $|m_2 - m_1| + |n_2 - n_1| = 1$. In the following proposition we obtain an integral representation of the Green's function for the isotropic time-independent diffusion equation on the infinite two-dimensional lattice by means of a discrete Fourier transform.

Proposition III.13. *Let Γ be the graph $\mathbb{Z} \times \mathbb{Z}$ with vertices labelled by $\{(m, n) \mid m, n \in \mathbb{Z}\}$. The Green's function for the corresponding homogeneous time-independent diffusion equation (2.6) is*

$$(3.81) \quad G((m_1, n_1), (m_2, n_2)) = \frac{1}{2\pi} \int_0^\pi \frac{\cos(d_- v) (\cos(v))^{d_+}}{(a + \sqrt{a^2 - \cos(v)})^{d_+} \sqrt{a^2 - \cos(v)}} dv$$

where $a = 1 + \alpha_0/4$, and $d_\pm = |m_2 - m_1| \pm |n_2 - n_1|$. In particular, if $(m_1, n_1) = (m_2, n_2)$ then

$$(3.82) \quad G((m, n), (m, n)) = \frac{1}{\pi a} K\left(\frac{1}{a^2}\right)$$

where K is the complete elliptic integral of the first kind defined by [1]

$$(3.83) \quad K(m) = \int_0^{\pi/2} \frac{1}{\sqrt{1 - m^2 \sin^2 \phi}} d\phi,$$

for $m^2 < 1$.

Proof. The approach for finding the Green's function is similar to that used for the Helmholtz equation [38, 61] and the Poisson equation [72] on lattices. We begin by noting that the problem is invariant under translations and reflections, from which it follows that G must only depend on the quantities $m = |m_2 - m_1|$ and $n = |n_2 - n_1|$. Hence

$$(3.84) \quad G((m_1, n_1), (m_2, n_2)) = G((m, n), (0, 0)) = g(m, n)$$

for some function $g(m, n) \in \ell^2(\mathbb{Z}^2)$. Applying the operator H_0 defined in (2.7), we see that $g(m, n)$ satisfies the difference equation

$$(3.85) \quad (4 + \alpha_0)g(m, n) - g(m-1, n) - g(m+1, n) - g(m, n-1) - g(m, n+1) = \delta_{m,0}\delta_{n,0}.$$

We next consider the discrete Fourier transform of (3.85). On $\mathbb{Z} \times \mathbb{Z}$ the Fourier transform $\mathcal{F} : \ell^1(\mathbb{Z} \times \mathbb{Z}) \rightarrow L^1((-\pi, \pi]^2)$ of a function f is given by

$$(3.86) \quad \hat{f}(\xi, \eta) = \mathcal{F}(f)(\xi, \eta) = \sum_{n, m \in \mathbb{Z}} e^{-i\xi m - i\eta n} f(m, n).$$

Thus, upon taking the Fourier transform of equation (3.85), we obtain

$$(3.87) \quad [(4 + \alpha_0) - e^{i\xi} - e^{-i\xi} - e^{i\eta} - e^{-i\eta}] \hat{g}(\xi, \eta) = 1,$$

where $\xi, \eta \in (-\pi, \pi]$. Using the identity

$$(3.88) \quad e^{i\xi} + e^{-i\xi} + e^{i\eta} + e^{-i\eta} = (e^{i(\xi+\eta)/2} + e^{-i(\xi+\eta)/2})(e^{i(\xi-\eta)/2} + e^{-i(\xi-\eta)/2})$$

yields

$$(3.89) \quad \hat{g}(\xi, \eta) = \frac{1}{4 \left[1 + \alpha_0/4 - \cos\left(\frac{\xi+\eta}{2}\right) \cos\left(\frac{\xi-\eta}{2}\right) \right]}.$$

Upon application of the inverse Fourier transform we find

$$(3.90) \quad g(m, n) = \frac{1}{(2\pi)^2} \int_{-\pi}^{\pi} \int_{-\pi}^{\pi} \frac{e^{im\xi + inn\eta}}{4 \left[1 + \alpha_0/4 - \cos\left(\frac{\xi+\eta}{2}\right) \cos\left(\frac{\xi-\eta}{2}\right) \right]} d\xi d\eta.$$

If we change variables, letting $u = (\xi + \eta)/2$ and $v = (\xi - \eta)/2$, we obtain

$$(3.91) \quad g(m, n) = \frac{1}{2(2\pi)^2} \int_{-\pi}^{\pi} e^{i(m-n)v} \int_{-\pi}^{\pi} e^{i(m+n)u} \frac{1}{1 + \frac{\alpha_0}{4} - \cos u \cos v} du dv.$$

If we let $a = 1 + \alpha_0/4$ and choose $z = e^{iu}$ we obtain

$$(3.92) \quad g(m, n) = \frac{1}{2(2\pi)^2 i} \int_{-\pi}^{\pi} e^{i(m-n)v} \oint_{C_1} \frac{z^{m+n}}{az - \frac{\cos v}{2}(z^2 + 1)} dz dv$$

where C_1 is the unit circle oriented counterclockwise. Integration then yields

$$(3.93) \quad g(m, n) = \frac{1}{4\pi} \int_{-\pi}^{\pi} e^{i(m-n)v} \frac{(\cos v)^{m+n}}{(a + \sqrt{a^2 - \cos^2 v})^{m+n} \sqrt{a^2 - \cos^2 v}} dv.$$

Using the fact that the above expression is the Fourier transform of an even function we can re-write it as a real integral, yielding

$$(3.94) \quad g(m, n) = \frac{1}{2\pi} \int_0^{\pi} \frac{\cos[(m-n)v] (\cos v)^{m+n}}{(a + \sqrt{a^2 - \cos^2 v})^{m+n} \sqrt{a^2 - \cos^2 v}} dv.$$

The expression for the Green's function given in (3.81) follows by employing the translation and reflection symmetries outlined above. To obtain the expression (3.82) we observe that $(m_2, n_2) = (m_1, n_1)$ corresponds to $m = n = 0$ and hence is given by

$$(3.95) \quad \begin{aligned} g(0, 0) &= \frac{1}{2\pi} \int_0^{\pi} \frac{1}{\sqrt{a^2 - \cos^2 v}} dv \\ &= \frac{1}{2\pi a} \int_{-\frac{\pi}{2}}^{\frac{\pi}{2}} \frac{1}{\sqrt{1 - (1/a)^2 \cos^2 \phi}} d\phi \\ &= \frac{1}{\pi a} \int_0^{\frac{\pi}{2}} \frac{1}{\sqrt{1 - (1/a)^2 \cos^2 \phi}} d\phi \\ &= \frac{1}{\pi a} K\left(\frac{1}{a^2}\right). \end{aligned}$$



CHAPTER IV

Optical Tomography on Graphs

4.1 Introduction

Inverse problems arise in numerous settings within discrete mathematics, including graph tomography [79, 48, 49, 45, 27] and resistor networks [32, 33, 34, 35, 50, 17, 16]. In such problems, one is typically interested in reconstructing a function defined on edges of a fixed graph or, in some cases, the edges themselves. Here we focus on recovering vertex properties of a graph from boundary measurements. The problem we consider is the discrete analog of optical tomography. Optical tomography is a biomedical imaging modality that uses scattered light as a probe of structural variations in the optical properties of tissue [6]. The inverse problem of optical tomography consists of recovering the potential of a Schrödinger operator from boundary measurements.

Let $G = (V, E)$ be a finite locally connected loop-free graph with vertex boundary

δV . We once again consider the time-independent diffusion equation [64]

$$(4.1) \quad (Lu)(x) + \alpha_0[1 + \eta(x)]u(x) = f(x), \quad x \in V,$$

$$(4.2) \quad t u(x) + \partial u(x) = g(x), \quad x \in \delta V,$$

which, in the continuous setting, describes the transport of the energy density of an optical field in an absorbing medium. Here we assume that the absorption of the medium is nearly constant with background absorption α_0 and inhomogeneities represented by the *vertex potential* η . In place of the Laplace-Beltrami operator, we introduce the combinatorial Laplacian L defined by

$$(4.3) \quad (Lu)(x) = \sum_{y \sim x} [u(x) - u(y)],$$

where $y \sim x$ if the vertices x and y are adjacent. We make use of the graph analog of Robin boundary conditions, where the normal derivative is defined by

$$(4.4) \quad \partial u(x) = \sum_{\substack{y \in V \\ y \sim x}} [u(x) - u(y)],$$

and t is an arbitrary nonnegative parameter, which interpolates between Dirichlet and Neumann boundary conditions. If the vertex potential η is non-negative, then there exists a unique solution to the diffusion equation (4.1) satisfying the boundary condition.

In Chapter III we presented an algorithm for solving the forward problem of determining u , given η . Our approach was a perturbative one, making use of known Green's functions for the time-independent diffusion equation (or Schrödinger equation) [5, 11, 12, 10, 19, 20, 21, 22, 72, 81], with η identically zero. The corresponding

inverse problem, which we refer to as graph optical tomography, is to recover the potential η from measurements of u on the boundary of the graph. More precisely, let $G = (V, E)$ be a connected subgraph of a finite graph $\Gamma = (\mathcal{V}, \mathcal{E})$ and let δV denote those vertices in \mathcal{V} adjacent to a vertex in V . In addition, let S, R denote fixed subsets of δV . We will refer to elements of S and R as sources and receivers, respectively. For a fixed potential η , source $s \in S$ and receiver $r \in R$, let $u(r, s; \eta)$ be the solution to (4.1) with vertex potential η and boundary condition (4.2), where

$$(4.5) \quad g(x) = \begin{cases} 1 & x = s, \\ 0 & x \neq s. \end{cases}$$

We define the Robin-to-Dirichlet map Λ_η by

$$(4.6) \quad \Lambda_\eta(s, r) = u(r, s; \eta).$$

The inverse problem is to recover η from the Robin-to-Dirichlet map Λ_η .

The remainder of this chapter is organized as follows. We begin by highlighting differences between discrete and continuous diffuse optical tomography. In Section 4.2, we give an example of a family of graphs for which exact recovery is impossible. In Section 4.3 we briefly review key results on the solvability of the forward problem and introduce the Born series. We obtain necessary conditions for the convergence of the inverse Born series depending on the measurement data and the graph. We also describe related stability and error estimates. Next, in Section 4.4 we discuss the numerical implementation of the inverse series and present the results of numerical

simulations. Following this, in Section 4.5 we extend our results to the case where measurements can be taken at multiple values of α_0 . Finally, in Section 4.6 we show how for a certain class of graphs it is possible to give an explicit algebraic formula for the potential in terms of the data.

4.2 Non-uniqueness of absorption recovery

Unlike in continuous media, in the discrete setting there are a number of conditions which prohibit the unique reconstruction of the vertex potential η . As is true for resistor networks [35], it is easy to construct large families of graphs for which any η is unrecoverable. Here we proceed by considering graphs with special path subgraphs, though the construction can be generalized easily to a large class of graphs, ie. those containing an unrecoverable subgraph.

Proposition IV.1. *Let $G = (V, E)$ be a graph containing a path $P = (V', E')$ of length four, connected at each end to a single vertex in the remainder of the graph $V \setminus V'$, as illustrated in Figure 4.1. Then, for each vertex potential $\eta : V \rightarrow \mathbb{R}$ there exists an infinite family of potentials which yield the same Robin to Dirichlet map. Explicitly, $\tilde{\eta}_s$ is given by*

$$(4.7) \quad \begin{aligned} \tilde{\eta}_s(x) = & \eta(x) \mathbf{1}_{V \setminus V'}(x) + \left(-\frac{2}{\alpha_0} - 1 \right) \mathbf{1}_{V'}(x) + \frac{\sigma(\beta + s + n_3)}{\alpha_0(\beta\gamma - 1)} \mathbf{1}_{x_1}(x) + \\ & \frac{\sigma + \beta\gamma - 1}{\alpha_0\sigma(s + n_3)} \mathbf{1}_{x_2}(x) + \frac{s + n_3}{\alpha_0} \mathbf{1}_{x_3}(x) + \\ & \frac{\sigma + \sigma\gamma(s + n_3) + \beta\gamma - 1}{\alpha_0(\beta\gamma - 1)(s + n_3)} \mathbf{1}_{x_4}(x), \end{aligned}$$

for $s > -n_3$, where

$$\begin{aligned}
 n_i &= 2 + \alpha_0[1 + \eta(x_i)], \quad i = 1, \dots, 4, \\
 \sigma &= n_1 n_2 n_3 n_4 - n_1 n_2 - n_1 n_4 - n_2 n_4 + 1, \\
 \beta &= n_1 n_2 n_3 - n_1 - n_3, \\
 \gamma &= n_2 n_3 n_4 - n_2 - n_4.
 \end{aligned}
 \tag{4.8}$$

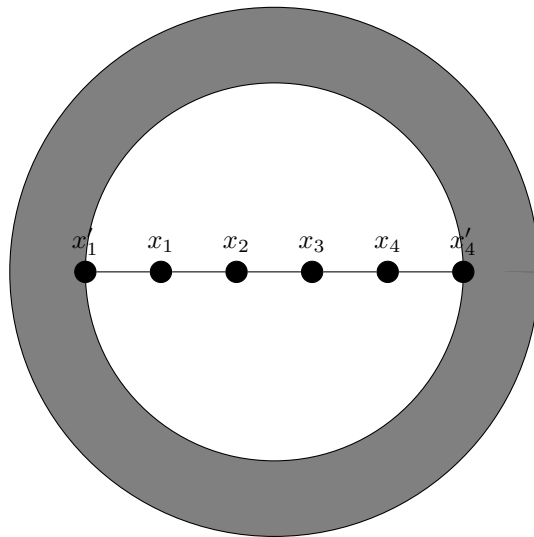


Figure 4.1: A graph $G = (V, E)$ with a path subgraph (V', E') of length 4. The remainder of the vertices $V \setminus V'$ and edges $E \setminus E'$ are represented by the grey annulus.

Proof. Let η be a vertex potential defined on all of V . Since the solution to the forward problem is unique, to each η we can associate a corresponding Robin-to-Dirichlet map $\Lambda_\eta : \ell^2(\delta V) \rightarrow \ell^2(\delta V)$. Our goal is to construct explicitly an infinite family of vertex potentials $\tilde{\eta}_s$ parametrized by $s \in \Omega \subset \mathbb{R}$, Ω open, such that $\Lambda_{\tilde{\eta}_s} = \Lambda_\eta$. In particular, we will show that this can be accomplished if we assume that $\text{supp}(\eta - \tilde{\eta}_s) \subset V'$.

Let g be an arbitrary source function supported on δV , and u the resulting solution of (4.1) on V , with vertex potential η . Note that only boundary sources are permitted and hence $f \equiv 0$ in (4.1). Consider also \tilde{u} , the solution of (4.1) obtained by replacing η with a new vertex potential $\tilde{\eta}$, with $\text{supp}(\eta - \tilde{\eta}) \subset V'$, and g held fixed. We wish to find an $\tilde{\eta}$ such that $\text{supp}(\eta - \tilde{\eta}) \subset V'$ and $\text{supp}(u - \tilde{u}) \subset V'$, for all sources g . If $V' = \{x_1, x_2, x_3, x_4\}$, and $\delta V' = \{x'_1, x'_4\}$, where x_1 and x_4 are adjacent to x'_1 and x'_4 , respectively, then it is sufficient to require that $u(x'_1) = \tilde{u}(x'_1)$ and $u(x'_4) = \tilde{u}(x'_4)$.

We seek suitable $(\tilde{u}, \tilde{\eta})$ by first considering the subgraph $V' \subset V$ with boundary $\delta V'$. For an arbitrary vertex potential $\tilde{\eta}$ on V' , we find a function ψ solving (4.1) on V' with η replaced by $\tilde{\eta}$ and subject to the boundary conditions (on $\delta V' \subset V \setminus V'$),

$$(4.9) \quad \psi(x'_1) = u(x'_1), \quad \text{and} \quad \psi(x'_4) = u(x'_4).$$

Initially, we assume no additional constraints on $\tilde{\eta}$, and add additional requirements as necessary. After obtaining an expression for ψ as a function of $\tilde{\eta}$, we extend it to a function, \tilde{u} , on all of V by setting $\tilde{u}|_{V \setminus V'} = u$. The resulting function \tilde{u} will not necessarily be a solution to (4.1) with potential $\tilde{\eta}$, unless $u(x_1) = \tilde{u}(x_1)$ and $u(x_4) = \tilde{u}(x_4)$ for all source functions g . This yields conditions on $\tilde{\eta}$ which can be solved to obtain potentials with the same Robin-to-Dirichlet map as our original η .

Step 1: solving for ψ

For ease of exposition, we begin by defining $n_i = 2 + \alpha_0[1 + \eta(x_i)]$, and $\tilde{n}_i = 2 + \alpha_0[1 + \tilde{\eta}(x_i)]$. We then construct the linear system

$$(4.10) \quad A\psi = \begin{pmatrix} 0 \\ 0 \\ 0 \\ 0 \\ \psi(x'_4) \\ \psi(x'_1) \end{pmatrix}$$

where

$$(4.11) \quad A = \begin{pmatrix} \tilde{n}_1 & -1 & 0 & 0 & 0 & -1 \\ -1 & \tilde{n}_2 & -1 & 0 & 0 & 0 \\ 0 & -1 & \tilde{n}_3 & -1 & 0 & 0 \\ 0 & 0 & -1 & \tilde{n}_4 & -1 & 0 \\ 0 & 0 & 0 & 0 & 1 & 0 \\ 0 & 0 & 0 & 0 & 0 & 1 \end{pmatrix}.$$

Observe that A is the restriction of (4.1) to $V' \subset V$, with vertex potential $\tilde{\eta}$ and Dirichlet boundary conditions $\psi(x'_1) = u(x'_1)$ and $\psi(x'_4) = u(x'_4)$. Upon solving (4.10)

for ψ we obtain

$$(4.12) \quad \psi = \frac{1}{\tilde{n}_1\tilde{n}_2\tilde{n}_3\tilde{n}_4 - \tilde{n}_1\tilde{n}_2 - \tilde{n}_1\tilde{n}_4 - \tilde{n}_2\tilde{n}_4 + 1} \begin{pmatrix} (\tilde{n}_2\tilde{n}_3\tilde{n}_4 - \tilde{n}_2 - \tilde{n}_4)u(x'_1) + u(x'_4) \\ (\tilde{n}_3\tilde{n}_4 - 1)u(x'_1) + \tilde{n}_1u(x'_4) \\ \tilde{n}_4u(x'_1) + (\tilde{n}_1\tilde{n}_2 - 1)u(x'_4) \\ u(x'_1) + (\tilde{n}_1\tilde{n}_2\tilde{n}_3 - \tilde{n}_1 - \tilde{n}_3)u(x'_4) \\ (\tilde{n}_1\tilde{n}_2\tilde{n}_3\tilde{n}_4 - \tilde{n}_1\tilde{n}_2 - \tilde{n}_1\tilde{n}_4 - \tilde{n}_2\tilde{n}_4 + 1)u(x'_4) \\ (\tilde{n}_1\tilde{n}_2\tilde{n}_3\tilde{n}_4 - \tilde{n}_1\tilde{n}_2 - \tilde{n}_1\tilde{n}_4 - \tilde{n}_2\tilde{n}_4 + 1)u(x'_1) \end{pmatrix}.$$

Step 2: constructing \tilde{u}

We next extend ψ to a function, \tilde{u} , on V via the following formula:

$$(4.13) \quad \tilde{u} = u \mathbf{1}_{V \setminus V'} + \psi \mathbf{1}_{V'},$$

where $\mathbf{1}_C$ denotes the indicator function on $C \subset V$. Note that this function need not be the solution to (4.1) with vertex potential $\tilde{\eta}$. In particular, we require that

1. $\tilde{u}(x_1) = u(x_1)$ and
2. $\tilde{u}(x_4) = u(x_4)$,

which together ensure that \tilde{u} will satisfy the necessary equations on $V \setminus V'$. Together these conditions imply that

$$(4.14) \quad \frac{\psi(x'_1) + (\tilde{n}_1\tilde{n}_2\tilde{n}_3 - \tilde{n}_1 - \tilde{n}_3)\psi(x'_4)}{\tilde{n}_1\tilde{n}_2\tilde{n}_3\tilde{n}_4 - \tilde{n}_1\tilde{n}_2 - \tilde{n}_1\tilde{n}_4 - \tilde{n}_2\tilde{n}_4 + 1} = \frac{\psi(x'_1) + (n_1n_2n_3 - n_1 - n_3)\psi(x'_4)}{n_1n_2n_3n_4 - n_1n_2 - n_1n_4 - n_2n_4 + 1},$$

$$\frac{(\tilde{n}_2\tilde{n}_3\tilde{n}_4 - \tilde{n}_2 - \tilde{n}_4)\psi(x'_1) + \psi(x'_4)}{\tilde{n}_1\tilde{n}_2\tilde{n}_3\tilde{n}_4 - \tilde{n}_1\tilde{n}_2 - \tilde{n}_1\tilde{n}_4 - \tilde{n}_2\tilde{n}_4 + 1} = \frac{(n_2n_3n_4 - n_2 - n_4)\psi(x'_1) + \psi(x'_4)}{n_1n_2n_3n_4 - n_1n_2 - n_1n_4 - n_2n_4 + 1}.$$

Step 3: constructing $\tilde{\eta}$

To guarantee that no possible measurement can distinguish $\{\tilde{n}_i\}$ from $\{n_i\}$, and hence distinguish $\{\tilde{\eta}_i\}$ from $\{\eta_i\}$, we require the new vertex potential values, $\{\tilde{n}_i\}$, to be independent of $\psi(x'_1)$ and $\psi(x'_4)$. This can be achieved by insisting that the coefficients of $\psi(x'_1)$ and $\psi(x'_4)$ on the left and right hand sides of (4.14) are equal. Hence, we obtain

(4.15)

$$\begin{aligned}\tilde{n}_1\tilde{n}_2\tilde{n}_3\tilde{n}_4 - \tilde{n}_1\tilde{n}_2 - \tilde{n}_1\tilde{n}_4 - \tilde{n}_2\tilde{n}_4 + 1 &= \sigma = n_1n_2n_3n_4 - n_1n_2 - n_1n_4 - n_2n_4 + 1, \\ \tilde{n}_1\tilde{n}_2\tilde{n}_3 - \tilde{n}_1 - \tilde{n}_3 &= \beta = n_1n_2n_3 - n_1 - n_3, \\ \tilde{n}_2\tilde{n}_3\tilde{n}_4 - \tilde{n}_2 - \tilde{n}_4 &= \gamma = n_2n_3n_4 - n_2 - n_4.\end{aligned}$$

Note that the constants σ , β , and γ are completely determined by the values of n_1, \dots, n_4 and hence by the original vertex potential η . We can now solve (4.15) for \tilde{n}_1 , \tilde{n}_2 , and \tilde{n}_4 in terms of \tilde{n}_3 , σ , β , and γ , which yields

$$(4.16) \quad \begin{aligned}\tilde{n}_1 &= \frac{\sigma[\beta + \tilde{n}_3]}{\beta\gamma - 1}, \\ \tilde{n}_2 &= \frac{\sigma + \beta\gamma - 1}{\sigma\tilde{n}_3}, \\ \tilde{n}_4 &= \frac{\sigma + \sigma\gamma\tilde{n}_3 + \beta\gamma - 1}{(\beta\gamma - 1)\tilde{n}_3}.\end{aligned}$$

Since \tilde{n}_3 is arbitrary, we can choose $\tilde{n}_3 = s + n_3$. Hence, we obtain an infinite family of vertex potentials, $\tilde{\eta}_s$, $s \in (-n_3, \infty) \subset \mathbb{R}$, which have the same Robin-to-Dirichlet

map as the original vertex potential η . Explicitly, $\tilde{\eta}_s$ is given by

$$(4.17) \quad \begin{aligned} \tilde{\eta}_s(x) = & \eta(x) \mathbf{1}_{V \setminus V'}(x) + \left(-\frac{2}{\alpha_0} - 1 \right) \mathbf{1}_{V'}(x) + \frac{\sigma(\beta + s + n_3)}{\alpha_0(\beta\gamma - 1)} \mathbf{1}_{x_1}(x) + \\ & \frac{\sigma + \beta\gamma - 1}{\alpha_0\sigma(s + n_3)} \mathbf{1}_{x_2}(x) + \frac{s + n_3}{\alpha_0} \mathbf{1}_{x_3}(x) + \\ & \frac{\sigma + \sigma\gamma(s + n_3) + \beta\gamma - 1}{\alpha_0(\beta\gamma - 1)(s + n_3)} \mathbf{1}_{x_4}(x), \end{aligned}$$

for $s > -n_3$, where

$$(4.18) \quad \begin{aligned} n_i &= 2 + \alpha_0[1 + \eta(x_i)], \quad i = 1, \dots, 4, \\ \sigma &= n_1 n_2 n_3 n_4 - n_1 n_2 - n_1 n_4 - n_2 n_4 + 1, \\ \beta &= n_1 n_2 n_3 - n_1 - n_3, \\ \gamma &= n_2 n_3 n_4 - n_2 - n_4. \end{aligned}$$

□

As an example of the above phenomenon, we consider the case where $G = (V, E)$ is an 8×8 lattice with edges deleted so that it contains a path of length four connected to the rest of the graph solely at its two endpoints, as shown in Figure 4.2.

Letting each boundary vertex serve as both as a source and as a receiver we observe that the problem is formally over-determined since we have 32×16 measurements and 64 internal nodes, though Proposition IV.1 guarantees that we cannot uniquely recover the potential. A plot of $\tilde{\eta}_s$ is shown in the left panel of Figure 4.3 for various values of s , where once again we have taken our initial η to be identically zero. The right plot of Figure 4.3 is the ℓ^1 -norm of the relative difference between the Robin to Dirichlet map for η and the Robin to Dirichlet map for $\tilde{\eta}_s$.

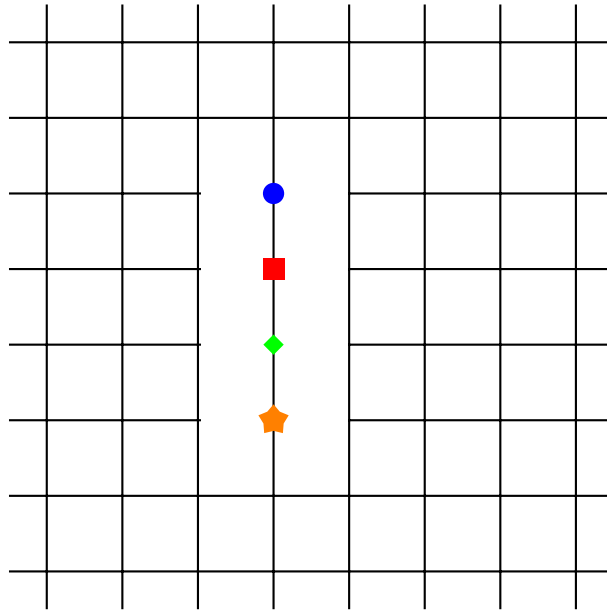


Figure 4.2: A graph G with edges deleted to create an interior path of length four, as required by the conditions of Proposition IV.1. The blue circle, red square, green diamond, and orange star mark the vertices x_1 , x_2 , x_3 , and x_4 , respectively.

4.3 Inverse Born series

4.3.1 Forward Born series

In this section we formulate the inverse Born series. We begin by reviewing some important properties of the Born series introduced in Chapter III, based in part on [43, 64].

We recall that the *background Green's function* [43] for (4.1) is the matrix G_0 whose i, j th entry is the solution to (4.1), with $\eta \equiv 0$, at the i th vertex for a unit source at the j th vertex. Under suitable restrictions this matrix can be used to construct the *Robin-to-Dirichlet map* Λ_η giving the solution of (4.1) on $R \subset \delta V$ to unit sources located in $S \subset \delta V$. To write a compact expression for Λ_η in terms of G_0 ,

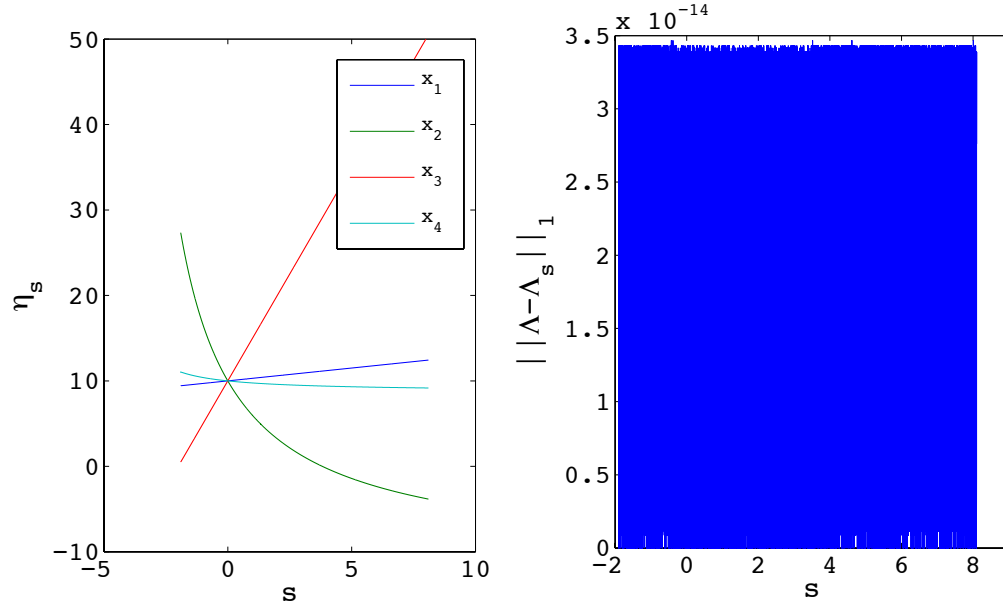


Figure 4.3: Left: Values of η restricted to an unconnected path subgraph of a lattice (see Figure 4.2), which are indistinguishable from $\eta \equiv 10$, for $\alpha = 0.2$. Right: ℓ^1 norm of the relative difference between the Robin to Dirichlet map of η and the Robin to Dirichlet map of $\tilde{\eta}_s$.

let D_η denote the matrix with entries given by

$$(D_\eta)_{i,j} = \begin{cases} \eta_i & \text{if } i = j, \\ 0 & \text{else.} \end{cases}$$

Additionally, for any two sets $U, W \subset V \cup \delta V$, let $G_0^{U;W}$ denote the submatrix of G_0 formed by taking the rows indexed by U and the columns indexed by W . For η sufficiently small we may write the Robin-to-Dirichlet map as a Neumann series

$$(4.19) \quad \Lambda_\eta(s, r) = G_0(r, s) - \sum_{j=1}^{\infty} K_j(\eta, \dots, \eta)(r, s), \quad r \in R, s \in S,$$

where $K_j : \ell^p(V^n) \rightarrow \ell^p(R \times S)$ is defined by

$$(4.20) \quad K_j(\eta_1, \dots, \eta_j)(r, s) = (-\alpha_0)^j G_0^{r;V} D_{\eta_1} G_0^{V;V} D_{\eta_2} \dots G_0^{V;V} D_{\eta_j} G_0^{V;s}.$$

We refer to the series (4.19) as the *forward Born series*.

In order to establish the convergence and stability of (4.19), we seek appropriate bounds on the operators $K_j : \ell^p(V \times \cdots \times V) \rightarrow \ell^p(\delta V \times \delta V)$. Note that if $|V|$ and $|\delta V|$ are finite then all norms are equivalent. However, since we are interested in the rate of convergence of the inverse series it will prove useful to establish bounds for arbitrary ℓ_p norms.

Proposition IV.2. *Let $p, q \in [1, \infty]$ such that $1/p + 1/q = 1$ and define the constants ν_p and μ_p by*

$$(4.21) \quad \nu_p = \alpha_0 \|G_0^{R;V}\|_{\ell^q(V) \times \ell^p(R)} \|G_0^{V;S}\|_{\ell^q(V) \times \ell^p(S)}, \quad \text{and} \quad \mu_p = \alpha_0 C_{G_0^{V;V}, q},$$

where

$$(4.22) \quad C_{G_0^{V;V}, q} = \max_{v \in V} \|G_0^{V;v}\|_{\ell^q(V)}.$$

The forward Born series (4.19) converges if

$$(4.23) \quad \mu_p \|\eta\|_p < 1.$$

Moreover, the N -term truncation error has the following bound,

$$(4.24) \quad \left\| \Lambda_\eta - \left(G_0 - \sum_{j=N}^{\infty} K_j(\eta, \dots, \eta) \right) \right\|_{\ell^p(R \times S)} \leq \nu_p \|\eta\|_p^{N+1} \mu_p^N \frac{1}{1 - \mu_p \|\eta\|_p}.$$

Remark IV.3. The bounds we obtain are similar to those found in the continuous setting [64], though here we present a novel proof of ℓ^2 -boundedness and extend our results to include $p \in [1, 2)$; a case not previously considered.

Before proving the proposition, we first establish the following useful identities.

Lemma IV.4. *Let M be an $n \times n$ matrix, and D_a, D_b be $n \times n$ diagonal matrices with diagonal entries given by vectors a and b , respectively. Let $M(k)$ denote the k th row of M , and*

$$(4.25) \quad C_{M,q} = \max_k \|M(k)\|_q,$$

for $1 \leq q \leq \infty$. Then for any vectors u^T and v , and $p, q \in [1, \infty]$, such that $1/p + 1/q = 1$,

$$(4.26) \quad |u^T D_a M D_b v| \leq C_{M,q} \|u\|_q \|a\|_p \|b\|_p \|v\|_\infty.$$

Proof. We begin by observing that if e_k is the k th canonical basis vector, $a = \sum_k D_a e_k$ and $I = \sum_k e_k e_k^T$, where I is the $n \times n$ identity matrix. Hence

$$(4.27) \quad \begin{aligned} |u^T D_a M D_b v| &\leq \left(\sum_k |u^T D_a e_k| \right) \max_k |M(k) D_b v|, \\ &\leq \|u\|_q \|a\|_p \max_k \sum_j |M(k) D_b e_j| \max_j |e_j^T v|, \\ &\leq \|u\|_q \|a\|_p \|b\|_p \max_k \|M(k)\|_q \max_j |e_j^T v|. \end{aligned}$$

□

We can iterate the result of the Lemma to obtain the following corollary.

Corollary IV.5. *Let M_1, \dots, M_{j-1} be $n \times n$ matrices and D_{a_1}, \dots, D_{a_j} be $n \times n$ diagonal matrices with diagonal elements given by the vectors a_1, \dots, a_j . If $M_i(k)$ and $C_{M_i,q}$ are defined as in the previous Lemma, then for all u and v ,*

$$(4.28) \quad |u^T D_{a_1} M_1 D_{a_2} \cdots M_{j-1} D_{a_j} v| \leq \|a_1\|_p \cdots \|a_j\|_p C_{M_1,q} \cdots C_{M_{j-1},q} \|u\|_q \|v\|_\infty,$$

where once again $p, q \in [1, \infty]$ and $1/p + 1/q = 1$.

We now return to the proof of Proposition IV.2.

Proof. Since D_{η_i} is a diagonal matrix, $D_{\eta_i} = \sum_{k \in V} \eta_i(k) e_k e_k^T$, where $\eta_i(k)$ is the k th component of the vector η_i and e_k is the canonical basis vector corresponding to the vertex k . From the definition of K_j , we see that

$$(4.29) \quad \|K_j(\eta_1, \dots, \eta_j)\|_p \leq \alpha_0^j \left(\sum_{r \in R, s \in S} \left[G_0^{r;V} D_{\eta_1} G_0^{V;V} D_{\eta_2} \cdots G_0^{V;V} D_{\eta_j} G_0^{V;s} \right]^p \right)^{1/p}.$$

The previous Corollary implies that

$$(4.30) \quad \left| G_0^{r;V} D_{\eta_1} \cdots D_{\eta_j} G_0^{V;s} \right| \leq \|\eta_1\|_p \cdots \|\eta_j\|_p C_{G_0^{V;V}, q}^{j-1} \|G_0^{r;V}\|_q \|G_0^{V;s}\|_\infty.$$

Thus

$$(4.31) \quad \begin{aligned} \|K_j\|_p &\leq \alpha_0^j \|G_0^{R,V}\|_{\ell^p(R) \times \ell^q(V)} \|G_0^{V,S}\|_{\ell^q(V) \times \ell^p(S)} C_{G_0^{V;V}, q}^{j-1}, \\ &\leq \nu_p \mu_p^{j-1}, \end{aligned}$$

where $\nu_p = \alpha_0 \|G_0^{R,V}\|_{\ell^q(V) \times \ell^p(R)} \|G_0^{V,S}\|_{\ell^q(V) \times \ell^p(S)}$ and $\mu_p = \alpha_0 C_{G_0^{V;V}, q}$, from which the result follows immediately. □

4.3.2 Inverse Born series

Proceeding as in [64], let $\phi \in \ell^2(R \times S)$ denote the *scattering data*,

$$(4.32) \quad \phi(r, s) = G_0(r, s) - \Lambda_\eta(r, s),$$

corresponding to the difference between the measurements in the background medium and those in the medium with the potential present. Note that if the forward Born series converges, we have

$$(4.33) \quad \phi(r, s) = \sum_{j=1}^{\infty} K_j(\eta, \dots, \eta).$$

Next, we introduce the ansatz

$$(4.34) \quad \eta = \mathcal{K}_1(\phi) + \mathcal{K}_2(\phi, \phi) + \mathcal{K}_3(\phi, \phi, \phi) + \dots ,$$

where each \mathcal{K}_n is a multilinear operator. Though ϕ can be thought of as an operator from $\ell^2(R)$ to $\ell^2(S)$, in (4.34) we treat it as a vector of length $|R| \cdot |S|$. Similarly, though it is often convenient to think of η as a (diagonal) matrix, in (4.34) it should be thought of as a vector of length $|V|$. Treating η and ϕ as matrices results in a different **approach** related to matrix completion [57]. With a slight abuse of notation, we also use K_1 to denote the $|R||S| \times |V|$ matrix mapping η (viewed as a vector) to $K_1\eta$, once again thought of as a vector.

To derive the inverse Born series, we substitute the ansatz (4.34) into the forward series (4.33) and equate tensor powers of ϕ . We thus obtain the following recursive expressions for the operators \mathcal{K}_j [64]:

$$(4.35) \quad \begin{aligned} \mathcal{K}_1 &= K_1^+, \\ \mathcal{K}_2 &= -\mathcal{K}_1 K_2 \mathcal{K}_1 \otimes \mathcal{K}_1, \\ \mathcal{K}_3 &= -(\mathcal{K}_2 K_1 \otimes K_2 + \mathcal{K}_2 K_2 \otimes K_1 + \mathcal{K}_1 K_3) \mathcal{K}_1 \otimes \mathcal{K}_1 \otimes \mathcal{K}_1, \\ \mathcal{K}_j &= -\left(\sum_{m=1}^{j-1} \mathcal{K}_m \sum_{i_1+\dots+i_m=j} K_{i_1} \otimes \dots \otimes K_{i_m} \right) \mathcal{K}_1 \otimes \dots \otimes \mathcal{K}_1, \end{aligned}$$

where K_1^+ denotes the (regularized) pseudoinverse of K_1 .

The following result provides sufficient conditions for the convergence of the inverse Born series for graphs where $|V| = |R \times S|$, corresponding to the case of a formally determined inverse problem.

Theorem IV.6. *Let $|V| = |R \times S|$ and $p \in [1, \infty]$. Suppose that the operator K_1 is invertible. Then the inverse Born series converges to the true potential η if $\|\phi\|_p < r_p$. Here the radius of convergence r_p is defined by*

$$(4.36) \quad r_p = \frac{C_p}{\mu_p} \left[1 - 2 \frac{\nu_p}{C_p} \left(\sqrt{1 + \frac{C_p}{\nu_p}} - 1 \right) \right],$$

where

$$(4.37) \quad C_p = \min_{\|\eta\|_p=1} \|K_1(\eta)\|_p$$

and ν_p, μ_p are defined in (4.21).

Remark IV.7. The convergence of the inverse Born series in the continuous setting was analyzed in [60]. It was found that certain smallness conditions on both $\|\mathcal{K}_1\|_p$ and $\|\mathcal{K}_1\phi\|_p$ are sufficient to guarantee convergence. Note that such a condition on $\|\mathcal{K}_1\|_p$ is not present in Theorem 5, Proposition 10 or Theorem 11. As explained below, this is due to the use of different techniques than in [60].

The proof of Theorem IV.6 depends on the following multi-dimensional version of Rouché's theorem.

Theorem IV.8. *[Theorem 2.5, 2] Let D be a domain in \mathbb{C}^n with a piecewise smooth boundary ∂D . Suppose that $f, g : \mathbb{C}^n \rightarrow \mathbb{C}^n$ are holomorphic on \bar{D} . If for each point*

$z \in \partial D$ there is at least one index j , $j = 1, \dots, n$, such that $|g_j(z)| < |f_j(z)|$, then $f(z)$ and $f(z) + g(z)$ have the same number of zeros in D , counting multiplicity.

Proof of Theorem IV.6. Put $n = |V| = |R \times S|$. Let $F : \mathbb{C}^n \times \mathbb{C}^n \rightarrow \mathbb{C}^n$ be the function defined by

$$(4.38) \quad F(\eta, \phi) = \phi - \sum_{j=1}^{\infty} K_j(\eta, \dots, \eta).$$

Note that F has n components F_1, \dots, F_n , each of which is well-defined and holomorphic for all ϕ if $\|\eta\|_p < 1/\mu_p$, since they are defined by a convergent Taylor series in ϕ and η . Let

$$(4.39) \quad C_p = \min_{\|\eta\|_p=1} \|K_1(\eta)\|_p,$$

which is non-zero for all p since K_1 is invertible. Then

$$(4.40) \quad \begin{aligned} \|F(\eta, 0)\|_p &\geq C_p \|\eta\|_p - \sum_{j=2}^{\infty} \|K_j(\eta, \dots, \eta)\|_p, \\ &\geq C_p \|\eta\|_p - \nu_p \sum_{j=2}^{\infty} \mu_p^{j-1} \|\eta\|_p^j, \\ &\geq C_p \|\eta\|_p - \nu_p \mu_p \|\eta\|_p^2 \frac{1}{1 - \mu_p \|\eta\|_p}, \end{aligned}$$

where the second inequality follows from the bounds on the forward operators obtained in the proof of Proposition IV.2. For $0 < \|\eta\|_p < 1/\mu_p$, $\|F(\eta, 0)\|_p$ is non-vanishing if

$$(4.41) \quad \|\eta\|_p < \frac{1}{\mu_p} \frac{C_p}{C_p + \nu_p}.$$

Suppose $\lambda \geq 1$. We then define

$$(4.42) \quad R_\lambda = \frac{1}{\mu_p} \frac{C_p}{C_p + \nu_p \lambda},$$

and let $\Omega_{1,\lambda} = \{\eta \in \mathbb{C}^n \mid \|\eta\|_p < R_\lambda\}$.

Next, we observe that $F(\eta, \phi) - F(\eta, 0) = \phi$ and hence if

$$(4.43) \quad \|\phi\|_p < \|F(\eta, 0)\|_p,$$

then

$$(4.44) \quad \|F(\eta, \phi) - F(\eta, 0)\|_p < \|F(\eta, 0)\|_p.$$

Note that

$$(4.45) \quad \|F(\eta, 0)\|_p \geq C_p \|\eta\|_p - \nu_p \mu_p \frac{\|\eta\|_p^2}{1 - \mu_p \|\eta\|_p},$$

and thus (4.43) holds if

$$(4.46) \quad \|\phi\|_p < C_p \|\eta\|_p - \nu_p \mu_p \frac{\|\eta\|_p^2}{1 - \mu_p \|\eta\|_p}.$$

If $\eta \in \partial\Omega_{1,\lambda}$, (4.43) holds if

$$(4.47) \quad \|\phi\|_p < R_\lambda C_p \left(1 - \frac{1}{\lambda}\right) \equiv r_{p,\lambda}.$$

Defining $\Omega_{2,\lambda} = \{\phi \in \mathbb{C}^n \mid \|\phi\|_p < r_{p,\lambda}\}$, we note the following: for all $(\eta, \phi) \in \Omega_{1,\lambda} \times \Omega_{2,\lambda}$, $F(\eta, 0) \neq 0$; and, for all $(\eta, \phi) \in \partial\Omega_{1,\lambda} \times \Omega_{2,\lambda}$, $\|F(\eta, \phi) - F(\eta, 0)\|_p < \|F(\eta, 0)\|_p$. By Theorem IV.8, $F(\eta, 0)$ and $F(\eta, \phi)$ have the same number of zeroes counting multiplicity on $\Omega_{1,\lambda} \times \Omega_{2,\lambda}$, namely precisely one. Thus, for all $\phi \in \Omega_{2,\lambda}$

there exists a unique $\eta = \psi(\phi)$ such that $F(\psi(\phi), \phi) = 0$. Since the unique zero must have multiplicity one,

$$(4.48) \quad \det \left(\{\partial_{\eta_j} F_i(\psi(\phi), \phi)\}_{i,j=1}^n \right) \neq 0.$$

Consequently, by the analytic implicit function theorem [Theorem 3.1.3, 69], ψ is analytic in a neighborhood of each $\phi \in \Omega_{2,\lambda}$, which is sufficient to prove that ψ is analytic on all of $\Omega_{2,\lambda}$. Hence ψ has a Taylor series converging absolutely for all $\phi \in \Omega_{2,\lambda}$. By construction, the terms in this series must be the same as those of the inverse Born series, since they are both power series for the same function. It follows that the inverse Born series must also converge for all $\phi \in \Omega_{2,\lambda}$. Optimizing over $\lambda \geq 1$, the inverse Born series converges for all $\phi \in \mathbb{C}^n$, such that

$$(4.49) \quad \|\phi\|_p < \frac{C_p}{\mu_p} \left[1 - 2 \frac{\nu_p}{C_p} \left(\sqrt{1 + \frac{C_p}{\nu_p}} - 1 \right) \right],$$

which completes the proof. □

Remark IV.9. We note that Theorem 6 is closely related to the problem of determining the domain of biholomorphy of a function of several complex variables, where the radii of analyticity of the function and its inverse are referred to as Bloch radii or Bloch constants [47, 46, 25]. In the context of nonlinear optimization a related result was obtained in [23], which also made use of Rouché's theorem.

Remark IV.10. The bound constructed in Theorem IV.6 is only a lower bound for the radius of convergence. In practice, the series converges well outside this range,

as the example in the next section confirms. Additionally, if in the proof of Theorem IV.6 we instead define $F(\eta, \phi)$ by

$$(4.50) \quad F(\eta, \phi) = \mathcal{K}_1\phi - \sum_{j=1}^{\infty} \mathcal{K}_1 K_j(\eta, \dots, \eta),$$

then it can easily be shown that the inverse series converges if

$$(4.51) \quad \|\mathcal{K}_1\phi\|_p < \tilde{r}_p := \frac{1}{\mu_p} \left[1 - 2\frac{\nu_p}{C_p} \left(\sqrt{1 + \frac{C_p}{\nu_p}} - 1 \right) \right].$$

Though the right-hand side is slightly more complicated, it is often easily computed and gives a better bound.

Figure 4.4 shows a plot of the bound on the radius of convergence,

$$r_p = \frac{C_p}{\mu_p} \left[1 - 2\frac{\nu_p}{C_p} \left(\sqrt{1 + \frac{C_p}{\nu_p}} - 1 \right) \right]$$

for various values of C_p/ν_p . For large graphs we expect the determinant of K_1 to be small, corresponding to a small value of C_p . In this regime we observe that the first term in the asymptotic expansion of (4.49) is

$$(4.52) \quad r_p = \frac{C_p^2}{4\nu_p\mu_p} + \mathcal{O}(C_p^3).$$

We now consider the stability of the limit of the inverse scattering series under perturbations in the scattering data. The following stability estimate follows immediately from Theorem IV.6.

Proposition IV.11. *Let E be a compact subset of $\Omega_p = \{\phi \in \mathbb{C}^n \mid \|\phi\|_p < r_p\}$, where r_p is defined in (4.36) and $p \in [1, \infty]$. Let ϕ_1 and ϕ_2 be scattering data belonging to*

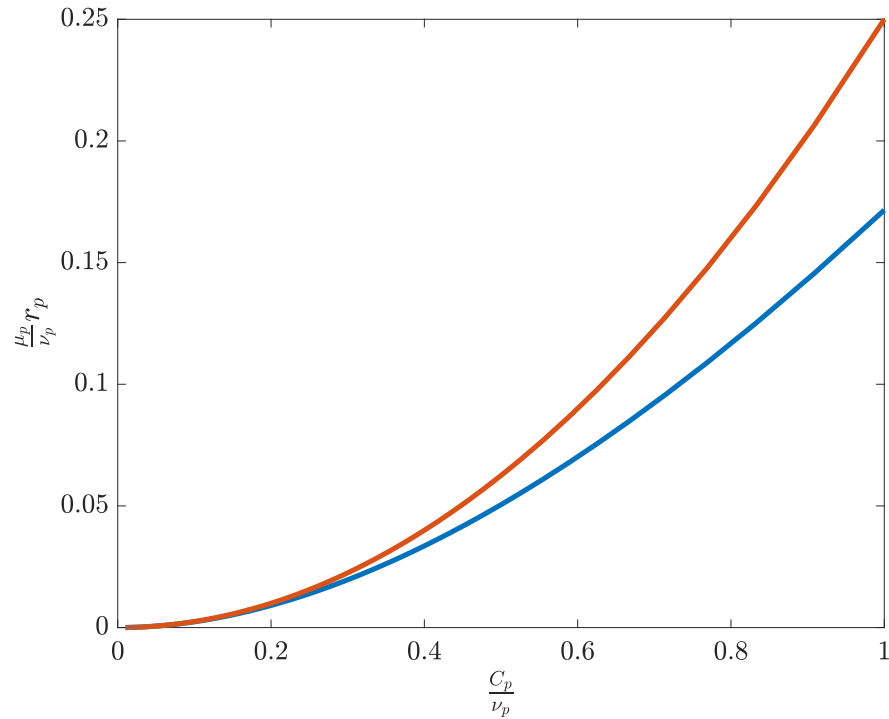


Figure 4.4: The bound on the radius of convergence of the inverse Born series as a function of C_p/ν_p . The radius r_p (multiplied by μ_p/ν_p) is shown in blue. The red curve is the asymptotic estimate given in (4.52).

E and ψ_1 and ψ_2 denote the corresponding limits of the inverse Born series. Then the following stability estimate holds:

$$\|\psi_1 - \psi_2\|_p \leq M \|\phi_1 - \phi_2\|_p ,$$

where $M = M(E, p)$ is a constant which is otherwise independent of ϕ_1 and ϕ_2 .

Proof. In the proof of Theorem IV.6 it was shown that ψ is analytic on Ω_p . In particular, it follows that there exists an $M < \infty$ such that

$$(4.53) \quad \|D\psi\|_p \leq M,$$

for all $\phi \in \Omega$. Here $D\psi$ is the differential of ψ and $\|\cdot\|_p$ is its induced matrix p -norm.

By the mean value theorem,

$$(4.54) \quad \|\psi_1 - \psi_2\|_p \leq M \|\phi_1 - \phi_2\|_p,$$

for all $\phi_1, \phi_2 \in \Omega$. □

Theorem IV.6 guarantees convergence of the inverse Born series, but does not provide an estimate of the approximation error. Such an estimate is provided in the next theorem.

Theorem IV.12. *Suppose that the hypotheses of Theorem IV.6 hold and $\|\phi\|_p < \tau r_p$, where $\tau < 1$. If η is the true vertex potential corresponding to the scattering data ϕ , then*

$$\left\| \eta - \sum_{m=1}^N \mathcal{K}_m(\phi, \dots, \phi) \right\|_{\infty} < M \left(\frac{1}{1-\tau} \right)^n \left(\frac{\|\phi\|_p}{\tau r_p} \right)^N \frac{1}{1 - \frac{\|\phi\|_p}{\tau r_p}}.$$

Proof. The proof follows a similar argument to one used to show uniform convergence of analytic functions on polydiscs, see [Lemma 1.5.8 and Corollary 1.5.9, 69] for example. By Theorem IV.6, since $\|\phi\|_p < r_p$, the inverse Born series converges. Moreover, the value to which it converges is precisely the unique potential η corresponding to the scattering data ϕ .

Let ψ_j be the j th component of the sum of the inverse Born series, which is of the form

$$(4.55) \quad \psi_j = \sum_{|\alpha|=0}^{\infty} c_{\alpha}^{(j)} \phi^{\alpha},$$

for suitable $c_\alpha^{(j)}$, consistent with (4.34). Here we have used the following notational convention: if $\alpha = (\alpha_1, \dots, \alpha_n)$ then $\phi^\alpha \equiv \phi_1^{\alpha_1} \dots \phi_n^{\alpha_n}$. Additionally, for a given multi-index α we define $|\alpha| = \alpha_1 + \dots + \alpha_n$. Note that each α in the sum has exactly n elements, though any number of them may be zero.

Let

$$\psi_j^{(N)} = \sum_{|\alpha|=0}^N c_\alpha^{(j)} \phi^\alpha,$$

and Δ_ϕ be the polydisc

$$\Delta_\phi = \left\{ z \in \mathbb{C}^n \mid |z_s| < |\phi_s| \frac{r_p}{\|\phi\|_p}, s = 1, \dots, n \right\}.$$

We note that $\phi \in \Delta_\phi \subseteq \{\phi \mid \|\phi\|_p < r_p\}$. It follows by Cauchy's estimate [Theorem 1.3.3, 69] that

$$(4.56) \quad |c_\alpha^{(j)}| \leq M \left(\frac{\|\phi\|_p}{r_p} \right)^{|\alpha|} \frac{1}{|\phi|^\alpha},$$

where $M = \max_{\|\phi\|_p < r_p} \|\psi\|_p$. To proceed, we employ the following combinatorial identity, [Example 1.5.7, 69],

$$(4.57) \quad \sum_{|\alpha|=0}^{\infty} t^{|\alpha|} = \frac{1}{(1-t)^n},$$

for all $t \in (-1, 1)$. In light of the above, we see that

$$M \sum_{|\alpha|=0} \left(\frac{\|\phi\|_p}{r_p} \right)^{|\alpha|} = M \left(\sum_{m=1}^{\infty} \left(\frac{\|\phi\|_p}{r_p} \right)^m \right)^n = M \left(\frac{1}{1 - \frac{\|\phi\|_p}{r_p}} \right)^n.$$

The function $1/(1-t)^n$ is bounded by

$$M \left(\frac{1}{1-\tau} \right)^n$$

for all $|t| < \tau < 1$. Thus the one-dimensional Cauchy estimate implies that the k th coefficient of its Taylor series, b_k , is bounded by

$$|b_k| \leq M \left(\frac{1}{1-\tau} \right)^n \frac{1}{\tau^k},$$

and so

$$(4.58) \quad \begin{aligned} \sum_{|\alpha| > N} \left(\frac{\|\phi\|_p}{r_p} \right)^{|\alpha|} &\leq M \sum_{k > N} \left(\frac{1}{1-\tau} \right)^n \left(\frac{\|\phi\|_p}{\tau r_p} \right)^k, \\ &= M \left(\frac{1}{1-\tau} \right)^n \left(\frac{\|\phi\|_p}{\tau r_p} \right)^N \frac{1}{1 - \frac{\|\phi\|_p}{\tau r_p}}. \end{aligned}$$

Hence, independent of j ,

$$(4.59) \quad \begin{aligned} \left| \psi_j - \psi_j^{(N)} \right| &= \left| \sum_{|\alpha| > N} c_\alpha^{(j)} \phi^\alpha \right|, \\ &\leq \sum_{|\alpha| > N} |c_\alpha^{(j)}| |\phi|^\alpha, \\ &\leq M \sum_{|\alpha| > N} \left(\frac{\|\phi\|_p}{r_p} \right)^{|\alpha|}, \\ &\leq M \left(\frac{1}{1-\tau} \right)^n \left(\frac{\|\phi\|_p}{\tau r_p} \right)^N \frac{1}{1 - \frac{\|\phi\|_p}{\tau r_p}}, \end{aligned}$$

from which the result follows immediately. \square

Remark IV.13. Note that in the previous theorem we can minimize our bound over $\tau \in (\|\phi\|_p/r_p, 1)$. Letting $\gamma = \|\phi\|_p/r_p$ the minimum occurs at

$$\tau_* = \frac{\gamma}{2} \left[\left(1 + \frac{N-\gamma}{\gamma(n+N)} \right) + \sqrt{\left(1 - \frac{N-\gamma}{\gamma(N+n)} \right)^2 + 4 \frac{1-\gamma}{\gamma(N+n)}} \right].$$

Finally, we conclude our discussion of the convergence of the inverse Born series by proving an asymptotic estimate for the truncation error. Specifically, we show that for a fixed number of terms N the error in the N -term inverse Born series goes to zero as η goes to zero. We note that our estimate does not apply to the case of fixed ϕ and $N \rightarrow \infty$ since $C_{N,a}x^N \rightarrow \infty$ for any fixed positive x .

Theorem IV.14. *Let $\|\eta\|_p \mu_p < a < 1$. Then there exists a constant $C_{N,a}$, depending on N such that*

$$(4.60) \quad \left\| \eta - \sum_{j=1}^N \mathcal{K}_j(\phi, \dots, \phi) \right\|_p \leq C_{N,a} \|\eta\|_p^{N+1}.$$

Proof. We begin by considering the truncated inverse Born series,

$$(4.61) \quad \eta_N(\phi) = \sum_{j=1}^N \mathcal{K}_j(\phi, \dots, \phi).$$

If $\mu_p \|\eta\|_p < 1$, ϕ is equal to its forward Born series, and hence

$$(4.62) \quad \eta_N - \eta = \sum_{j=1}^N \sum_{i_1, \dots, i_j=1}^{\infty} \mathcal{K}_j[K_{i_1}(\eta, \dots, \eta), \dots, K_{i_N}(\eta, \dots, \eta)] - \eta.$$

Using (4.35) we find that

$$(4.63) \quad \eta_N - \eta = \sum_{j=1}^n \sum_{i_1 + \dots + i_j > N}^{\infty} \mathcal{K}_j[K_{i_1}(\eta, \dots, \eta), \dots, K_{i_N}(\eta, \dots, \eta)],$$

which follows from the construction of the inverse Born series. Therefore

$$\begin{aligned}
\|\eta_N - \eta\|_p &\leq \sum_{j=1}^N \|\mathcal{K}_j\|_p \nu_p^j \sum_{k>N}^{\infty} \mu_p^{k-j} \|\eta\|_p^k, \\
&\leq \sum_{j=1}^N \|\mathcal{K}_j\|_p \left(\frac{\nu_p}{\mu_p}\right)^j \sum_{k>N}^{\infty} \mu_p^k \|\eta\|_p^k, \\
(4.64) \quad &\leq \sum_{j=1}^N \|\mathcal{K}_j\|_p \left(\frac{\nu_p}{\mu_p}\right)^j \|\eta\|_p^{N+1} \mu_p^{N+1} \sum_{k=0}^{\infty} (\mu_p \|\eta\|_p)^k, \\
&= \sum_{j=1}^N \|\mathcal{K}_j\|_p \nu_p^j \mu_p^{N+1-j} \|\eta\|_p^{N+1} \frac{1}{1 - \mu_p \|\eta\|_p}.
\end{aligned}$$

In order to proceed, we require a bound on $\|\mathcal{K}_j\|_p$. As in [64], we begin by observing that if $p \in [1, \infty]$, $j > 2$,

$$\begin{aligned}
\|\mathcal{K}_j\|_p &\leq \|\mathcal{K}_1\|_p^j \sum_{m=1}^{j-1} \|\mathcal{K}_m\|_p \sum_{i_1+\dots+i_m=j} \|K_{i_1}\|_p \cdots \|K_{i_m}\|_p, \\
&\leq \|\mathcal{K}_1\|_p^j \sum_{m=1}^{j-1} \|\mathcal{K}_m\|_p \sum_{i_1+\dots+i_m=j} \left(\frac{\nu_p}{\mu_p}\right)^m \mu_p^j, \\
(4.65) \quad &= \|\mathcal{K}_1\|_p^j \sum_{m=1}^{j-1} \|\mathcal{K}_m\|_p \binom{j-1}{m-1} \left(\frac{\nu_p}{\mu_p}\right)^m \mu_p^j, \\
&\leq \nu_p \mu_p^{j-1} \|\mathcal{K}_1\|_p^j \left(\sum_{m=1}^{j-1} \|\mathcal{K}_m\|_p\right) \sum_{m=0}^{j-2} \binom{j-1}{m} \left(\frac{\nu_p}{\mu_p}\right)^m,
\end{aligned}$$

where we have shifted the index m in the last expression. It follows immediately

from the binomial theorem that

$$\begin{aligned}
\|\mathcal{K}_j\|_p &\leq \|\mathcal{K}_1\|_p^j \nu_p \left[(\mu_p + \nu_p)^{j-1} - \nu_p^{j-1} \right] \left(\sum_{m=1}^{j-1} \|\mathcal{K}_m\|_p \right), \\
(4.66) \quad &\leq [\|\mathcal{K}_1\|_p (\mu_p + \nu_p)]^j \left(\sum_{m=1}^{j-1} \|\mathcal{K}_m\|_p \right), \\
&\leq \|\mathcal{K}_1\|_p (\mu_p + \nu_p) \|\mathcal{K}_{j-1}\|_p + \frac{\nu_p}{\mu_p + \nu_p} [\|\mathcal{K}_1\|_p (\mu_p + \nu_p)]^j \|\mathcal{K}_{j-1}\|_p, \\
&\leq \|\mathcal{K}_1\|_p (\mu_p + \nu_p) \left[1 + (\mu_p + \nu_p)^{j-1} \|\mathcal{K}_1\|_p^{j-1} \right] \|\mathcal{K}_{j-1}\|_p.
\end{aligned}$$

Further note that if $j = 2$, then

$$(4.67) \quad \|\mathcal{K}_2\|_p \leq \|\mathcal{K}_1\|_p^3 \nu_p^2 \leq \|\mathcal{K}_1\|_p^3 (\mu_p + \nu_p)^2.$$

For ease of notation, let $r = (\mu_p + \nu_p) \|\mathcal{K}_1\|_p$ and note that

$$\begin{aligned}
\|\mathcal{K}_j\|_p &\leq \|\mathcal{K}_1\|_p (\mu_p + \nu_p) \left[1 + (\mu_p + \nu_p)^{j-1} \|\mathcal{K}_1\|_p^{j-1} \right] \|\mathcal{K}_{j-1}\|_p, \\
(4.68) \quad &\leq r \left[1 + r^{j-1} \right] \|\mathcal{K}_{j-1}\|_p, \\
&\leq \|\mathcal{K}_1\|_p r^j 2^j \left[\max\{1, r\} \right]^{\frac{j(j-1)}{2}}.
\end{aligned}$$

If we define $C = \max\{1, r\}$, then it follows from (4.64) and (4.68)

$$\begin{aligned}
\|\eta_N - \eta\|_p &\leq \frac{\|\eta\|_p^{N+1} \mu_p^{N+1} \|\mathcal{K}_1\|_p}{1 - \mu_p \|\eta\|_p} \sum_{j=1}^N \left(\frac{2\nu_p r}{\mu_p} \right)^j C^{\frac{j^2}{2}}, \\
(4.69) \quad &\leq \frac{\|\eta\|_p^{N+1} \mu_p^{N+1} \|\mathcal{K}_1\|_p}{1 - \mu_p \|\eta\|_p} \frac{1 - (2\nu_p \mu_p^{-1} r)^{N+1}}{1 - 2\nu_p \mu_p^{-1} r} C^{\frac{N^2}{2}}, \\
&\leq \tilde{C}(N) \frac{\|\eta\|_p^{N+1}}{1 - \mu_p \|\eta\|_p}.
\end{aligned}$$

Thus, for $\|\eta\|_p < \mu_p^{-1} a < \mu_p^{-1}$,

$$(4.70) \quad \|\eta_N - \eta\|_p \leq C'(N) \|\eta\|_p^{N+1}$$

for some constant $C'(N)$. □

4.4 Implementation

4.4.1 Regularizing \mathcal{K}_1

In the previous section we found that the norm of \mathcal{K}_1 plays an essential role in controlling the convergence of the inverse Born series. In practice, for large graphs $\|\mathcal{K}_1\|_p$ is too large to guarantee convergence of the inverse series. Moreover, even if the series converges, a modest amount of noise can lead to large changes in the recovered potential. Regularization improves the stability and radius of convergence of the inverse Born series by employing a regularized pseudoinverse, K_1^+ in place of the true inverse K_1^{-1} in the definition of \mathcal{K}_1 . In our numerical studies we compute \mathcal{K}_1 using a Tikhonov-regularized singular value decomposition of K_1 [66]. In the following we denote the regularization parameter by ϵ , noting that when $\epsilon = 0$ no regularization has been performed.

4.4.2 Numerical examples

In the following we present numerical reconstructions for a 12×12 lattice with boundary vertices connected to the outermost layer of vertices, as illustrated in Figures 4.5-4.9. Note that each outgoing edge connects to a boundary vertex. The scattering data is obtained by solving the forward problem by applying a direct solver to the linear system (4.1). As is often the case in biomedical applications, we consider a homogeneous medium with a small number of large inclusions.

Figures 4.5–4.9 show typical results of the inverse Born series reconstruction. Note that due to the rapid increase in the number of terms at each order in the

inverse Born series, it is seldom practical to proceed beyond the first few terms of the series. As such, in each of our experiments it is not possible to say whether the series converges, since we are well beyond the radius of convergence guaranteed by Theorem 5. Instead, we consider the behavior of the first five terms. If the sum grows exponentially in the order of truncation then we say that the series diverges.

In Figure 4.6 the potential η is scaled by a factor of 10 compared to Figure 4.5. The inverse Born series diverges for the larger potential, and regularization is necessary to ensure convergence. Though this regularization improves the rate of convergence of the inverse Born series, it no longer converges to the true potential. We note, however, that there is still good qualitative recovery of the potential. Moreover, the method of regularization we have used here, Tikhonov regularization, has a smoothing effect on the recovered potential in the continuous setting. The same effect is evident in the transition from Figure 4.6 to Figure 4.7 where the regularization parameter, ϵ , has been increased from 10^{-7} to 10^{-5} . Figure 4.8 shows the effect of changing the boundary condition parameter t . In particular, decreasing t appears to shrink the radius of convergence, necessitating a larger regularization parameter. Finally, in Figure 4.9 we see the effect of partial boundary data. Note that a larger regularization parameter is required since the forward operator K_1 is more ill-conditioned.

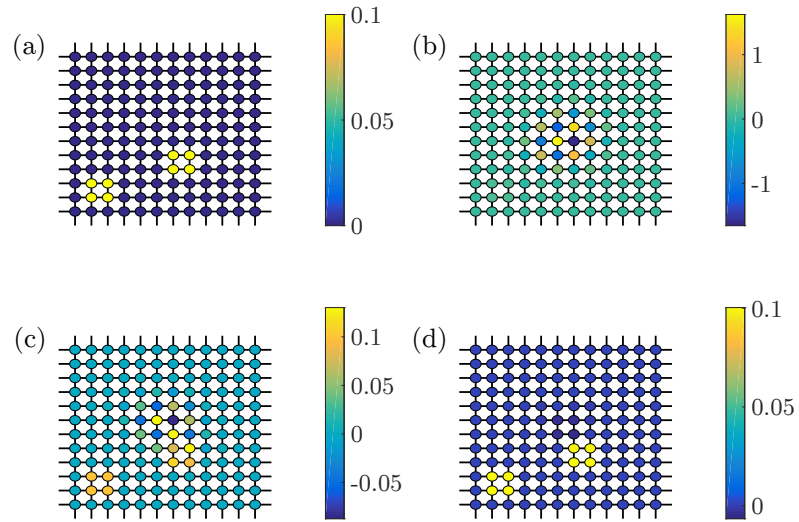


Figure 4.5: a) True potential b) first term of the inverse Born series, c) first two terms of the inverse Born series, d) first five terms of the inverse Born series. Here $\alpha_0 = 0.1$, $t = 1$, $\epsilon = 0$, and every boundary vertex is both a source and a receiver. $\mu_2 = 0.0874$, $\nu_2 = 0.4702$, and $\tilde{r}_2 = 3.7 \times 10^{-7}$.

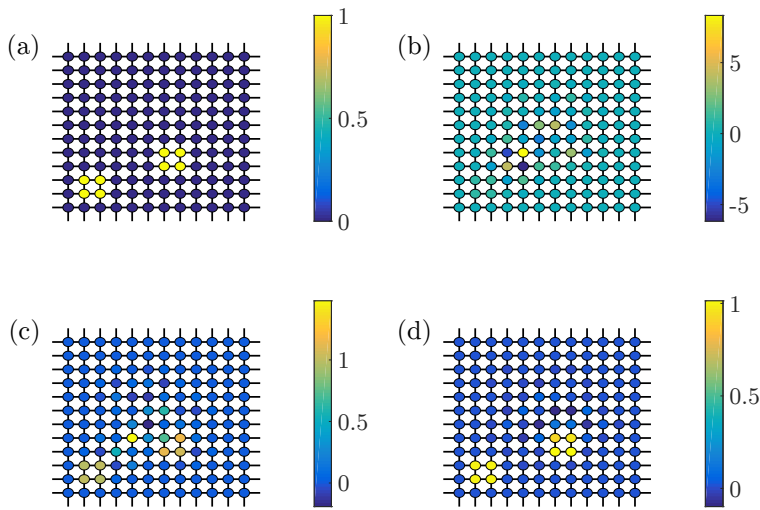


Figure 4.6: a) True potential b) first term of the inverse Born series, c) first two terms of the inverse Born series, d) first five terms of the inverse Born series. Here $\alpha_0 = 0.1$, $t = 1$, $\epsilon = 10^{-7}$, and every boundary vertex is both a source and a receiver. $\mu_2 = 0.0874$, $\nu_2 = 0.4702$, and $\tilde{r}_2 = 1.215 \times 10^{-6}$. Note that without the regularization the inverse Born series diverges.

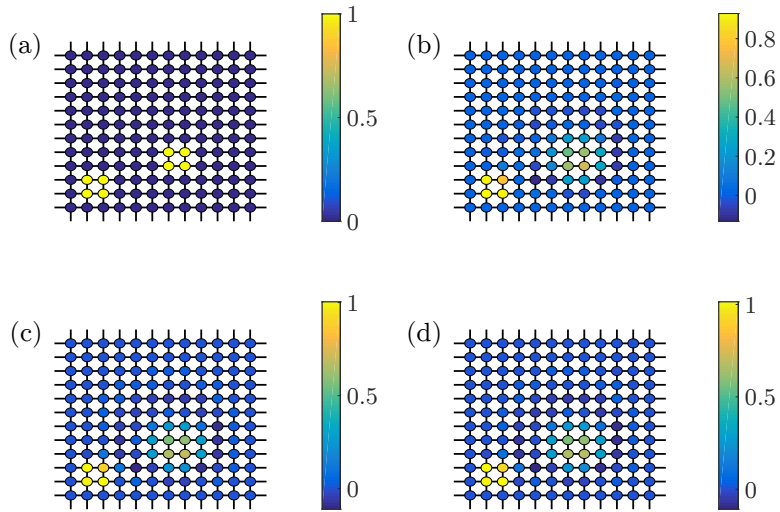


Figure 4.7: a) True potential b) first term of the inverse Born series, c) first two terms of the inverse Born series, d) first five terms of the inverse Born series. Here $\alpha_0 = 0.1$, $t = 1$, $\epsilon = 10^{-5}$, and every boundary vertex is both a source and a receiver. $\mu_2 = 0.0874$, $\nu_2 = 0.4702$, and $\tilde{r}_2 = 1.224 \times 10^{-4}$.

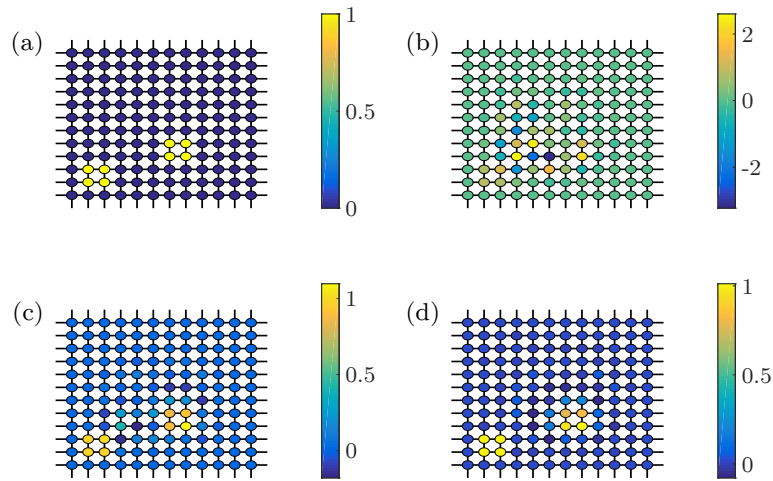


Figure 4.8: a) True potential b) first term of the inverse Born series, c) first two terms of the inverse Born series, d) first five terms of the inverse Born series. Here $\alpha_0 = 0.1$, $t = 0$, $\epsilon = 10^{-5}$, and every boundary vertex is both a source and a receiver. $\mu_2 = 0.1738$, $\nu_2 = 10.7463$, and $\tilde{r}_2 = 2.677 \times 10^{-6}$.

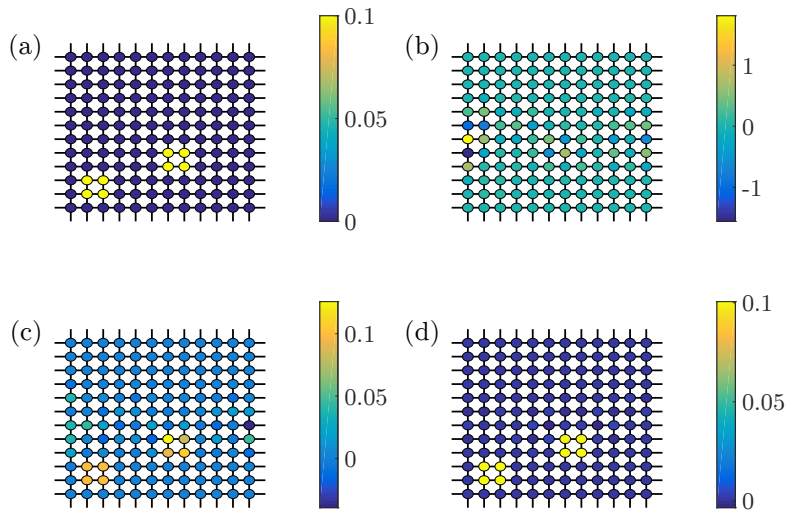


Figure 4.9: a) True potential b) first term of the inverse Born series, c) first two terms of the inverse Born series, d) first five terms of the inverse Born series. Here $\alpha_0 = 0.1$, $t = 1$, $\epsilon = 10^{-9}$, and every boundary vertex on the top and bottom edges of the lattice is both a source and a receiver. $\mu_2 = 0.0874$, $\nu_2 = 0.2351$, and $\tilde{r}_2 = 2.656 \times 10^{-7}$.

4.5 Incorporating potential structure

The inverse Born series algorithm can be extended to take into account additional constraints on the vertex potential η , such as restrictions on its support or requirements that it is constant on some subset of the domain, allowing the recovery of vertex potentials which would otherwise be unrecoverable using the inverse Born series described above.

Theorem IV.15. *Let ϕ be the measurement data and F be a linear mapping from $\mathbb{R}^k \rightarrow \mathbb{R}^{|V|}$, where $k \leq |V|$. Moreover, suppose that η is in the image of F and let η' be its pre-image,*

$$(4.71) \quad \eta' = F^{-1}(\eta).$$

Then

$$(4.72) \quad \eta' = \mathcal{K}'_1(\phi) + \mathcal{K}'_2(\phi, \phi) + \cdots + \mathcal{K}'_n(\phi, \dots, \phi) + \cdots,$$

and

$$(4.73) \quad \begin{aligned} \mathcal{K}'_1 &= (K_1 \circ F)^+, \\ \mathcal{K}'_2 &= -\mathcal{K}'_1 \circ K_2 \circ ((F \circ \mathcal{K}_1) \otimes (F \circ \mathcal{K}_1)), \\ \mathcal{K}'_n &= -\sum_{j=1}^{n-1} \mathcal{K}'_j \circ \left(\sum_{i_1+\dots+i_j=n} K_{i_1} \otimes K_{i_2} \otimes \cdots \otimes K_{i_j} \right) \circ ((F \circ \mathcal{K}_1) \otimes \cdots \otimes (F \circ \mathcal{K}_1)), \end{aligned}$$

where $(K_1 \circ F)^+$ denotes the (regularized) pseudoinverse of $(K_1 \circ F)$.

Proof. We begin by rewriting the discrete time-independent diffusion equation as

$$(4.74) \quad \begin{aligned} Lu + \alpha_0[I + D_{F(\eta')}]u - A_{V,\delta V}^T v &= \mathbf{0}, \\ -A_{V,\delta V} u + Dv &= \mathbf{g}, \end{aligned}$$

where $D_{F(\eta')}$ is the diagonal matrix whose diagonal elements are given by the vector $F(\eta')$. If $\Lambda'_{\eta'} : \ell^2(\mathbb{R}^k) \rightarrow \ell^2(R \times S)$ denotes the Robin-to-Dirichlet map for the modified system (4.74) and η is in the image of F , then

$$(4.75) \quad \Lambda'_{\eta'} = \Lambda_\eta.$$

Thus the forward Born series of (4.74) is given by

$$(4.76) \quad \Lambda'_{\eta'}(s, r) = G_0(r, s) - \sum_{n=1}^{\infty} K_n(F(\eta'), \dots, F(\eta')).$$

Following the construction of the inverse Born series, we let ϕ represent the measured data, and consider the ansatz

$$(4.77) \quad \eta' = \mathcal{K}'_1(\phi) + \mathcal{K}'_2(\phi, \phi) + \dots + \mathcal{K}'_n(\phi, \dots, \phi) + \dots$$

We see immediately that

$$(4.78) \quad \begin{aligned} \mathcal{K}'_1 \circ K_1 \circ F &= I, \\ \mathcal{K}'_1 \circ K_2 \circ (F \otimes F) + \mathcal{K}'_2 \circ ((K_1 \circ F) \otimes (K_1 \circ F)) &= 0, \\ \dots \\ \sum_{j=1}^n \mathcal{K}'_j \circ \left(\sum_{i_1+\dots+i_j=n} K_{i_1} \otimes K_{i_2} \otimes \dots \otimes K_{i_j} \right) \circ (F \otimes \dots \otimes F) &= 0. \end{aligned}$$

If $(K_1 \circ F)^+$ denotes the (regularized) pseudoinverse of $(K_1 \circ F)$, then we obtain

(4.79)

$$\mathcal{K}'_1 = (K_1 \circ F)^+,$$

$$\mathcal{K}'_2 = -\mathcal{K}'_1 \circ K_2 \circ ((F \circ \mathcal{K}_1) \otimes (F \circ \mathcal{K}_1)),$$

$$\mathcal{K}'_n = -\sum_{j=1}^{n-1} \mathcal{K}'_j \circ \left(\sum_{i_1+\dots+i_j=n} K_{i_1} \otimes K_{i_2} \otimes \dots \otimes K_{i_j} \right) \circ ((F \circ \mathcal{K}_1) \otimes \dots \otimes (F \circ \mathcal{K}_1)).$$

□

We observe that bounds on the radius of convergence, truncation error, and stability of the modified inverse Born series can be easily obtained using arguments similar to those made in Section 4.3. Theorem IV.15 can easily be applied to incorporate measurements from multiple values of α_0 , provided the vertex potential η is independent of the value of α_0 . In optical tomography, this corresponds to varying the optical wave wavelength so that the absorption coefficients of the background medium and the inhomogeneities to be imaged have the same wavelength dependence.

In particular, let $\Gamma = (E, V)$ be a graph and suppose we have measurements for $\alpha_0 = (\alpha_i)_1^m$. Let $\Gamma' = \{\Gamma_1, \dots, \Gamma_m\}$ be the graph with vertices $V' = \{V_1, \dots, V_m\}$ and edges $E' = \{E_1, \dots, E_m\}$, consisting of m copies of Γ . Here the subscript denotes the copy of E , V , or Γ to which we are referring. Let $\pi : V' \rightarrow V$ denote the projection map taking a vertex in V_i or δV_i to the corresponding vertex in V or δV , respectively. Finally, for a given vertex potential, η , on Γ let η' denote the corresponding potential

on Γ' . Thus, for each vertex $v \in V'$,

$$(4.80) \quad \eta'(v) = \eta(\pi(v)).$$

Next we construct the following modified time-independent diffusion equation

$$(4.81) \quad \begin{aligned} L_i u_i + \alpha_i [I + D_{\eta'}] u_i - (A_i)_{V, \delta V}^T v_i &= \mathbf{0}, \\ -(A_i)_{V, \delta V} u_i + D v_i &= \mathbf{g}_i, \end{aligned}$$

where u_i and v_i , $i = 1, \dots, m$, are supported on V_i and δV_i , respectively, and L_i is the Laplacian corresponding to the i th subgraph. As before $D_{\eta'}$ denotes the diagonal matrix with entries given by η' .

Note that Γ' consists of m disconnected components, and hence the solution in one component is independent of the solution in another. If $W, U \subset V_i \times \delta V_i$ let $G_i^{W;U}$ denote the submatrix of G_i consisting of the rows indexed by W and the columns indexed by U . It follows that the background Green's function for (4.81) is given by

$$(4.82) \quad G_0 = \begin{pmatrix} G_1^{V_1;V_1} & & & & G_1^{V_1;\delta V_1} & & & & \\ & G_2^{V_2;V_2} & & & & G_2^{V_2;\delta V_2} & & & \\ & & \ddots & & & & \ddots & & \\ & & & G_m^{V_m;V_m} & & & & G_m^{V_m;\delta V_m} & \\ \hline G_1^{\delta V_1;V_1} & & & & G_1^{\delta V_1;\delta V_1} & & & & \\ & G_2^{\delta V_2;V_2} & & & & G_2^{\delta V_2;\delta V_2} & & & \\ & & \ddots & & & & \ddots & & \\ & & & G_m^{\delta V_m;V_m} & & & & G_m^{\delta V_m;\delta V_m} & \end{pmatrix}$$

Thus, if $\mathbf{u} = (u_1, \dots, u_m, v_1, \dots, v_m)^T$ solves (4.81) when $\eta' \equiv 0$, and

$$\mathbf{g} = (0, \dots, 0, g_1, \dots, g_m)^T,$$

then

$$(4.83) \quad \mathbf{u} = G_0 \mathbf{g}.$$

Using this we can define the operators K_1, \dots, K_n for (4.81), where we replace G_0

by

(4.84)

$$G'_0 = \left(\begin{array}{cccc|cccc} \frac{\alpha_1}{\alpha_0} G_1^{V_1;V_1} & & & & \frac{\alpha_1}{\alpha_0} G_1^{V_1;\delta V_1} & & & \\ & \frac{\alpha_2}{\alpha_0} G_2^{V_2;V_2} & & & & \frac{\alpha_2}{\alpha_0} G_2^{V_2;\delta V_2} & & \\ & & \ddots & & & & \ddots & \\ & & & \frac{\alpha_m}{\alpha_0} G_m^{V_m;V_m} & & & & \frac{\alpha_m}{\alpha_0} G_m^{V_m;\delta V_m} \\ \hline \frac{\alpha_1}{\alpha_0} G_1^{\delta V_1;V_1} & & & & \frac{\alpha_1}{\alpha_0} G_1^{\delta V_1;\delta V_1} & & & \\ & \frac{\alpha_2}{\alpha_0} G_2^{\delta V_2;V_2} & & & & \frac{\alpha_2}{\alpha_0} G_2^{\delta V_2;\delta V_2} & & \\ & & \ddots & & & & \ddots & \\ & & & \frac{\alpha_m}{\alpha_0} G_m^{\delta V_m;V_m} & & & & \frac{\alpha_m}{\alpha_0} G_m^{\delta V_m;\delta V_m} \end{array} \right),$$

to account for the different α value in each component.

We now enforce the condition that η is identical on each copy of Γ , and hence is independent of α . The map $F : \ell^p(V_1) \rightarrow \ell^p(V_1 \times \cdots \times V_m)$ in (4.71) is defined by

$$(4.85) \quad F\{\eta\}(v) = \eta(\pi(v)).$$

Using this we form the modified inverse Born series operators in (4.79) and thus construct the modified inverse Born series. Provided that $(\mathcal{K}_1 \circ F)$ is invertible and the measured data ϕ is sufficiently small, by Theorem IV.6 the inverse Born series converges to the true (unique) value of η . Since η is the α -independent absorption of the vertices in Γ , we have constructed a reconstruction algorithm using data from

multiple α_0 . To illustrate this algorithm we consider a path of length 10, noting that it cannot be imaged using the standard inverse Born series, that is with one value of α_0 . Observe that, more generally, any graph containing a path of length greater than six in its interior, connected to the remainder of the graph only at its endpoints, the corresponding K_1 is not invertible. In fact, it can be shown that for such graphs that the absorption η cannot be uniquely determined from the data ϕ .

To illustrate the effect of the number of α_i on recovery, we choose one boundary vertex to act both as source and receiver and take $\alpha_i = 0.1 \left(1 + 4\frac{i}{N-1}\right)$, $i = 0, \dots, N-1$, for $N = 8, 16, 24$, and 32 ; see Figure 4.10. Here η is chosen to be a function supported on the interior vertices 2, 3 and 6, with a height of 0.01. In each case the sum of the first 6 terms of the inverse Born series is taken with the Tikhonov regularization parameter $\epsilon = 10^{-10}$). The effect of regularization on the recovery of the potential is similar to that obtained in the results presented in Section 3.

4.6 Inversion through Internal Polling

4.6.1 Internal Polling

In the internal polling approach to vertex data recovery we allow ourselves to select a fixed number of internal vertices to which we attach our boundary vertices. By polling the system in this way we wish to recover the absorption at each interior vertex. As before we consider the time-independent diffusion equation

$$(4.86) \quad \begin{aligned} \mathcal{L}u + \alpha_0(I + \eta)u &= f, & \text{on } V \\ t u + \partial u &= g, & \text{on } \partial V. \end{aligned}$$

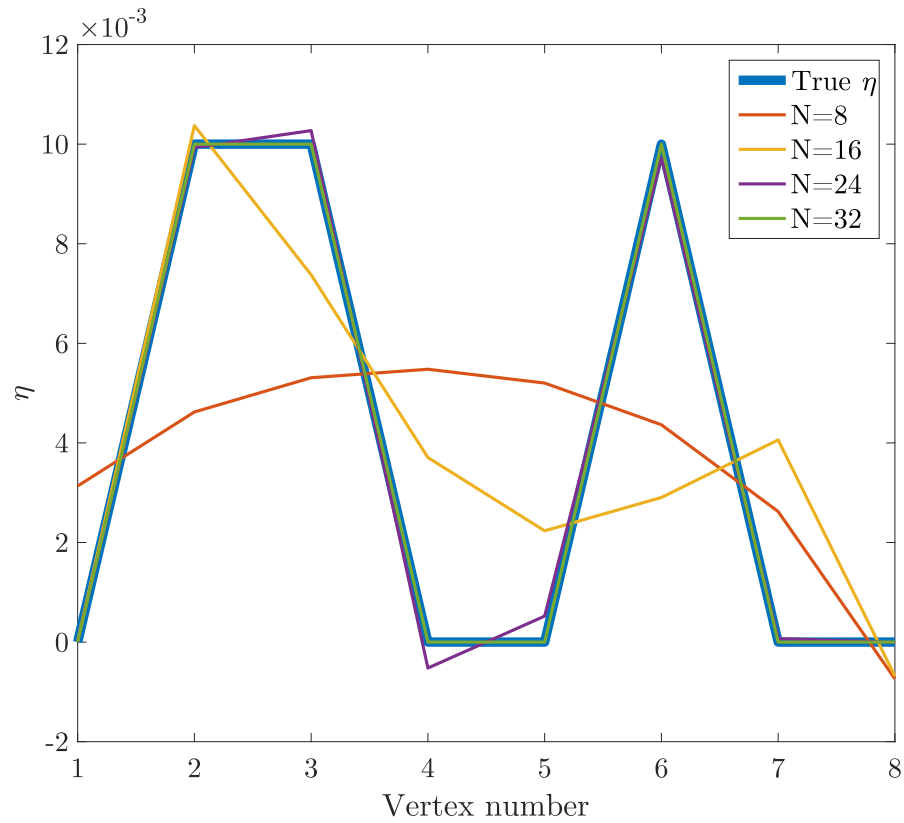


Figure 4.10: Reconstructions using the multi-frequency inverse Born series for $\alpha_i = 0.1 \left(1 + 4\frac{i}{N-1}\right)$, $i = 0, \dots, N-1$, $t = 0.01$, and $\epsilon = 10^{-10}$.

Typically we take f to be identically zero and g is assumed to be supported on one vertex. As in Chapter III, we can write this as a linear system,

$$(4.87) \quad \begin{aligned} \tilde{\mathcal{L}}u + \alpha_0(I + \eta)u - A_{V,\delta V}^T v &= \mathbf{0} \\ -A_{V,\delta V}u + Dv &= \mathbf{g}, \end{aligned}$$

where $\tilde{\mathcal{L}}$ is the restriction of the Laplacian to the interior vertices, $A_{V,\delta V}$ is the interior to boundary adjacency matrix, D is a diagonal matrix, u is taken to be the solution restricted to interior vertices and v is the solution on the boundary.

It is also convenient to consider solutions to the unperturbed problem (u_i, v_i) satisfying the system

$$(4.88) \quad \begin{aligned} \tilde{\mathcal{L}}u_i + \alpha_0 u_i - A_{V,\delta V}^T v_i &= \mathbf{0} \\ -A_{V,\delta V} u_i + Dv_i &= \mathbf{g}. \end{aligned}$$

If we let $\phi = u_i - u$ and $\psi = v_i - v$ then we obtain

$$(4.89) \quad \begin{aligned} \tilde{\mathcal{L}}\phi + \alpha_0(I + \eta)\phi - A_{V,\delta V}^T \psi &= \alpha_0 \eta u_i \\ -A_{V,\delta V} \phi + D\psi &= 0. \end{aligned}$$

Now suppose that each interior vertex is connected to at least one boundary vertex and

$$(4.90) \quad A_{V,\delta V}^\dagger A_{V,\delta V} = I,$$

where I is the $|V| \times |V|$ identity matrix. In this case, using Schur complements we can prove the following proposition, which guarantees an exact recovery of the absorption at all interior vertices.

Proposition IV.16. *Suppose the columns of $A_{V,\delta V}$ are linearly independent and let $A_{V,\delta V}^\dagger$ denote its pseudoinverse. Further suppose that we are given the solution (u_i, v_i) to the unperturbed problem everywhere, as well as ψ , the solution to the perturbed problem on the boundary. Provided that $u_i - A_{V,\delta V}^\dagger D\psi$ is nowhere vanishing, we find that*

$$(4.91) \quad \eta_i = \frac{(A\psi)_i}{\alpha_0 [u_i - A_{V,\delta V}^\dagger D\psi]_i}, \quad i = 1, \dots, |V|,$$

where $(\cdot)_i$ denotes the i th component of a vector and

$$(4.92) \quad A = \tilde{\mathcal{L}}A_{V,\delta V}^\dagger D + \alpha_0 A_{V,\delta V}^\dagger D - A_{V,\delta V}^T.$$

Proof. Using the second line of the system (4.89) we can solve for ϕ in terms of ψ to obtain

$$(4.93) \quad \phi = A_{V,\delta V}^\dagger D\psi.$$

We can then substitute that equation into the first equation of (4.89), which yields

$$(4.94) \quad \tilde{\mathcal{L}}A_{V,\delta V}^\dagger D\psi + \alpha_0 A_{V,\delta V}^\dagger D\psi - A_{V,\delta V}^T\psi = \alpha_0 \eta (u_i - A_{V,\delta V}^\dagger D\psi).$$

Recalling that η is a diagonal matrix, we let $\underline{\eta}$ be the vector whose components are the diagonal elements of η , and let U be the diagonal matrix whose non-zero entries are the corresponding components of $u_i - A_{V,\delta V}^\dagger D\psi$. If A is defined as in (4.92) then we find

$$(4.95) \quad A\psi = \alpha_0 U \underline{\eta}.$$

Provided that U is invertible, which is equivalent to saying that $u_i - A_{V,\delta V}^\dagger D\psi$ is non-vanishing, we obtain

$$(4.96) \quad \underline{\eta} = \alpha_0^{-1} U^{-1} A\psi.$$

The result follows immediately by observing that

$$(4.97) \quad (U^{-1})_{ij} = \begin{cases} \frac{1}{(u_i - A_{V,\delta V}^\dagger D\psi)_i}, & \text{if } i = j, \\ 0, & \text{otherwise.} \end{cases}$$

□

As an example, consider the complete graph on n vertices, choosing the boundary so that each interior vertex is connected to a single unique boundary vertex. Additionally, we suppose that each boundary vertex has both a receiver and a unit source, so that g in (4.86) is identically one. The following proposition guarantees exact absorption recovery in this case. Note that we assume g is identically one to obtain a compact expression for the absorption, but similar results can be obtained for any non-zero source function.

Proposition IV.17. *Consider the complete graph on n vertices with full boundary, and suppose that the set of receivers, V_R , is the whole boundary vertex set, δV . Moreover, assume that the source function g is identically one. If $\psi(x')$ is the measured solution on the boundary then the absorption η is given by*

$$(4.98) \quad \eta(x) = \frac{(\sigma - 1)(1 + t) [(1 + t)(n + \alpha_0) - 1]\psi(x) - (1 + t) \left(\sum_{x' \in \delta V} \psi(x') \right)}{\alpha_0 \left(1 - (1 + t)^2(\sigma - 1)\psi(x) \right)}.$$

Proof. We begin by observing that $A_{V, \delta V}$ from Proposition IV.16 is the identity matrix,

$$(4.99) \quad D = (1 + t)I,$$

and

$$(4.100) \quad \tilde{\mathcal{L}} = (n + 1)I - \mathbf{1}^T \mathbf{1},$$

where I is the $n \times n$ identity matrix and $\mathbf{1}$ is the n -vector of all 1's. Thus,

$$(4.101) \quad A\psi = [(1 + t)(n + \alpha_0) - 1]\psi - (1 + t) \left(\sum_{x' \in \delta V} \psi(x') \right) \mathbf{1}.$$

Recall from Chapter 2 that

$$(4.102) \quad u_i(x) = \frac{1}{(1+t)(\sigma-1)},$$

and hence from (4.91) we obtain

$$(4.103) \quad \eta(x) = \frac{(\sigma-1)(1+t)}{\alpha_0} \frac{[(1+t)(n+\alpha_0)-1]\psi(x) - (1+t) \left(\sum_{x' \in \delta V} \psi(x') \right)}{1 - (1+t)^2(\sigma-1)\psi(x)}.$$

□

CHAPTER V

Conclusion and Further Work

5.1 Conclusion

In this thesis we analyzed a discrete analog of the time-independent diffusion equation, considering both the forward problem, which we call diffuse scattering on graphs, as well as the corresponding inverse problems, which we call diffuse optical tomography on graphs.

For the forward problem we used Born series to construct perturbative solutions to time-independent diffusion equations. Since our method relied on knowledge of the Green's function for the homogeneous (background) problem, we reviewed a few useful families of graphs for which the homogeneous Green's functions could be explicitly constructed and outlined a method for finding Green's functions for Cayley graphs for both abelian and non-abelian groups.

For the inverse problem we presented and analyzed an algorithm based on the inverse Born series, proving estimates characterizing the domain of convergence, approximation errors, and stability of our approach. Our convergence results rep-

resent a substantial improvement over existing proofs of convergence for continuous problems, which require a smallness condition on the pseudoinverse of the forward operator. Finally, we presented a modification to our inversion algorithm which allows for the incorporation of additional information on the structure of the potential. Numerical experiments were performed to validate the algorithms. It was found that in practice our approach works well beyond the domain of convergence guaranteed by the analysis.

5.2 Future work

5.2.1 The inverse Born series in infinite dimensions

A natural direction for future work is to apply the techniques used in the discrete setting to continuous problems. As mentioned previously, the current bounds for the radius of convergence of inverse Born series for partial differential equation problems require that the norm of the linearized operator K_1 is bounded by a constant ν , and the norm of its regularized pseudoinverse, \mathcal{K}_1 , is bounded by $1/(\nu + \mu)$, where $\mu > 0$. If \mathcal{K}_1 is the true inverse of K_1 this is a contradiction since for any f in the domain of K_1 ,

$$\|f\| = \|\mathcal{K}_1 K_1 f\| \leq \frac{\nu}{\nu + \mu} \|f\|.$$

More generally, if \mathcal{K}_1 is any operator taking the range of K_1 to the domain of K_1 such that $\|\mathcal{K}_1\| < 1/(\mu + \nu)$, then

$$\|f - \mathcal{K}_1 K_1 f\| \geq \left(1 - \frac{\nu}{\mu + \nu}\right) \|f\|.$$

Now suppose that K_1 is a compact operator between Hilbert spaces and has a singular value decomposition

$$K_1 = \sum_{j=1}^{\infty} \sigma_j u_j \otimes v_j^*,$$

with $\sigma_1 > \sigma_2 > \dots \geq 0$. Many common methods for computing regularized pseudoinverses are based on applying a function ψ_ϵ to σ_j , where $\psi_\epsilon(\sigma_j) \rightarrow 1/\sigma_j$ as $\epsilon \rightarrow 0$ for any fixed j , and typically $0 \leq \psi_\epsilon(\sigma_j) \leq \sigma_j^{-1}$. It follows that

$$(5.1) \quad \mathcal{K}_1 K_1 = \sum_{j=1}^{\infty} \sigma_j \psi_\epsilon(\sigma_j) v_n \otimes v_n^*,$$

and hence in this setting the boundedness condition is equivalent to

$$\sigma_1 \left(\max_k \psi_\epsilon(\sigma_k) \right) \leq \frac{\nu}{\nu + \mu}.$$

Moreover,

$$\|v_j - \mathcal{K}_1 K_1 v_j\| = 1 - \sigma_j \psi_\epsilon(\sigma_j) \geq 1 - \frac{\sigma_j}{\sigma_1} \frac{\mu}{\nu + \mu}.$$

Hence, unless the largest singular values of K_1 are approximately the same size, the error in the approximation $\mathcal{K}_1 K_1 f \approx f$ will increase quickly with the number of singular vectors.

Our approach does not require the above additional smallness condition. In particular, for discrete systems if \mathcal{K}_1 is the true inverse of K_1 , then provided the data is sufficiently small, the inverse Born series is guaranteed to converge to the exact solution. A natural aim is then to extend our result to the infinite-dimensional setting, in order to remove the smallness condition for the convergence of the inverse Born series in the setting of partial differential equations.

5.3 Operator bounds and the Inverse Born series

In Chapter IV our analysis of the convergence and stability of the inverse Born series required bounding both the smallest and largest singular values of K_1 , as well as the norms of K_2, K_3, \dots . Such a dependence is inescapable, since it is in these operators that the structure of the graph, the sources, and the receivers is encoded. The task of producing suitable bounds for a general graph is, however, a difficult one. In particular, Proposition IV.1 suggests that deleting a single edge can make K_1 non-invertible, producing a graph with a non-invertible absorption to measurement map. This suggests the following general question.

Question V.1. *Characterize those graphs, or families of graphs, for which the map taking absorption vectors to boundary data is invertible.*

Additionally, when comparing with continuous media and physical applications we often wish to consider families of graphs in the limit where the number of vertices is taken to infinity. For example, if a mesh is used to approximate a domain then it is natural to consider what happens when the mesh is refined. Bounding the behaviour of operators in this limit is an interesting approach to studying the effects of regularization when dealing with pseudo-inverses of certain integral operators. Hence the following question is a natural one.

Question V.2. *For what families of graphs can suitable asymptotic bounds on the largest and smallest singular values of K_1 be determined, and what are the implications of these bounds for the continuum limit?*

Note that in general we expect that the smallest singular value will go to zero as the graph size goes to infinity. Though for the complete graph with boundary we have an explicit formula, the problem remains open for many other families of graphs, including those most often employed in discretizing continuous problems.

5.4 Sparsity and internal polling

When considering physical or computational applications of inverse problems we are often given additional information *a priori* about the inhomogeneities in the absorption which we wish to recover. For example, it is often natural to assume that the support of the inhomogeneities in question is small, or at least the inhomogeneities in the absorption can be approximated well by a sparse vector, which corresponds to the presence of a relatively small number of point absorbers in an otherwise-homogeneous medium. Our inverse problem then becomes to find the sparsest vector η , such that the resulting Robin-to-Dirichlet map (Λ_η) is equal to the measurement data (Φ). In other words, thinking of η , Φ , and Λ_η as vectors, we solve the exact recovery problem

$$(5.2) \quad \operatorname{argmin} \|\eta\|_0 \quad \text{such that} \quad \Lambda_\eta = \Phi,$$

where $\|\eta\|_0$ denotes the number of non-zero entries of η . Note that unlike traditional compressed sensing our objective function $\|\Lambda_\eta - \Phi\|_2$ has a nonlinear dependence on η . In the absence of noise, if η is exactly k -sparse we might expect (5.2) to recover the true vertex potential exactly. Here we assume that there is no sparser vector $\tilde{\eta}$ which yields the same Robin-to-Dirichlet map. In the presence of noise we replace

(5.2) by

$$(5.3) \quad \operatorname{argmin} \|\eta\|_0 \quad \text{such that} \quad \|\Lambda_\eta - \Phi\|_2 < \epsilon,$$

or

$$(5.4) \quad \operatorname{argmin}_\eta \|\Lambda_\eta - \Phi\|_2 \quad \text{such that} \quad \|\eta\|_0 \leq k.$$

In (5.3) we seek the sparsest vector which yields a Robin-to-Dirichlet map which is within a given tolerance of our measurements, while in (5.4) we seek the vector with fewer than k non-zero entries whose Robin-to-Dirichlet map, Λ_η , is closest to the measured data, Φ . In theory, an exhaustive search over all possible vectors could be used to solve (5.2)-(5.4), though such an approach is computationally infeasible. Thus we have the following question for future research.

Question V.3. *Find an efficient algorithm to solve (5.2), (5.3), or (5.4), together with conditions assuring the successful recovery of η .*

We observe that Proposition IV.1 provides a pathological example which any such conditions must rule out in order for the algorithm to have any chance of recovering the correct vertex potential. These results suggest that suitable conditions must be placed upon the underlying graph, the distance between the point absorbers, or both.

One specific case in which sparsity can be implemented is via internal polling. In the internal polling approach to vertex data recovery, we allow ourselves to select a fixed number of internal vertices to which we attach our boundary vertices. By

polling the system in this way we wish to recover the absorption at each interior vertex. We consider the time-independent diffusion equation

$$(5.5) \quad \begin{aligned} \mathcal{L}u + \alpha_0(I + \eta)u &= f, & \text{on } V \\ t u + \partial u &= g, & \text{on } \partial V. \end{aligned}$$

As before, we can write this as a linear system,

$$(5.6) \quad \begin{aligned} \tilde{\mathcal{L}}u + \alpha_0(I + \eta)u - A_{V,\delta V}^T v &= \mathbf{0} \\ -A_{V,\delta V}u + Dv &= \mathbf{g}, \end{aligned}$$

where $\tilde{\mathcal{L}}$ is the restriction of the Laplacian to the interior vertices, $A_{V,\delta V}$ is the interior to boundary adjacency matrix, D is a diagonal matrix, u is taken to be the solution restricted to interior vertices and v is the solution on the boundary.

Once again we also consider solutions to the unperturbed problem (u_i, v_i) , which satisfy

$$(5.7) \quad \begin{aligned} \tilde{\mathcal{L}}u_i + \alpha_0 u_i - A_{V,\delta V}^T v_i &= \mathbf{0} \\ -A_{V,\delta V}u_i + Dv_i &= \mathbf{g}. \end{aligned}$$

If we let $\phi = u_i - u$ and $\psi = v_i - v$ then we obtain

$$(5.8) \quad \begin{aligned} \tilde{\mathcal{L}}\phi + \alpha_0(I + \eta)\phi - A_{V,\delta V}^T \psi &= \alpha_0 \eta u_i \\ -A_{V,\delta V}\phi + D\psi &= 0. \end{aligned}$$

In Proposition IV.16 we showed that if

$$(5.9) \quad A_{V,\delta V}^\dagger A_{V,\delta V} = I,$$

where I is the $|V| \times |V|$ identity matrix, then we can recover η exactly. The assumptions on the graph geometry and the number of measurements are, in general, too restrictive for this result to be applicable to a broad range of families of graphs. If we relax the requirement that the recovery be exact, or assume that the absorption η is sparse, then we can employ sparse recovery methods to achieve good approximations with fewer measurements.

Consider the system of equations in equation (5.8). We wish to obtain the diagonal matrix η from measurements taken only on the boundary, ie. with access solely to $\psi = v_i - v$. It is convenient to first multiply the second equation by -1 and let $A_{V,\delta V}$ denote the adjacency matrix between δV and V so that it has non-zero entries. Our first step is to solve

$$(5.10) \quad A_{V,\delta V}\phi = D\psi$$

for ϕ .

In the internal polling approach, before taking measurements we are able to choose the connections between internal and boundary vertices, or equivalently, to design the adjacency matrix $A_{V,\delta V}$. We do so assuming that the difference ϕ from the unperturbed problem is equal, or close in norm, to an exactly k -sparse vector.

One way to construct a suitable $A_{V,\delta V}$ is to let $A_{V,\delta V}$ be the adjacency matrix of another graph Γ with good expansion properties. In particular, if $n = |V|$ and $m = |\delta V|$ then we choose Γ to be an (n, m, d, k, ϵ) a bipartite, unbalanced, degree d

expander with n vertices on the left and m vertices on the right. These parameters ensure that if U is a neighbourhood on the left of size at most k , then the size of its neighbourhood is almost $d|U|$. Formally, we require that $|N(U)| \geq (1 - \epsilon)d|U|$. Such expanders can be constructed deterministically for $m = O(k 2^{(\log \log n)^{O(1)}})$ and randomly for m as low as $O(k/\epsilon^2 \log(n/k))$.

We next observe the following fact.

Theorem V.4. [14] *There is an $m \times n$ matrix $A_{V,\delta V}$ that is the adjacency matrix of an expander such that for any ϕ , given $A_{V,\delta V}\phi = D\psi$, we can recover $\hat{\phi}$ such that*

$$(5.11) \quad \|\phi - \hat{\phi}\|_1 \leq C(\epsilon)\|\phi - \phi_k\|_1.$$

The inversion algorithm is a linear program of the form

$$(5.12) \quad \hat{\phi} = \operatorname{argmin}\|z\|_1 \quad \text{s.t.} \quad A_{V,\delta V}z = D\psi$$

with $O(n)$ variables and $O(m+n)$ constraints. Furthermore, if there is noise in our measurements; i.e.,

$$A_{V,\delta V}\phi = D\psi + \nu,$$

then the linear program in Equation 5.12 returns $\hat{\phi}$ with the guarantee

$$\|\phi - \hat{\phi}\|_1 \leq C(\epsilon)\|\phi - \phi_k\|_1 + \frac{\|\nu\|_1}{d}.$$

Heuristic arguments indicate that the time to solve such a linear program is approximately $\sqrt{n}T$ where T is the time it takes to multiply $A_{V,\delta V}$ times a vector, if the interior point method is used [14].

After solving for ϕ in (5.10) we can then proceed as in Proposition IV.16, with $\hat{\phi}$ in place of $A_{V,\delta V}^\dagger D\phi$, to obtain

$$(5.13) \quad \eta_i \approx \frac{[(\tilde{\mathcal{L}} + \alpha_0)\hat{\phi} - A_{V,\delta V}^T \psi]_i}{\alpha_0[u_i - \hat{\phi}]_i}, \quad i = 1, \dots, |V|,$$

where the subscripts in the numerator and denominator denote the i th component of the vector.

5.5 Fast summation of the inverse Born series

The first few terms of the inverse Born series are useful for computing relatively cheaply a good approximation to the true potential, provided the smallness condition is met and the background Green's function is already known. However, in many cases it becomes computationally expensive to compute beyond the sixth or seventh order due to the exponential growth in the number of sub-terms associated with each \mathcal{K}_n . An important direction for future research is to construct algorithms for efficiently computing, storing and applying the \mathcal{K}_n .

Increasing the efficiency of the code would not, however, remove the bottleneck associated with the exponential growth in the number of terms required at each order. Thus, it is natural to ask if it is possible to eliminate this restriction. In some cases the answer is yes.

Suppose there is only one source (a similar argument holds if there is only one receiver). Then,

$$(5.14) \quad \Lambda = G_0^{R;V} \left[I + D_\eta G_0^{V;V} \right]^{-1} D_\eta G_0^{V;s},$$

where Λ is a column vector of length $|R|$, $G_0^{R;V}$ is an $|R| \times |V|$ matrix, $G_0^{V;V}$ is a $|V| \times |V|$ matrix and $G_0^{V;s}$ is a column vector of length $|V|$. Here we also scale G_0 so that the factors of α_0^2 are included in the operators. Additionally, recall that D_a is a diagonal matrix with entries given by the vector a . We will sometimes also denote this by $D[a]$. Then

$$K_1(\eta) = G_0^{R;V} D_\eta G_0^{V;s} = G_0^{R;V} D_{G_0^{V;s}} \eta$$

and hence

$$\mathcal{K}_1 = (G_0^{R;V} D_{G_0^{V;s}})^+.$$

For ease of exposition we take \mathcal{K}_1 to be the inverse of K_1 , whence it follows that both $G_0^{R;V}$ and $D_{G_0^{V;s}}$ are invertible and thus

$$[I + D_\eta G_0^{V;V}] (G_0^{R;V})^{-1} \Lambda = D_\eta G_0^{V;s}.$$

Hence

$$D_\eta \left[G_0^{V;s} - G_0^{V;V} (G_0^{R;V})^{-1} \Lambda \right] = (G_0^{R;V})^{-1} \Lambda,$$

and thus if $\left[G_0^{V;s} - G_0^{V;V} (G_0^{R;V})^{-1} \Lambda \right]$ does not vanish then

$$\eta = \left(D \left[G_0^{V;s} - G_0^{V;V} (G_0^{R;V})^{-1} \Lambda \right] \right)^{-1} (G_0^{R;V})^{-1} \Lambda.$$

In terms of \mathcal{K}_1 this may be re-written as

$$\eta = \left(I - D[G_0^{V;s}]^{-1} D \left[G_0^{V;V} D[G_0^{V;s}] \mathcal{K}_1[\Lambda] \right] \right)^{-1} \mathcal{K}_1[\Lambda].$$

Expanding in powers of Λ we obtain

$$\begin{aligned}
 (5.15) \quad \eta &= \sum_{j=0}^{\infty} \left(D[G_0^{V;s}]^{-1} D \left[G_0^{V;V} D[G_0^{V;s}] \mathcal{K}_1[\Lambda] \right] \right)^j \mathcal{K}_1[\Lambda] \\
 &= \sum_{j=0}^{\infty} \left(D[G_0^{V;s}]^{-1} D \left[G_0^{V;V} D_{\tilde{\eta}} G_0^{V;s} \right] \right)^j \tilde{\eta},
 \end{aligned}$$

where $\tilde{\eta} = \mathcal{K}_1[\Lambda]$. Evidently, for this setup the inverse Born series may be re-written so that there is only one term at each order which contributes. Note that the evaluation of (5.15) only requires one matrix-vector multiply which can be pre-computed. The remainder is elementwise arithmetic. A natural question is if reductions of this sort are possible when there is more than one source. In numerical experiments it has been observed that such cancellations do occur, though no general theory has been developed to explain or quantify these cancellations.

Bibliography

- [1] Milton Abramowitz and Irene A. Stegun. *Handbook of Mathematical Functions*. National Bureau of Standards, 1964.
- [2] L.A. Aizenberg and A.P. Yuzhakov. *Integral Representations and Residues in Multidimensional Complex Analysis*. Translations of Mathematical Monographs. American Mathematical Society, 1983.
- [3] K. Ando. Inverse scattering theory for discrete Schrödinger operators on the hexagonal lattice. *Annales Henri Poincaré*, 14(2):347–383, October 2013.
- [4] Omer Angel, Alexander E. Holroyd, Dan Romik, and Bálint Virág. Random sorting networks. *Advances in Mathematics*, 215(2):839 – 868, 2007.
- [5] C. Araúz, A. Carmona, and A.M. Encinas. Overdetermined partial boundary value problems on finite networks. *J. Math. Anal. Appl.*, 423(1):191–207, 2014.
- [6] S R Arridge. Optical tomography in medical imaging. *Inverse Problems*, 15(2):R41, 1999.

- [7] Simon Arridge, Shari Moskow, and John C Schotland. Inverse Born series for the Calderon problem. *Inverse Problems*, 28, 2012.
- [8] Simon R Arridge and John C Schotland. Optical tomography: forward and inverse problems. *Inverse Probl.*, 25, 2009.
- [9] Patrick Bardsley and Fernando Guevara Vasquez. Restarted inverse Born series for the Schrödinger problem with discrete internal measurements. *Inverse Problems*, 30(4):045014, 2014.
- [10] E. Bendito, A. M. Encinas, and A. Carmona. Eigenvalues, eigenfunctions and Green's functions on a path via Chebyshev polynomials. *Appl. Anal. Discrete Math.*, 3:282–302, 2009.
- [11] Enrique Bendito, Angeles Carmona, and Andrés M. Encinas. Solving Boundary Value Problems on Networks Using Equilibrium Measures. *J. Funct. Anal.*, 171(1):155–176, 2000.
- [12] Enrique Bendito, Angeles Carmona, and Andrés M. Encinas. Potential Theory for Schrödinger operators on finite networks. *Rev. Mat. Iberoamericana*, 21:771–818, 2005.
- [13] Alain Bensoussan and Jose-Luis Menaldi. Difference equations on weighted graphs. *J. of Convex Anal.*, 12(1):13–44, 2005.
- [14] R. Berinde, A.C. Gilbert, P. Indyk, H. Karloff, and M.J. Strauss. Combining geometry and combinatorics: A unified approach to sparse signal recovery. In

Communication, Control, and Computing, 2008 46th Annual Allerton Conference on, pages 798–805, 2008.

- [15] A. Beurling and J. Deny. Espaces de dirichlet i, le cas élémentaire. *Acta Math.*, 99:203–224, 1958.
- [16] Liliana Borcea, Vladimir Druskin, Fernando Guevara Vasquez, Alexander, and V. Mamonov. Resistor network approaches to electrical impedance tomography. In *Inside Out, Mathematical Sciences Research Institute Publications*, 2011.
- [17] Liliana Borcea, Fernando Guevara Vasquez, and Alexander V. Mamonov. A discrete Liouville identity for numerical reconstruction of Schrödinger potentials, January 2016.
- [18] Justin Boyer, Jack J. Garzella, and Fernando Guevara Vasquez. On the solvability of the discrete conductivity and schrödinger inverse problems. *SIAM Journal on Applied Mathematics*, 76(3):1053–1075, 2016.
- [19] A. Carmona, A. M. Encinas, and M. Mitjana. Discrete elliptic operators and their Green operators. *Linear Algebra Appl.*, 442(2):115–134, 2014.
- [20] A. Carmona, A. M. Encinas, and M. Mitjana. Green matrices associated with generalized linear polyominoes. *Linear Algebra Appl.*, 468:38–47, 2015.
- [21] A. Carmona, A. M. Encinas, and M. Mitjana. Perturbations of discrete elliptic operators. *Linear Algebra Appl.*, 468:270–285, 2015.

- [22] P. Cartier. Fonctions harmoniques sur un arbre. *Sympos. Math.*, 9:203–270, 1972.
- [23] H.C. Chang, W. He, and N. Prabhu. The analytic domain in the implicit function theorem. *Journal of Inequalities in Pure and Applied Mathematics*, 4(1), 2003.
- [24] Chi-Kin Chau and Prithwish Basu. Analysis of latency of stateless opportunistic forwarding in intermittently connected networks. *IEEE/ACM Trans. Netw.*, 19(4):1111–1124, August 2011.
- [25] Huaihui Chen and Paul M. Gauthier. On Bloch’s constant. *Journal d’Analyse Mathématique*, 69(1):275–291, 1996.
- [26] G. Choquet and J. Deny. Modèles finis en théorie du potentiel. *J. Anal. Math.*, 5:77–135, 1956.
- [27] Fan Chung, Mark Garrett, Ronald Graham, and David Shallcross. Distance realization problems with applications to internet tomography. *Journal of Computer and System Sciences*, 63(3):432 – 448, 2001.
- [28] Fan R.K. Chung. *Spectral Graph Theory*. American Mathematical Society, 1997.
- [29] Fan R.K. Chung and S. T. Yau. Discrete Green’s functions. *Journal of Combinatorial Theory (A)*, 91:191–214, 2000.
- [30] Philippe G. Ciarlet. *Introduction to Numerical Linear Algebra and Optimisation*. Cambridge University Press, 1 edition, 1989.

- [31] Jozsef Cserti, Gyula David, and Attila Piroth. Perturbation of infinite networks of resistors. *American Journal of Physics*, 70(2):153–159, 2002.
- [32] E. Curtis, E. Mooers, and J. Morrow. Finding the conductors in circular networks from boundary measurements. *ESAIM: Mathematical Modelling and Numerical Analysis - Modélisation Mathématique et Analyse Numérique*, 28(7):781–814, 1994.
- [33] Edward B. Curtis and James A. Morrow. Determining the Resistors in a Network. *SIAM Journal on Applied Mathematics*, 50(3):918–930, 1990.
- [34] Edward B. Curtis and James A. Morrow. The Dirichlet to Neumann Map for a Resistor Network. *SIAM Journal on Applied Mathematics*, 51(4):1011–1029, 1991.
- [35] Edward B. Curtis and James. A Morrow. *Inverse Problems for Electrical Networks*. World Scientific Publishing, 2000.
- [36] Petros Drineas and Michael W. Mahoney. Effective Resistances, Statistical Leverage, and Applications to Linear Equation Solving. *CoRR*, abs/1005.3097, 2010.
- [37] R. J. Duffin. Discrete potential theory. *Duke Math. J.*, 20:233–251, 1953.
- [38] Eleftherios N. Economou. *Green's Functions in Quantum Physics*. Springer Berlin Heidelberg, 2006.

- [39] Robert B. Ellis. Discrete Green's functions for products of regular graphs, 2003.
- [40] Robert B. Ellis, III. *Chip-Firing Games with Dirichlet Eigenvalues and Discrete Green's Functions*. PhD thesis, University of California, San Diego, San Diego, 2002.
- [41] Andrew R Fisher, Andrew J Schissler, and John C Schotland. Photoacoustic effect for multiply scattered light. *Phys. Rev. E*, 76, 2007.
- [42] F. P. Gantmacher and M. G. Krein. *Oscillation matrices and kernels and small vibrations of mechanical systems*. AMS Chelsea Publishing, 2002.
- [43] A.C. Gilbert, J.G. Hoskins, and J. C. Schotland. Diffuse scattering on graphs. *Linear Algebra and its Applications*, 496:1–35, 2016.
- [44] Martin Grötschel, Michael Jünger, and Gerhard Reinelt. Facets of the linear ordering polytope. *Math. Program.*, 33(1):43–60, 1985.
- [45] F. Alberto Grünbaum and Laura Felicia Matusевич. A nonlinear inverse problem inspired by three-dimensional diffuse tomography: Explicit formulas. *International Journal of Imaging Systems and Technology*, 12(5):198–203, 2002.
- [46] Lawrence A. Harris. On the size of balls covered by analytic transformations. *Monatshefte für Mathematik*, 83(1):9–23, 1977.
- [47] Lawrence A. Harris. Fixed point theorems for infinite dimensional holomorphic functions. *Journal of the Korean Mathematical Society*, 41(1):175–192, 2004.

- [48] Gabor T. Herman and Attila Kuba, editors. *A Recursive Algorithm for Diffuse Planar Tomography*. Birkhäuser Boston, Boston, MA, 1999.
- [49] Atsushi Imiya, Akihiko Torii, and Kosuke Sato. Proceedings of the workshop on discrete tomography and its applications tomography on finite graphs. *Electronic Notes in Discrete Mathematics*, 20:217 – 232, 2005.
- [50] David V. Ingerman. Discrete and Continuous Dirichlet-to-Neumann Maps in the Layered Case. *SIAM Journal on Mathematical Analysis*, 31(6):1214–1234, 2000.
- [51] H. Isozaki and H. Morioka. Inverse scattering at a fixed energy for discrete Schrödinger operators on the square lattice. *ArXiv e-prints*, August 2012.
- [52] T. Kayano and M. Yamasaki. Dirichlet finite solution of Poisson equations on an infinite network. *Hiroshima Math. J.*, 12:569–579, 1982.
- [53] Richard W. Kenyon and David B. Wilson. Spanning trees of graphs on surfaces and the intensity of loop-erased random walk on \mathbb{Z}^2 , 2011.
- [54] Kimberly Kilgore, Shari Moskow, and John C Schotland. Inverse Born Series for Scalar Waves. *Journal of Computational Mathematics*, 30(6):601–614, 2012.
- [55] G. Kirchhoff. On the Solution of the Equations Obtained from the Investigation of the Linear Distribution of Galvanic Currents. *Circuit Theory, IRE Transactions on*, 5:4–7, 1958.

- [56] I. Koutis, G.L. Miller, and R. Peng. A nearly- $o(m \log n)$ time solver for sdd linear systems. In *Foundations of Computer Science (FOCS), 2011 IEEE 52nd Annual Symposium on*, pages 590–598, 2011.
- [57] Howard W. Levinson and Vadim A. Markel. Solution of the inverse scattering problem by t-matrix completion, 2014.
- [58] Yu-Ru Lin, Hari Sundaram, Yun Chi, Junichi Tatemura, and Belle L. Tseng. Blog Community Discovery and Evolution Based on Mutual Awareness Expansion. In *Proceedings of the IEEE/WIC/ACM International Conference on Web Intelligence, WI '07*, pages 48–56, Washington, DC, USA, 2007. IEEE Computer Society.
- [59] Vadim A. Markel, Joseph A. O’Sullivan, and John C. Schotland. Inverse problem in optical diffusion tomography. iv. Nonlinear inversion formulas. *J. Opt. Soc. Am. A*, 20(5):903–912, May 2003.
- [60] Vadim A. Markel and John C. Schotland. On the convergence of the Born series in optical tomography with diffuse light. *Inverse Problems*, 23(4):1445, 2007.
- [61] P.A. Martin. Discrete scattering theory: Green’s function for a square lattice. *Wave Motion*, 43(7):619 – 629, 2006.
- [62] Frédéric Mila, C. A. Stafford, and Sylvain Capponi. Persistent currents in a möbius ladder: a test of interchain coherence of interacting electrons. *Phys. Rev. B*, 57:1457–1460, Jan 1998.

- [63] Peter D. Miller. *Applied Asymptotic Analysis*. American Mathematical Society, 2006.
- [64] Shari Moskow and John Schotland. Convergence and Stability of the Inverse Scattering Series for Diffuse Waves. *Inverse Problems*, 24, 2008.
- [65] Shari Moskow and John C Schotland. Numerical studies of the inverse Born series for diffuse waves. *Inverse Problems*, 25(9):095007, 2009.
- [66] F. Natterer. *The Mathematics of Computerized Tomography*. SIAM, 2001.
- [67] Richard Oberlin. Discrete inverse problems for Schrödinger and Resistor networks. Technical report, University of Washington, July 2000.
- [68] Huaijun Qiu and Edwin R. Hancock. Clustering and Embedding Using Commute Times. *IEEE Transactions on Pattern Analysis and Machine Intelligence*, 29:1873–1890, 2007.
- [69] Volker Scheidemann. *Introduction to Complex Analysis in Several Variables*. Birkhäuser Verlag, 2005.
- [70] Jean-Pierre Serre. *Linear Representations of Finite Groups*. Springer-Verlag, 1977.
- [71] Jonathan Simon. Knots and chemistry. In *New Scientific Applications of Geometry and Topology*, volume 45 of *Proceedings of Symposia in Applied Mathematics*, pages 97–130, Providence, Rhode Island, 1992. American Math Society.

- [72] Paolo M. Soardi. *Potential theory on infinite networks*. Lecture Notes in Mathematics. Springer-Verlag, 1994.
- [73] Daniel A. Spielman and Nikhil Srivastava. Graph sparsification by effective resistances. In *Proceedings of the 40th Annual ACM Symposium on Theory of Computing*, STOC '08, pages 563–568, New York, NY, USA, 2008. ACM.
- [74] Satoshi Tanda, Taku Tsuneta, Yoshitoshi Okajima, Katsuhiko Inagaki, Kazuhiko Yamaya, and Noriyuki Hatakenaka. Crystal topology: A mobius strip of single crystals. *Nature*, 417:397–398, 2002.
- [75] Audrey Terras. *Fourier analysis on finite groups and applications*. Cambridge University Press, 1999.
- [76] Robb Thomson, S. J. Zhou, A. E. Carlsson, and V. K. Tewary. Lattice imperfections studied by use of lattice Green's functions. *Phys. Rev. B*, 46:10613–10622, Nov 1992.
- [77] H. Urakawa. Heat kernel and Green kernel comparison theorems for infinite graphs. *J. Funct. Anal.*, 146:206–235, 1997.
- [78] H. Urakawa. Spectra of the Discrete and Continuous Laplacians on graphs and Riemannian Manifolds. *Inter. Informations Sci.*, 3:95–109, 1997.
- [79] Y. Vardi. Network Tomography: Estimating Source-Destination Traffic Intensities from Link Data. *Journal of the American Statistical Association*, 91(433):365–377, 1996.

- [80] Nisheeth K Vishnoi. Laplacian Solvers and Their Algorithmic Applications. *Theoretical Computer Science*, 8(1-2):1–141, 2012.
- [81] M. Yamasaki. The equation $\Delta u = qu$ on an infinite network. *Mem. Fac. Sci. Shimane Univ.*, 21:31–46, 1987.
- [82] Xiaojin Zhu, Zoubin Ghahramani, and John Lafferty. Semi-Supervised Learning Using Gaussian Fields and Harmonic Functions. In *Proceedings of the Twentieth International Conference on Machine Learning, ICML, 2003*.